STUDIES ON SURFACE PROPERTIES AND CATALYTIC ACTIVITY OF SOME CHROMITES AND RELATED SPINELS

Kochurani George

Department of Applied Chemistry
Cochin University of Science and Technology
Kochi-682 022, Kerala, India.

Ph. D Thesis submitted to Cochin University of Science and Technology in partial fulfillment of the requirements for the award of the Degree of

Doctor of Philosophy

December 2006

Studies on Surface Properties and Catalytic Activity of Some Chromites and Related Spinels

Ph. D Thesis in the field of Catalysis

Author:

Kochurani George

Research Fellow,
Department of Applied Chemistry,
Cochin University of Science and Technology,
Kochi, Kerala, India-682 022
E mail: ranig@cusat.ac.in, rani_geo2003@yahoo.com

Research Advisors:

Dr. S. Sugunan

Professor in Physical Chemistry,
Department of Applied Chemistry,
Cochin University of Science and Technology,
Kochi, Kerala, India-682 022
E mail: ssg@cusat.ac.in

Dr. P.V. Mohanan

Lecturer,
Department of Applied Chemistry,
Cochin University of Science and Technology,
Kochi, Kerala, India-682 022
E mail: mohan@cusat.ac.in

Department of Applied Chemistry,

Cochin University of Science and Technology,

Kochi, Kerala, India-682 022

December 2006

…….To my Family

CERTIFICATE

Certified that the work presented in this thesis entitled **"Studies on Surface Properties and Catalytic Activity of Some Chromites and Related Spinels"** is an authentic record of the bonafide research work done by Ms. Kochurani George, under our guidance and supervision at the Department of Applied Chemistry, Cochin University of Science and Technology, and it has not been included in any other thesis submitted previously for the award of any degree.

Dr. P.V. Mohanan	**Dr. S. Sugunan**
(Supervising Guide)	(Supervising Co-Guide)
Lecturer,	Professor,
Department of Applied Chemistry,	Department of Applied Chemistry,
CUSAT.	CUSAT.

Kochi-22

20-12-2006

DECLARATION

I hereby declare that the work presented in this thesis entitled **"Studies on Surface Properties and Catalytic Activity of Some Chromites and Related Spinels"** is based on the original research work done by me under the guidance of Dr. P.V. Mohanan, Lecturer in Department of Applied Chemistry, Cochin University of Science and Technology and Dr. S. Sugunan, Professor in Department of Applied Chemistry, Cochin University of Science and Technology and it has not been included in any other thesis submitted previously for the award of any degree.

Kochurani

Kochi-22
20-12-2006

Kochurani George

ACKNOWLEDGEMENTS

I owe a debt of gratitude to all as I reflect on this thesis. I am grateful to my teacher Dr.S. Sugunan, not only for his able guidance but also for encouraging me throughout my work. His constructive comments and suggestions have played a key role in formulating my attitude and aptitude towards research.

I thank Dr. P.V. Mohanan for his support and co-operation during the period of this work. I am grateful to Dr. M.R.Prathapachandrakurup Kurup, Head, Department of Applied Chemistry, CUSAT for providing the necessary facilities for research. The valuable suggestions offered by Dr.S. Prathapan in proposing the mechanisms of many reactions are remembered with a lot of gratitude.

My heartfelt gratitude to Dr. K. K. Mohammed Rasheed, Sud Chemie, Cochin, for providing me the facility to do one part of my work there. Assistance provided by Mr. Anees is also remembered with gratitude.

At this moment, let me express my indebtedness towards all the teachers who opened the door of knowledge to me. I extend a special word of thanks to Dr. Sunny Kuriakose, Reader, Research and Post Graduate Department of Chemistry, St. Thomas College, Pala for leading me to the world of research. I extend my earnest thanks to all my teachers of St. Thomas College Pala and Pavanatma College Murickassery.

I thank Mr. Suresh and Mr. Kumar, Service Engineers, Chemito for their help during technical difficulties. The whole- hearted technical assistance provided by Mr. Kasmir Das, Mr. Jose and Mr. Gopi Menon, Department of Instrumentation is acknowledged with gratitude. I thank the scientists of STIC, CUSAT and IISc Bangalore for helping me with the analysis.

It is very difficult to find a person such as Sr.Ritty, my councilor and the most supportive person in CUSAT, without whose inspiration and support, I could not have moved with my work in its critical stages. No words of gratitude are enough for all the moments of help she had given in making my research life fruitful and memorable. I feel intensely grateful to my friends Jyothish, Sankar, Devi and Vandana for their help in literature survey and in some analysis part.

I would like to record my sincere thanks to my colleagues Sanjay, Suja, Radhika and Maya for their well-timed suggestions and encouragement during the course of this work. I am grateful to all my physical chemistry labmates who were one of the main reasons why it was fun working with catalysis. I also owe a lot to my friends of the Department of Applied Chemistry for creating a really positive atmosphere. The days spent with my friends of Athulya hostel has left warm memories in my heart.

It is beyond words to express my sincere gratitude to my beloved parents, loving brother and sister in law, sisters and brothers in law, the greatest gift that god has given me on this earth, for their constant support, encouragement and prayers. Their appreciation and support even in my small achievements, has always been a source of motivation for me. I thank them for being with me in all crests and troughs of my life. I am sure that I would not have been able to achieve anything without their support, help and prayers.

Financial assistance from CSIR-New Delhi, India is acknowledged with gratitude.

Above all, my gratitude towards the power that controls everything, without his blessings and mercy we cannot accomplish anything in this world. Thank God.

Kochurani George

PREFACE

The science and practice of catalysis is central to most activities in chemical industry. In recent years, catalysis has become an important route to the improvement of environmental quality by helping in the abatement of air pollution and the reduction of industrial waste. The phenomenon of catalysis is very widespread in chemistry and has enormous practical consequences in our daily lives. The area of catalysis is sometimes referred to as a "foundational pillar" of green chemistry. Catalytic reactions often reduce energy requirements and decrease separations due to increased selectivity; they may permit the use of renewable feedstocks or minimize the quantities of reagents needed.

Chromium oxide based catalysts are partners in many industrial processes. Spinel chromites are known for a long time now and have been exploited for a number of communications and defense applications. In spite of this development in the technology of spinel chromites, the scientists now prefer to examine the structure, cation distribution, transport properties and catalytic activities of these materials in a methodical mode to evolve the correlations between them. The present work is oriented to study the catalytic properties of some transition metal substituted copper chromite spinels prepared by co-precipitation method.

The thesis is structured into seven chapters. First chapter deals with a brief introduction and literature survey on spinels. Second chapter explains the materials and methods employed in the work. Results and discussions of the characterization techniques are described in the third chapter. The subsequent three chapters describe the catalytic activities of spinels in some industrially as well as eco-friendly important oxidation reactions. Last chapter comprises the summary of the investigations and the conclusions drawn from the earlier chapters.

CONTENTS

Page No.

CHAPTER 1 General Introduction

CHAPTER 2 Materials and Methods

CHAPTER 3 Characterization and Surface Properties

CHAPTER 4 Oxidation of Hydrocarbons

CHAPTER 7 Summary and Conclusions

CHAPTER 1

GENERAL INTRODUCTION

Abstract

Catalyzed reactions are becoming more important in the synthesis of fine chemicals and pharmaceuticals. Catalysts have been used in the chemical industry for hundreds of years, and many large-scale industrial processes can be carried out only with the aid of catalysts. Catalytic reactions often reduce energy requirement and decreases separations due to increased selectivity; they may permit the use of renewable feedstock or minimize the quantities of reagents needed. While most of these reactions are promoted by soluble, homogeneous catalysts, a strong case can be made for an increase in the extent to which heterogeneous catalysts should be used in these synthetic sequences. Heterogeneous catalysis is a field where new challenges appear continuously, more and more charming and interestingly. Spinel catalysts based on chromium play a significant role in the greening of fine chemicals manufacturing processes. A wide range of important reactions can be effectively catalyzed by these materials, which can be designed to provide good activity as well as high degree of reaction product selectivity.

1.1 Catalysis

The phrase catalysis was coined by Jöns Jakob Berzelius in 1835 who was the first to note that certain chemicals speed up a reaction. Other early chemists involved in catalysis were Alexander Mitscherlich who in 1831 referred to contact processes and Johann Wolfgang Döbereiner who spoke of contact action and whose lighter based on hydrogen and a platinum sponge became a huge commercial success in the 1820's.

A catalyst is a substance that alters the rate at which a chemical reaction approaches equilibrium without, itself, being permanently involved in the reaction. The key word in this definition is "permanently" since there is ample evidence showing that the catalyst and the reactant interact before a reaction can take place. The outcome of this interaction is a reactive intermediate from which the products are formed. This substrate-catalyst interaction can take place homogeneously with both the reactants and the catalyst in the same phase, usually the liquid, or it can occur at the interface between two phases. These heterogeneously catalyzed reactions generally utilize a solid catalyst with the intersection taking place at either the gas/solid or liquid/solid interface.

Since a catalyst merely alters the rate of a reaction, it cannot be used to initiate a reaction that is thermodynamically unfavorable. The enthalpy of the reaction as well as other thermodynamic factors are a function of the nature of the reactants and the products only and, thus, cannot be modified by the presence of a catalyst. Kinetic factors such as the reaction rate, activation energy, nature of the transition state, and so on, are the characteristics that can be affected by a catalyst.

Catalysts work by providing an alternative mechanism involving a different transition state and lower activation energy. The effect of this is that more molecular collisions have the energy needed to reach the transition state. Hence, catalysts can perform reactions that, albeit thermodynamically feasible, would not run without the presence of a catalyst, or perform them much faster, more specific, or at lower temperatures. This means that catalysts reduce the amount of energy needed to start a chemical reaction. Catalysts cannot make energetically unfavorable reactions possible — they have no effect on the chemical equilibrium of a reaction because the rate of both the forward and the reverse reaction are equally affected. The net free energy change of a reaction is the same whether a catalyst is used or not; the catalyst just makes it easier to activate.

The SI derived unit for measuring the catalytic activity of a catalyst is the katal, which is moles per second. The degree of activity of a catalyst can also be described by the turn over number or TON and the catalytic efficiency by the turn over frequency (TOF). The biochemical equivalent is the enzyme unit.

Catalysts can be either heterogeneous or homogeneous. Biocatalysis is often seen as a separate group. Heterogeneous catalysts are present in different phases from the reactants (e.g. a solid catalyst in a liquid reaction mixture), whereas homogeneous catalysts are in the same phase (e.g. a dissolved catalyst in a liquid reaction mixture).

A simple model for heterogeneous catalysis involves the catalyst providing a surface on which the reactants (or substrates) temporarily become adsorbed. Bonds in the substrate become weakened sufficiently for new bonds to be created. The bonds between the products and the catalyst are weaker, so the products are released. Different possible mechanisms for reactions on surfaces are known, depending on how the adsorption takes place. For example, in the Haber process to manufacture ammonia, finely divided iron acts as a heterogeneous catalyst. Active sites on the metal allow partial weak bonding to the reactant gases, which are adsorbed onto the metal surface. As a result, the bond within the molecule of a reactant is weakened and the reactant molecules are held in close proximity to each other. In this way the particularly strong triple bond in nitrogen is weakened and the hydrogen and nitrogen molecules are brought closer together than would be the case in the gas phase, so the rate of reaction increases. Other heterogeneous catalysts include vanadium (V) oxide in the Contact process, nickel in the manufacture of margarine, alumina and silica in the cracking of alkanes and platinum rhodium palladium in catalytic converters. In car engines, incomplete combustion of the fuel produces carbon monoxide, which is toxic. The electric spark and high temperatures also allow oxygen and nitrogen to react and form nitric oxide and nitrogen dioxide, which are responsible for photochemical smog and acid rain. Catalytic converters reduce such emissions by adsorbing CO and NO onto a catalytic surface, where the gases undergo a redox reaction. Carbon dioxide and nitrogen are desorbed from the surface and emitted as relatively harmless gases.

In homogeneous catalysis the catalyst is a molecule, which facilitates the reaction. The reactant(s) coordinate to the catalyst (or *vice versa*), are transformed to product(s), which are then released from the catalyst. Examples of homogeneous catalysts are H^+ (aq) which acts as a catalyst in esterification, and chlorine free radicals in the break down of ozone. Chlorine free radicals are formed by the action of ultraviolet radiation on chlorofluorocarbons (CFCs). They react with ozone forming oxygen molecules and regenerating chlorine free radicals.

In nature, enzymes are catalysts in the metabolic pathway. In biochemistry, catalysis is also observed with enzymes, ribozymes and deoxyribozymes. In biocatalysis, enzymes are used as catalyst in organic chemistry.

1.2. Metal Oxides in Heterogeneous Catalysis

Historically, oxide catalysts have been used primarily for vapour phase reactions in the petroleum and petrochemical industries. Recent work, however, has shown that these catalysts can also be effective in promoting a number of synthetically useful reactions. While simple oxides show activity for some oxidations they are more commonly used as solid acids or bases. Complex oxides can range in composition from the simple, amorphous, binary oxides to the more complex ternary and quaternary systems. The use of zeolites and clays can impart shape selectivity to a number of reactions; a feature that makes these systems particularly appealing for use in synthesis.

Oxide catalysts fall into two general categories. They are either electrical insulators or they can act as semiconductors. Insulator oxides are those in which the cationic material has a single valence so they have stoichiometric M: O ratios. The simple oxides, MgO, Al_2O_3, and SiO_2 and the more complex zeolites, which are aluminosilicates, fall into this category. These materials are not effective as oxidation catalysts and find most use as acids[1] or bases[2,3].

Semiconductor oxides are most commonly used in oxidations. They are materials in which the metallic species is relatively easily cycled between two valence states. These can be two different positive oxidation states as in Fe_2O_3, V_2O_5, TiO_2, CuO or NiO or the inter conversion between the positive ion and neutral metal as with the more easily reduced oxides such as ZnO[4] and CdO[5]. Basically, some oxides are semiconductors because they can have either a slightly excess or deficiency of electrons. In the former case there is a net negative charge so the material is referred to as an n-type semiconductor. A net positive charge gives a p-type semiconductor. These two types are appreciably different in their adsorption and reaction characteristics.

Many oxide catalysts are materials having two or more cationic components. If the oxides are crystalline the crystal structure can determine the oxide composition. For instance perovskites have the general formula ABO_3, Scheelites are ABO_4, spinels are AB_2O_4 and palmeirites are $A_3B_2O_8$[6]. In other cases where specific crystallinity is not observed the cationic ratio can vary over a wide range. The most common methods used to prepare complex oxides are co-precipitation followed by calcinations and a solid-state procedure involving the heating of precursor salts or oxides in appropriate ratios. Co-precipitation occurs when a solution of two or more metal salts is treated with a precipitating agent, usually an alkali hydroxide, carbonate or bicarbonate. The resulting precipitate may contain not only the insoluble oxides, hydroxides and/or carbonates but also a mixed metal species if the solubility equilibria are favorable and the precipitation time is sufficient for the formation of such compounds. This material is then washed, dried and calcined at an elevated temperature to decompose any hydroxides or carbonates and give the desired metal oxide. The critical factor with this procedure is the distribution of the components evenly throughout the solid. Unfortunately, this is usually not the case. Since the solubility constants of the individual components will not be identical so in the early stages of the precipitation one component may be present in excess while in the later stages the second or third component may predominate[7,8]. This difference in solubility can be magnified if the basic precipitant is added to a solution of metal salts. The initial quantity of base will be diluted by the metal solution so precipitation of the material with the lowest solubility will occur preferentially. This will also use up some of the base resulting in a further decrease in its concentration. As more base is added, its concentration will increase and the more soluble species will then be precipitated.

A more uniform precipitate is obtained if the metal ion solution is added to the base but even here some discrimination can be observed. As the metal solution is added, the base concentration decreases. A further decrease is brought about by the precipitation of some of the basic anions. Homogeneous precipitation appears to take place when the metal salt solution and the base are added together at such a rate as to maintain the reacting mixture at a constant pH[8].

Another way of effecting a nearly constant pH in the reaction mixture is to introduce the base by the aqueous hydrolysis of urea[9]. A TiO_2-SiO_2 catalyst was prepared by adding an acid solution of $TiCl_4$ and tetraethoxy silane to ammonium hydroxide. A second batch of catalyst was prepared by adding urea to the acid solution and heating the resulting mixture at 95°C for several hours. In both the cases, the resulting precipitates were washed, dried and calcined at 500°C. Even though the NaOH precipitated material had a larger surface area than that prepared using urea hydrolysis as a source of the base, the later material was considerably more acidic, presumably because of the more homogeneous character of the precipitate[9].

Another procedure that produces a more homogeneous mixed oxide involves the aqueous hydrolysis of metal alkoxides. Adding water to an alcoholic solution of tetraethoxy silane and titanium tetraisopropoxide gives a gel composed of the mixed oxides[10]. When an acid catalyst is used the hydrolysis of the alkoxides takes place very rapidly, but the condensation of the resulting metal hydroxides is slow. This result in the formation of linear chains with little cross-linking and gives a material that on calcinations collapses to a microporous solid of limited usefulness in catalysis. In base, the hydrolysis of the alkoxides takes place more slowly but the condensation of the hydroxides is rapid. Thus, as the hydrolyzed species is formed it becomes attached to a growing nucleus that is extensively cross-linked. On heating these clusters form mesoporous solids that are stable to elevated temperature treatment and, then, useful for catalytic processes[10].

The addition of a small amount of ammonium hydroxide to an alcoholic solution of tetraethoxy silane and aluminium triisobutoxide gave an aluminosilicate gel that on washing, drying and calcination at 300-900°C produced an amorphous aluminosilicate that was an effective solid acid catalyst[11].

The advantage of using a co-precipitation procedure for the production of mixed oxides is that the ratio of the cations in the resulting mixed oxide can be varied over a wide range of compositions. This facilitates optimizing the oxide composition for a particular application. In the case of the TiO_2-SiO_2 mixed oxides, the one containing 20% TiO_2 and 80% SiO_2 was shown to be particularly effective as a support for V_2O_5 oxidation catalysts. Changing the Ti: Si ratio from this value resulted in a decrease in the oxidation activity of the supported catalysts[12,13].

1.3 Chromites

Mixed metal oxides with chromium (III) oxides as their main components are known as chromites. The electronic effect of chromium (III) in tetrahedral and octahedral sites is given in figure 1.1. Cr (III) in octahedral site is stabilized with all the orbitals half filled. So Cr (III) always prefer octahedral site and is a normal spinel[14].

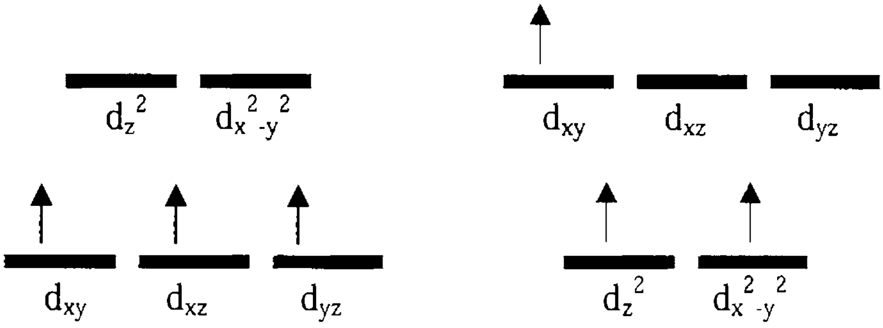

Figure 1.1: Electronic effect of chromium in octahedral and tetrahedral sites

1.4 Spinels

Spinels are mixed metal oxides with general formula AB_2O_4; where A and B are cations with oxidation states 2 and 3 respectively occupying the tetrahedral and octahedral sites of a face centered cubic array of the anions. Chromites belong to the group of spinels and simple chromites as well as mixed chromites are known. They exhibit interesting structural and catalytic properties, which are governed by their chemical composition.

1.4.1 Methods of preparation

Chromites can be prepared by almost all the existing techniques of solid-state chemistry. For the exact reproducibility of the particles, utmost care must be taken during the preparation stages. Minor changes in the preparation method can drastically alter their properties.

Ceramic method is the oldest method for the preparation of chromites. The precursor compounds are generally chromium oxide (Cr_2O_3) and oxides or carbonates of the other cations in the desired chromite and these are ground well by mechanical milling[15-19]. But this method cannot produce fine particles and extended milling introduces significant quantities of undesired impurities and the distribution in the particle size becomes extremely wide. The major drawback found for this method is the lack of homogeneity of the materials prepared. Again, the high temperature (~1200°C) required to complete solid-state reactions leads to drastic decrease in surface area of the resulting material by sintering and therefore catalytic properties are affected.

Co-Precipitation is a very suitable method for the creation of homogeneous catalyst components or for the moulding of precursors with a definite stoichiometry, which can easily be converted to the active catalyst. This method is based on the stoichiometric mixing of aqueous solutions of nitrates of Cr^{3+} and of divalent Mn, Co, Ni, Cu, Zn, Mg, Ba etc; in the concentrations required for the chromite composition and their simultaneous precipitation in the form of hydroxides by $NaOH/NH_4OH$[20-25]. This is followed by filtration, washing and calcination of the products to form the oxide. The morphology, the texture, the structure and the size of the particles can be accurately controlled by altering the pH and/or temperature of the solution. By this method, chromite particles with a narrow size distribution may be obtained with high purity.

The precursor method allows the preparation of chromites with a precise stoichiometry[26,27]. It involves the synthesis of a compound (precursor) in which the reactants are present in a required stoichiometry. Upon heating in air (1200-1500 K), the precursor decomposes to yield the chromite. Particles with high purity and various size ranges can be obtained by this method.

Sol-Gel techniques are receiving much attention because they can be applied to a wide variety of materials; they offer the possibility of controlling not only the size and distribution of particles, but also their shape[28]. A broad range of chromites with any desired shape can be prepared by this technique. The process involves the preparation of a sol, which is a dispersion of a solid and a dispersed phase in a liquid (dispersion medium). The sol is prepared by mixing concentrated solutions containing the cations of interest, with an organic solvent as dispersion medium. The sol is then destabilized by adding water, leading to the formation of a gel. This is transformed to the solid phase by high pressure heating whereby the liquid contained in the gel is transformed into supercritical vapors.

In addition to the above-discussed methods, some other methods like *chemical vapours transport method*[29] high temperature *aerosol decomposition process*[30] and *citrate route*[31-33] are also applied in the chromite synthesis.

1.4.2 Spinel Structure

The spinel structure was first determined by Bragg and Nishikava[34]. In the ideal structure of a spinel the anions form a face centered cubic (fcc) close packing in which the cations partly occupy the tetrahedral and octahedral interstices. The unit cell contains 32 anions forming 64 tetrahedral interstices and 32 octahedral interstices; of these 8 tetrahedral and 16 octahedral sites are occupied by cations. These are called A- and B- sites respectively. The general formula of compounds with spinel structure is AB_2O_4.The unit cell of an ideal spinel is shown in figure 1.2.

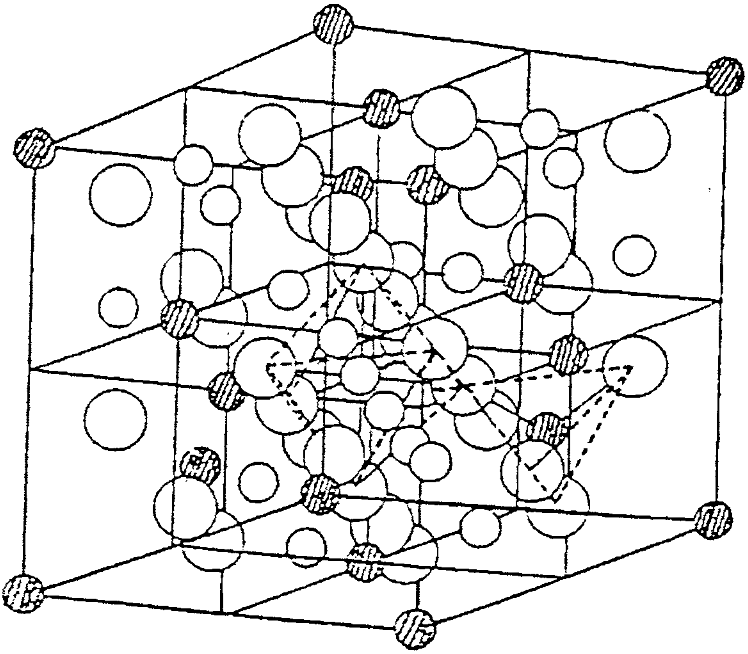

Figure 1.2. The unit cell of an ideal spinel structure. Hatched circles indicate A cations, unhatched circles indicate B cations and large unhatched circle indicate oxygen anions

It is convenient to divide the unit cell into eight edges of length a/2 to show the arrangements of A and B sites. (figure 1.3). The space group is Fd^3m (Oh^7). The oxygen atoms have four-fold coordination, formed by three B cations and A cation. The nearest neighbors of a tetrahedral site, octahedral site and oxygen anion site are shown in figure 1.4.

The ideal situation is never realized, as the oxygen anions in the spinel structures are generally not located at the exact positions of the fcc sub lattice. The interstices available in an ideal close packed structure of rigid oxygen anions can incorporate only those metal ions with radius $r_{tetra} \leq 0.30A^{\circ}$ in tetrahedral sites and only those ions with radius, $r_{octa} \leq 0.55A^{\circ}$ in octahedral sites. So in order to accommodate larger cations such as Co, Cu, Mn, Mg, Ni and Zn the lattice has to be expanded. The difference in the expansion of the tetrahedral and octahedral sites is characterized by a parameter called oxygen parameter (*u*).

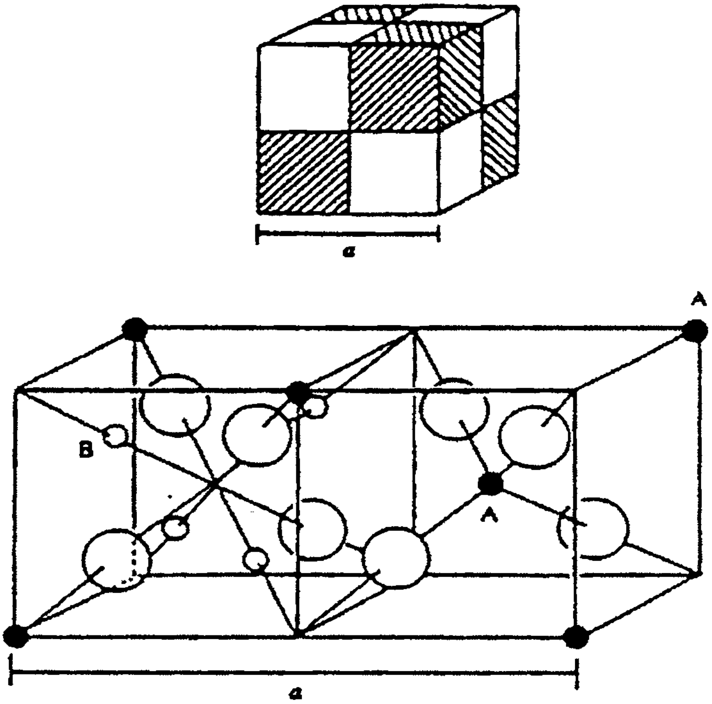

Figure 1.3. The spinel structure. The unit cell can be divided into octants; tetrahedral cations A, octahedral cations B and oxygen atoms (large circles) are shown in two octants

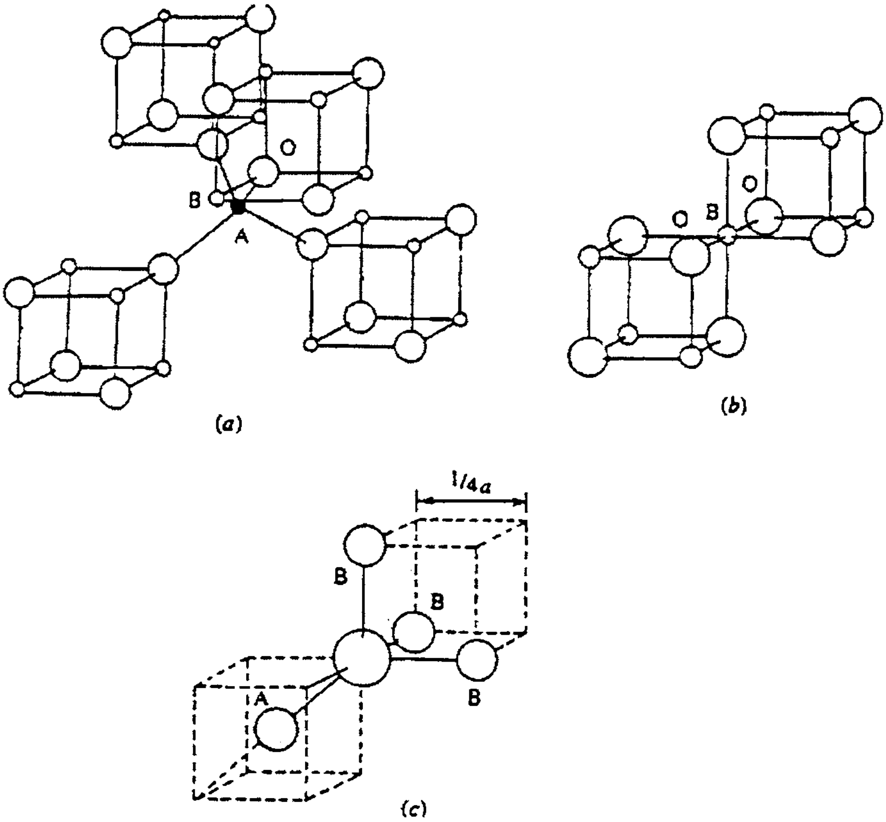

Figure 1.4. Nearest neighbors of (a) tetrahedral sites, (b) an octahedral site and (c) oxygen anion

In all ideal spinels, the parameter *u* has a value in the neighborhood of 0.375. But in the actual spinel lattice this ideal pattern is slightly deformed, usually corresponds to u > 0.375. *u* increases because the anions in the tetrahedral sites are forced to move in the [111] direction to give space to the larger A cations, but without changing the overall F'4_{3m} symmetry. Octahedra become smaller and assume Fd'$_{3m}$

symmetry[35,36]. Interatomic distances as a function of the unit cell parameter 'a' and the oxygen parameter u is given in the table 1.1.

Table: 1.1 Inter atomic distances and site radii in spinels AB_2O_4, as a function of unit cell edge (a) and oxygen parameter (u).

Tetra-tetra separation A-A	$a\ (3/4)^{1/2}$
Tetra-octa separation A-B	$a\ (11/8)^{1/2}$
Octa-octa separation B-B	$a\ (2/4)^{1/2}$
Tetra- O separation A-O	$a\ [(3(u\text{-}0.25)]^{1/2}$
Octa- O separation B-O	$a\ (3u^2-2.75u+43/64)^{1/2}\ a(5/8-u)$
O-O tetrahedral edge O-O	$a\ [2\ (2u-0.5)]^{1/2}$
O-O shared octa edge O-O	$a\ [2\ (1-2u)]^{1/2}$
O-O unshared octa edge O-O	$a\ (4u^2-3u+11/16)^{1/2}$
Tetrahedral radius	$a\ [3\ (u-0.25)]^{1/2}-R_o$
Octahedral radius	$a\ (3u^2-2.75u+43/64)^{1/2}-R_o\ a\ (5/8-u)-R_o$

u is defined with unit cell origin at an A site and R_o is the oxide ion radius

1.4.3 Distribution of metal ions over different sites

Normal, Inverse and Random spinels

An interesting property of compounds with spinel structure is the so-called cation distribution, ie the distribution of the cations present among the two types of sites, viz, tetrahedral and octahedral ones. As mentioned earlier, the general formula of the spinel is AB_2O_4, where A and B cations occupy the tetrahedral and octahedral sites respectively. Many different cation combinations may form a spinel structure and it is almost enough to combine any three cations with a total charge of eight to balance the charge of the anions. The following combinations are known.

$A= {}^{+}2$,	$B= {}^{+}3$	as in	$CuCr_2O_4$
$A= {}^{+}4$,	$B= {}^{+}2$	as in	Co_2GeO_4
$A= {}^{+}1$,	$B= {}^{+}3, {}^{+}4$	as in	$LiFeTiO_4$
$A= {}^{+}1$,	$B= {}^{+}3$	as in	$Li_{0.5}Fe_{2.5}O_4$
$A= {}^{+}1$,	$B= {}^{+}2, {}^{+}5$	as in	$LiNiVO_4$
$A= {}^{+}6$,	$B= {}^{+}1$	as in	Na_2WO_4

Verway and Heilman[37] have discussed the structure and cation distribution of the spinels. If A denotes a divalent cation and B, a trivalent one, the cation distribution is usually indicated as (A) $[B_2]$ O_4, where the square bracket indicate the octahedral occupancy and the cation in the parenthesis are located in the tetrahedral sites. This is the so-called normal distribution, in which the tetrahedral sites are occupied only by the A-type ions and the octahedral sites by B-type ions. The A-ions of a normal spinel occupy the 8 tetrahedral sites of the Oh^7 space group and have a point symmetry T_d. The B ions of a normal spinel occupy the 16 octahedral sites of the Oh^7 space group and have the point symmetry D_{3d}. Second distribution type is (B) [AB] O_4, as pointed out by Barth and Posnjak[38]. In this case the B cations occupy the Td sites and all the A cations together with the other half of the B cations occupy the octahedral sites. This type of spinel configuration is called inverse spinel. It is common to describe the structure of a spinel by the parameter,λ defined as the fraction of B ions in the tetrahedral sites. The value of λ ranges from zero for normal spinels and 0.5 for those having inverse composition. Cation distribution (as λ values) in a number of common spinels is given in the table 1.2. Datta and Roy[39] and Hafner and Laves[40] have shown that there are many intermediate or random spinels, which are in between pure normal and pure inverse arrangements. This can be represented as $(A_{1-x}B_x)$ $[A_xB_{(2-x)}]$ O_4, where, x is the degree of inversion with a value of zero for normal and one for the inverse distribution. This intermediate spinel structure is due to the average distribution of all the ions about the entire spinel cation position. (table 1.3).

Table 1.2: Value of λ for spinels, AB_2O_4

A^{2+} / B^{3+}	Mg^{2+}	Mn^{2+}	Fe^{2+}	Co^{2+}	Ni^{2+}	Cu^{2+}	Zn^{2+}
Al^{3+}	0	0	0	0	0.38	-	0
Cr^{3+}	0	0	0	0	0	0	0
Fe^{3+}	0.45	0.1	0.5	0.5	0.5	0.5	0
Mn^{3+}	-	0	-	-	-	-	0
Co^{3+}	-	-	-	0	-	-	0

Table 1.3: Cation distribution, lattice parameter (a) and oxygen parameter (*u*) for several spinels

	Distribution	a (A°)	*u*
Normal	$(Cd)[Fe_2]$	8.7050	0.3935
	$(Zn)[Fe_2]$	8.5632	0.3865
Inverse	$(Fe)[CoFe]$	8.3500	0.3810
	$(Fe)[CuFe]$	8.3690	0.3800
	$(Fe^{3+})[Fe^{2+}Fe^{3+}]$	8.3940	0.3798
	$(Fe)[Li_{0.5}Fe_{1.5}]$	8.3300	0.3820
	$(Fe)[NiFe]$	8.3390	0.3823
Random	$(Mg_{(1-x)}Fe_x)[Mg_xFe_{(2-x)}]$	8.3600	0.3820(x=0.10)
	$(Mn_{(1-x)}Fe_x)[Mn_xFe_{(2-x)})]$	8.5110	0.3865(x=0.85)
	$(Mo_{(1-x)}Fe_x)[Mo_xFe_{(2-x)}]$	8.5010	0.3751(x=0.50)

1.4.4 Factors influencing the cation distribution

The interesting and useful electrical, magnetic and catalytic properties of spinels depend not only on the kinds of cations in the lattice, but also their distribution over the available crystal sites. It is thus of major importance to understand the factors that contribute to the total lattice energy in spinels i.e. (i) Elastic energy (ii) Electrostatic (Madelung) energy (iii) Crystal field stabilization energy (iv) d-orbital splitting and (v) polarization effects.

The elastic energy refers to the degree of distortion of the crystal structure due to the difference in ionic radii assuming that ions adopt a spherical shape. Smaller cations, with ionic radii of 0.225-0.4A°, should occupy tetrahedral sites, while cations of radii 0.4-0.73A° should enter octahedral sites. This distribution leads to a minimum in lattice strain. Since trivalent cations are usually smaller than divalent ones, a tendency towards the inverse arrangement would be expected.

The Madelung constant of the spinel structure has been calculated by Verwey et al.[41] as a function of oxygen parameter u and the charge distribution among A- and B- sites. Their results showed that this energy is dependent on the u-parameter. For $u>0.379$, the normal distribution is more stable, while for lower u values the inverse arrangement possesses a higher Madelung constant. The presence of two kinds of cations in octahedral sites in inverse spinels leads to an additional contribution to the Madelung energy. The critical u value then becomes 0.381[42]. Madelung energy is higher for the normal spinel if $u > 0.381$ and the inverse ordered spinel is more stable for $u < 0.381$.

Crystal field factors used to help account for the site preferences in spinels. Romeijn[43] was the first one who suggested the application of the crystal field theory to understand the cation site preference in spinels. Dunitz and Orgel[44] and simultaneously Mc Clare[45] has calculated the octahedral site preference energies of transition metal ions in oxides using crystal field theory (CFT) and is given in the table 1.4.

Table 1.4. CFSE for transition metal ions on tetrahedral and octahedral spinel sites

Number of d electrons	Theoretical cfs in terms of Dq		Cations	Estimated octahedral site preference energies, eV
	Octahedral	Tetrahedral		
1	4	6	Ti^{3+}	0.33
2	8	12	V^{3+}	0.53
3	12	8	V^{2+}	1.37
			Cr^{3+}	2.02
4	6	4	Mn^{3+}	1.10
			Cr^{2+}	0.74
5	0	0	Fe^{3+}	0
			Mn^{2+}	0
6	4	6	Fe^{2+}	0.17
			Co^{3+}	0.82
7	8	12	Co^{2+}	0.09
8	12	8	Ni^{2+}	0.99
9	6	4	Cu^{2+}	0.68
10	0	0	Zn^{2+}	0

The data show that the systems with d^5 and d^{10} configurations have no CFSE and hence no site preference. The d^3 system has the highest octahedral site preference energy. The d^4 and d^9 ions can be further stabilized by Jahn-Teller distortion. In the regular octahedral symmetry, octahedron of surrounding anions is elongated or compressed in the z-direction to give D_{4h} symmetry, the doublet (e_g) and triplet (t_{2g})

levels split[46]. The splitting of the doublet is larger. In the case of elongation, the dz^2 orbital is stabilized compared to the dx^2-y^2 orbital. Cu [Cr_2] O_4, Fe [CuFe] O_4, Cr [NiCr] O_4 and Mn [ZnMn] O_4 are examples of tetragonally distorted spinels.

Another factor which plays a role in cation distribution is d-orbital splitting energy. Although, the CFSE contribution to the total bonding energy of a system is only about 5-10%; it may be the deciding factor when other contributions are reasonably constant. The crystal field contribution for spinels can assess by considering the difference in CFSE for octahedral compared to tetrahedral coordination for the metal ions involved. For purpose of estimating this difference, it can be assumed that the oxide ions will provide a moderately weak crystal field similar to that for water.

Polarization may simply be considered as the degree of distortion of the electronic charge density around an ion. This can arise from the negligible distortion and effective removal of an electron from one ion towards its neighbor, giving rise to a purely covalent bond and a purely ionic bond respectively. With regard to transition metal ions in spinels, only spherically symmetric ions (d^5 and d^{10}) can show tendency for covalency. In this case, tetrahedral sites are preferred. Cations which show covalent affinity for tetrahedral environments are Fe^{3+}, Ga^{3+} and more slightly Zn^{2+} and Cd^{2+}. Spinels with the former cations tend, therefore, to be inverse while those with the latter tend to be normal.

When the various factors are counter balancing, there can be a completely random arrangement of metal ions among the 8 tetrahedral and 16 octahedral sites.

1.4.5 Spinels as Catalysts

Mixed metal oxides possessing spinel structure exhibit interesting solid-state and catalytic properties. Individual metal oxides loose their catalytic activity rapidly owing to ageing and formation of coke over the catalyst surface. The spinel lattice imparts extra stability to the catalysts under various reaction conditions so that these systems have sustained activities for longer periods[47]. Copper based catalysts have attained considerable importance, owing to their selective properties in reactions involving hydrogen[48].

Metal chromite spinels are of considerable interest because of their technological applications as catalysts and refractories[49-54]. Chromia possesses an interesting electrical, magnetic as well as surface properties that affect its usage as an industrial catalyst in many reactions[55]. Such reactions include oxidative dehydrogenation of isobutene[56], ethane[57], selective oxidation of H_2S[58], carbon monoxide oxidation[59] and ethylene polymerization[60]. The presence of chromium in various oxidation states enables an easy exchange of electron between the oxide and the adsorbed species of the catalytic reactions, the oxide being in a position to accept electrons as well as to give them up. Chromia can be considered as a host oxide in preparing the catalyst viz spinels. Metal chromites seem to be a good example for the surface electron transfer cycle between two different valence states. The efficiency of this cycle is favored by the ease of establishing the known redox process $Cr^{3+} \rightarrow Cr^{6+} \rightarrow Cr^{3+}$. Such a concept would indicate an activity of chromites for redox reactions. This cycle is controlled by the extent to which the divalent cation can exchange electrons with the surface chromia ions[61,62].

Oxidative dehydrogenation (ODH) of hydrocarbons is the one of the most important reactions studied using spinel catalysts. Krishnasamy et al. have studied the ODH of ethylbenzene over Zn-Fe-Cr ternary spinel systems[63]. They concluded that both acidic and basic sites are responsible for the catalytic activity. Mathew et al. prepared ferrites of copper and cobalt and studied the ODH of ethylbenzene[64]. They have the same conclusion as proposed by Krishnasamy and explained the results with the mechanism of dehydrogenation of ethylbenzene proposed by Wang[65] and

Krouse[66]. Strong basic sites facilitate the formation of toluene whereas strong acid centers result in high yield of benzene. The active site balanced with acidic and basic sites is important for an efficient ethylbenzene dehydrogenation. Antonio et al. studied the ODH of 1-butene into butadiene on non- stoichiometric zinc ferrites synthesized by co-precipitation and hydrothermal methods[67]. They reported the parallelism between the macroscopic magnetization of the ferrites and their capacity of transforming 1-butene into butadiene, CO_2 and 2- butane by an ODH reaction. This suggests that the "freezing" of the magnetic moments in the octahedral sites could cause the catalytic behavior. Sloczynski et al. have studied the ODH of propane on $Ni_xMg_{1-x}Al_2O_4$ spinel systems and reported that the activity and selectivity towards propene increases with increase in Ni content. It is suggested that the nickel ions surrounded by oxygen in the spinel structure are proposed as active center for ODH of propene[68].

Branched higher alcohols, such as isobutanol or isoamyl alcohol, could provide the raw materials needed to produce novel cetane enhancers for diesel fuel, e.g. methyl isobutyl ether (MIBE). Branched alcohols could be of interest per se as oxygenated additives for motor gasoline. Improvements in the catalytic higher alcohol synthesis from syn gas are necessary in order for the reaction pathway to become economically viable. A commercially available Zn/Cr spinel catalyst is Engelhard Zn-0312. Epling et al. doped this commercial catalyst with varying amount of potassium and cesium[69-72]. Their results indicate that a better catalyst for the production of an equimolar mixture of isobutanol and methanol can be achieved by promoting the Zn/Cr spinel by Cs rather than K and Cr, which are found to be unnecessary for higher alcohol synthesis and possibly detrimental. Further, the authors prepared a series of Zn/Cr/Mn spinel catalysts promoted with Cs and Pd in which some of the Cr atoms have been replaced by Mn and the resulting data indicate that Mn improves the catalytic properties of Cs promoted spinels[73,74]. Roberts et al.[75] have studied the synthesis of higher alcohols from H_2/CO mixtures in a slurry reactor with Cs promoted zinc chromite catalyst in decahydro naphthalene as slurry liquid. Compared with unpromoted zinc chromite, the Cs promoted catalyst shifted the product distribution away from methanol to higher alcohols.

Alcohol decomposition is a widely studied reaction on spinel catalysts. Abu Zied et al.[76] studied the ethanol decomposition over Cd-Cr-O systems and their results showed that the samples containing the chromate phase is more active than the catalysts containing chromite phase. They have also reported[77] the ethanol decomposition on silver/chromia catalysts and suggested that lower activity of silver chromite is due to the stable phase towards reduction during the catalytic activity measurements. Robert and Shreiber[78] studied the methanol dehydrogenation in a slurry reactor with copper chromite and Fe/Ti catalysts. Their research supports the concept of in situ formaldehyde generation via methanol dehydrogenation and provides a basis for carrying out 'one pot' synthesis in which the generated formaldehyde reacts with another molecule to form the desired product in a temperature range 598 to 673 K.

Nitrogen oxides and soot particles emitted from diesel engines have been causing serious problems to global environments and human health. Ternary AB_2O_4 (A = Mg, Co, Cu, Ni and Zn and B = Cr, Fe and Mn) spinel type oxides catalyses simultaneous removal of NO_x and diesel soot to form CO_2, N_2 and nitrous oxide and the superiority of the spinels to constituent simple metal oxides and their mixtures is confirmed[79]. The catalytic performance of the spinels depend significantly on the constituent metal cation and $CuFe_2O_4$ is the excellent system with highest selectivity to nitrogen formation, lowest selectivity to nitrous oxide and provides intermediate ignition temperature of soot[80]. Sloczynski et al.[81] studied the selective catalytic reduction of NO with ammonia over a series of chromium spinels. They concluded that the catalytic activity and selectivity to N_2O depend on the nature of the divalent metal.

Carbon monoxide oxidation is one of the environmentally friendly reactions studied on spinel catalysts. Copper manganese oxide mixtures based on $CuMn_2O_4$ is a long established catalyst for the removal of toxic gases and vapors since its discovery in 1920[82]. Gedevanishvili et al.[83] have studied CO oxidation on spinel based pigment system consisting of mixed manganese, copper and iron oxides. Application of a reduction followed by oxidation type of heat treatment on fresh catalyst induced the formation of fine clusters on the surface of the catalyst particles. This refined morphology with high density of defects led to a great improvement in catalytic activity. Ghose et al. studied the activity of Cu^{2+} ions on the tetrahedral and octahedral sites of copper spinel oxide for CO oxidation[84] and concluded that in oxidation reactions, the catalytic activity is higher when copper is present in the tetrahedral sites of the spinel lattice. They have also studied the reaction on aluminium and magnesium substituted copper chromite spinel oxide catalysts[85]. From the results they concluded that the catalytic activity of $CuCr_2O_4$ for the oxidation of CO is due to Cr ions above 500K and the activity per Cr ion increases with Cr dilution due to weaker interaction of the surface Cr ions with its near neighbors. The activity below 500K is due to Cu^{2+} ions and their reduction to Cu^{+} ions lead to a decrease in the catalytic activity.

Nanosized nickel ferrite powders synthesized from fly ash via a chemical synthesis route[86] showed a good response towards CO oxidation. It was concluded that lower crystal size enhanced CO adsorption and consequently its oxidation. NiMn2O4 was reported to be a good catalyst for CO oxidation by Mehandjiev et al.[87]. Thormahlen et al. studied the influence of CO_2, C_3H_6, NO, H_2, H_2O, or SO_2 on the low-temperature oxidation of CO on a cobalt-aluminate spinel catalyst[88]. When the catalytic activity was tested with only CO and O_2 present in the feed gas, complete conversion was reached at room temperature. When other compounds were present in the gas mixture, they inhibited CO oxidation. The main reason for the loss of activity is suggested to originate from the compounds adsorption and formation of different species on the cobalt oxide surface, which seems to inhibit the reduction and/or re-oxidation process of the metal oxide surface and/or the adsorption of CO.

Alkylation of hydrocarbons is another reaction studied on spinel catalysts. Sugunan and co-workers studied the alkylation of aniline and phenol with methanol over Zn-Co-Fe ternary spinel systems[89-91]. Their results showed that a controlled interplay of surface acid-base properties and polarity of respective reacting molecules determines the efficiency of a particular reaction. In the case of aniline methylation, surface basicity plays a dominating role, where as for phenol methylation surface acidity plays a dominating role. Ghorpade et al.[92] studied the liquid phase Friedel Craft's alkylation of benzene using $CuCr_{2-x}Fe_xO_4$ spinel catalysts; $CuFe_2O_4$ gave the highest yield. They concluded Lewis acidity of the catalyst is mainly responsible for the good catalyst performance. Choudhary et al.[93] studied the same reaction using $MgGa_2O_4$ spinel systems and reported that the catalytically active species in this catalyst are Ga_2O_3 and $GaCl_3$ dispersed on MgO. Grabowska et al.[94] reported zinc aluminate spinel as an efficient catalyst for obtaining thymol by gas phase catalytic alkylation of m-cresol with isopropanol. They have obtained both O- and C-alkylated products at low temperature, while at high temperature thymol was the main product of the reaction.

1.5 Acid-Base Properties

Surface acidity and basicity investigations have received considerable attention in recent years, since they play an important role in many catalytic reactions. In the case of reactions that have been recognized to be catalyzed by acid sites on a catalyst surface, basic sites also act more or less as active sites in cooperation with acid sites. A catalyst having suitable acid-base pairs sometimes show pronounced activity, even if the acid- base strength of a bi- functional catalyst is much weaker than the strength of the simple acid or base. For example, ZrO_2, which is weakly acidic and basic shows higher activity for C-H bond cleavage than highly acidic SiO_2-Al_2O_3 or highly basic MgO[95]. A systematic investigation of the activity and selectivity of a catalyst and acid-base property (strength, amount and type) enables the development of an optimum catalyst with desired acid base properties for a specified reaction. Development in this area has given rise to numerous methods for exploring these properties.

1.5.1 Temperature Programmed Desorption of basic molecules

This method is based on desorbing volatile amines such as ammonia, pyridine, n-butyl amine or quinoline, that was pre- adsorbed on a solid, by heating it at a programmed rate. This simple and inexpensive method is normally used to measure the number and strength of acid sites on solid catalysts[96, 97]. An excess of the base is adsorbed and what is considered to be physically adsorbed is then removed by prolonged evacuation. Whatever left on the surface, after this, is considered to be chemically adsorbed and that is a measure of total acid strength and the area under the desorption peak as a measure of the number of acid centers.

The ammonia-TPD method is widely employed to characterize the acidity of solid catalysts[98-110]. Ammonia is an excellent probe molecule for testing the acidic properties of solid catalysts, because its strong basicity and small molecular size allow the determination of acidic sites of any strength and type [99,100]. Though ammonia TPD method is unable to distinguish the type of acid sites (Lewis and Bronsted) it gives the total acidity and acidity of solid catalyst at any temperature region. TPD of ammonia involves saturation of the surface with ammonia under some set of adsorption conditions, followed by linear ramping of the temperature of the sample in a flowing inert gas (Helium or N_2) stream. The concentration of ammonia in the effluent gas is estimated by titration or mass spectrometry. The experiment can also be carried out in a microbalance and weight loss in the sample can be followed continuously.

1.5.2 Cyclohexanol Decomposition

The amphoteric nature of alcohols enables them to interact with both acidic and basic sites. The utility of alcohol decomposition as a test reaction for acid-base property studies of metal oxides is well established[111-115]. It was observed that metal oxides catalyze both dehydration and dehydrogenation of alcohols. Dehydration of alcohols leads to an olefin and dehydrogenation forms as aldehyde (in the case of primary alcohols) or a ketone (in the case of secondary alcohol) and hydrogen. At elevated temperatures, decomposition may involve C-C bond cleavage giving products like CO, CO_2 etc. At near ambient temperatures, ether can be a major product. According to the general concept, dehydration is an acid catalyzed reaction, whereas dehydrogenation, which proceeds by a concerted mechanism, is due to the combined effect of both acidic and basic sites on the system, whereas the ratio of the dehydrogenation activity to the dehydration activity gives the basicity of the system[116,117].

One of the most widely studied alcohol decomposition reaction for the acidity-basicity correlation is the cyclohexanol decomposition. The amphoteric nature of cyclohexanol permits its interaction with both acidic and basic sites. As a result of this, dehydration and dehydrogenation are catalyzed by the oxide systems forming cyclohexene and cyclohexanone. (scheme 1.1)

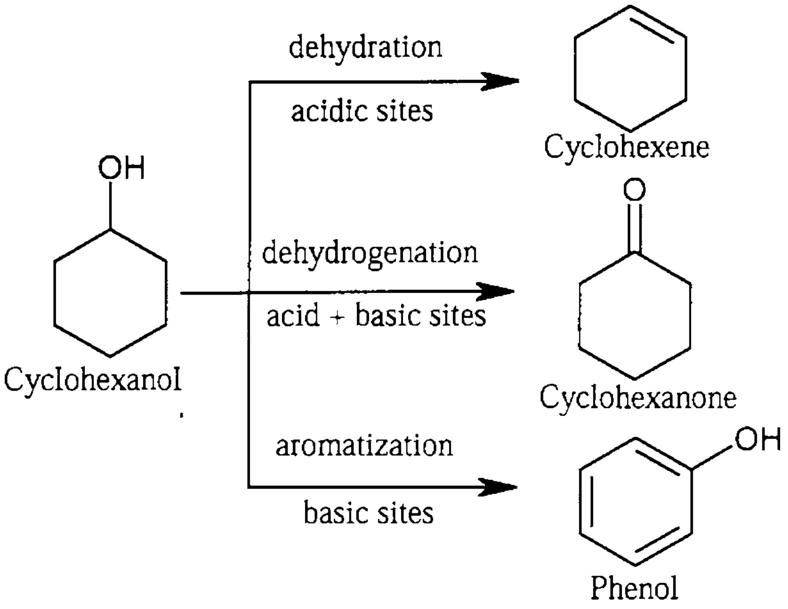

Scheme 1.1: Scheme of cyclohexanol decomposition

Haneda et al.[111] studied the acid-base properties on alumina supported catalysts and correlated the results with cyclohexanol decomposition data. Bezouhanava et al.[118] have noticed cyclohexanol decomposition as an easy and reliable method to determine the functionality of metal oxide catalysts. They correlated the dehydrogenation activity to the existence of basic sites originating from the lattice oxygen. Stronger acid sites are needed for dehydration of cyclohexanol compared to other secondary and tertiary alcohols. The influence of copper ions in the octahedral sites of spinel catalysts on the transformation of cyclohexanol to cyclohexanone was studied by Jebarathinam et al.[119]. Their investigations indicated that the Cu^{+} at the octahedral sites is more active than Cu^{0} for the dehydrogenation of cyclohexanol. The same authors studied the effect of Zn^{2+} in $NiFe_2O_4$ matrix on the catalytic decomposition of cyclohexanol. Introduction of Zn^{2+} creates strong basic sites and facilitated the dehydrogenation of cyclohexanol to cyclohexanone[120].

Catalytic decomposition of cyclohexanol over $Mg_{1-x}Zn_xAl_2O_4$ reported by Joshi and co workers established the correlation among transport properties, surface acidity and catalytic behavior[121].

1.5.3 Cumene cracking

Cumene cracking reaction can be considered as one of the test reactions for the acidity measurement of catalysts[122-125]. Generally cumene conversion gives dehydrogenation as well as dealkylated products. α-methyl styrene, the dehydrogenation product is attributed to the Lewis acidity of the catalyst and Bronsted acidity of the catalysts is responsible for benzene, the dealkylated product. Ethyl benzene, styrene and toluene are also formed as side products. (scheme 1.2)

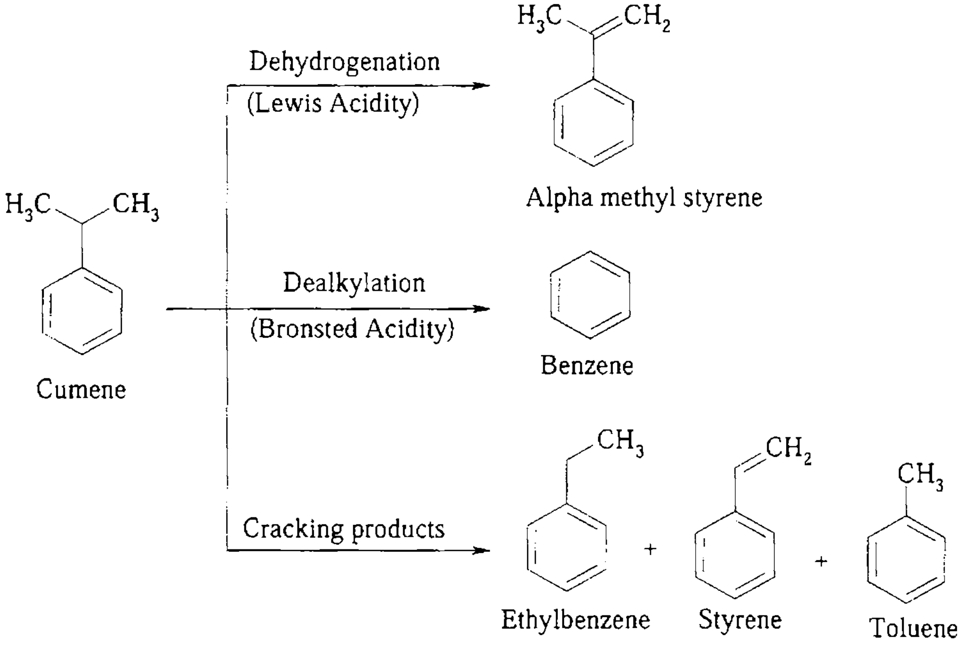

Scheme 1.2: Scheme of Cumene cracking

It is well known that acidity of the mixed oxide supports has a substantial effect on the activity of cumene cracking. Rana et al.[126] studied cumene cracking functionalities on sulfided Co (Ni) Mo/ TiO_2-SiO_2 catalysts. They concluded that the cumene cracking activity over supported catalysts is attributed to the Bronsted sites like sulfhydryl groups. Parida et al.[124] reported the preparation and textural characterization of sulfated titania-silica mixed oxides and their correlation with the catalytic activity for cumene cracking. A good correlation was found between the cumene cracking and the acidity of the catalyst. A number of workers studied the cumene cracking and correlated the results with the acidity of the catalysts [122, 127-131].

1.6 Reactions Selected for the Present Study

(i) Oxidation of benzyl alcohol

Catalytic conversion of primary alcohols to aldehydes is essential for the preparation of fragrances and food additives as well as many organic intermediates[132]. Pd and Pt metals supported on alumina are among the mostly used metal catalysts in the selective oxidation of alcohols. Such systems tend to deactivate quickly due to the strongly adsorbed products or by-products formed during the reaction. Section A of chapter 4, covers a thorough discussion of the reaction.

(ii) Oxidation of styrene

The styrene oxidation is of considerable academic and commercial interest for the synthesis of important products like benzaldehyde and phenyl acetaldehyde[133]. A detailed discussion of this reaction is given in section B of chapter 4.

(iii) Oxidation of cyclohexane

Oxidation of cyclohexane is one of the important bulk processes for the production of polyamide fibers and plastics such as Nylon-6 and Nylon-6,6.

Cyclohexanol and cyclohexanone (K/A oil) are the oxidation products of cyclohexane[134]. Industrially the process is carried out at 423-433 K in the presence of cobalt-based homogeneous catalyst[135]. The process is low in energy efficiency with plenty of by-products and waste. Section C of chapter 4 deals with a detailed discussion of the reaction.

(iv) Oxidation of ethylbenzene

Oxidation of ethylbenzene is an important reaction in chemical industry for the production of acetophenone as they are important intermediates for perfumes, drugs and pharmaceuticals[136]. Industrial production of this ketone is by Friedel-Craft's acylation using anhydrous aluminium chloride. A detailed description of this reaction is given in section D of chapter 4.

(v) Oxidative dehydrogenation of ethyl benzene

Oxidative dehydrogenation of ethylbenzene produces styrene as the major product, is one of the fundamental materials used to obtain synthetic rubbers and numerous thermoplastics. The industrial process for dehydrogenation of ethylbenzene to styrene employs an iron oxide promoted catalyst[137,138]. In chapter 5, we discuss the selective formation of styrene from ethylbenzene by dehydrogenation.

(vi) Oxidation of carbon monoxide

Oxidation of carbon monoxide to carbon dioxide is one of the widely studied environmentally friendly reactions[139,140]. There is an increasing demand to reduce emissions from vehicles equipped with Otto engines. It is a big challenge to find efficient catalysts that can convert the emissions immediately after a cold start. Chapter 6 covers a thorough discussion of the reaction.

1.7 Objectives of the Present Work

Mixed metal oxides possessing spinel structure exhibit interesting solid-state and catalytic properties. The spinel lattice imparts extra stability to the catalysts under various reaction conditions so that these systems have sustained activities for longer periods. These spinel oxides are cheap and their preparation method is simple. These attractive features of spinel oxides promoted us to prepare chromite spinels via co-precipitation method and investigate their catalytic properties for some oxidation reactions. The main objectives of the present work can be summarized as follows.

- To prepare chromites containing Mn, Fe, Co, Ni, Cu and Zn by homogeneous co-precipitation method and characterize these by various physico-chemical methods such as Powder XRD, EDX, BET surface area, FT-IR and TGA.
- To evaluate the surface acidity of the catalysts by temperature programmed desorption of ammonia.
- To study the vapour phase decomposition of cyclohexanol and cumene cracking reaction to correlate the results with surface acidity.
- To assess the catalytic activity of the systems for liquid phase oxidation of benzyl alcohol, styrene, cyclohexane and ethylbenzene.
- To study the catalytic activity of the systems for oxidative dehydrogenation of ethylbenzene to styrene, an industrially important product.
- Another important objective of the work is to evaluate the catalytic activity of the systems for the oxidation of carbon monoxide to carbon dioxide, an environmentally friendly reaction

References

[1] J. M. Thomas, Sci. Am. 266 (1992) 112

[2] H. Hattori, Mater. Chem. Phys. 18 (1988) 533

[3] H. Hattori, Stud.Surf.Sci.Catal. 78 (Heterog. Catal. Fine Chem.; 111) (1993) 35

[4] G. C. Bond, Heterogeneous Catalysis, Principles and applications, Clarendon Press, Oxford, 1987, Chap.4

[5] A. Holden, The nature of solids, Columbia Univ. Press, New York, 1965, Chapt XIV

[6] W. R. Moser, J. Happel, Catalytic chemistry of Solid-state Inorganics, Eds; Ann.N.Y.Acad.Sci; 272 (1976) 1

[7] P. Courty, C. Marcilly, Stud.Surf.Sci.Catal. 1 (1976) 119

[8] P. Courty, C. Marcilly, Stud.Surf.Sci.Catal. 1 (1983) 485

[9] K. Tanabe, M. Itoh, K. Morishige, H. Hattori, Stud.Surf.Sci.Catal. 1 (1976) 65

[10] M. Schraml-Marth, K. L. Walther, A. Wokaum, B. E. Handy, A. Baiker, J. Non-Cryst.solids. 143 (1992) 93

[11] T. Lopez, M. Azomozo, J. Gomez, J. Non-Cryst. Solids 147 (1992) 769

[12] A. Baiker, P. Dollenmeir, M. Blinski, A. Reller, Appl.Catal. A 35 (1987) 351

[13] A. Baiker, A. Wokaum, Naturwissenschaften, 76 (1989) 168

[14] Lessing P, Ceram. Bull. 68 (1989) 1002

[15] S. J. Yoon, S. H. Lee, K. H. Kim, K. S. Ahn, Mater. Chem. Phys. 73 (2002) 330

[16] Z. Wang, S. K. Saxena, P. Lazor, H. S. C. O. Neill, J. Phys. Chem. Solids 64 (2003) 425

[17] A. K. M. Zakaria, M. A. Asgar, F. U. Ahmed, S. M. Yunus, J. Magn. Magn. Mater 265 (2003) 311

[18] K. H. Janil, S. S. Laghate, H. H. Joshi, A. Banarjee, R. G. Kulkarni, J. Alloys

Compd. 326 (2001) 117

[19] H. Nayak, D. Bhatta, Thermochim. Acta. 389 (2002) 109

[20] J. Janas, T. Machej, J. Sloczynski, E. Wloch, Pol. J. Chem. 6 (1997) 79

[21] W. S. Epling, G. B. Hoflund, D. M. Minahan, Appl.Catal.A 183 (1999) 335

[22] J. M. C. Bueno, M. Gazzano, M. Goncalves, A. Vaccari, Appl. Catal. A 103 (1993) 69

[23] N. J. Jebarathinam, M. Eswaramoorthy, V. Krishnasamy, Appl. Catal. A 145 (1996) 57

[24] J. A. T. Antonio, N. Nava, M. Martinez, X.Bokhimi, Appl.Catal.A. 234 (2002) 137

[25] K. E. Jeong, D. C. Kim, S. K. Ihm, Catal. Today 87 (2003) 29

[26] K. Kaddouri, C. Mazzocchia, E. Tempesti, R. Nomen, J. sempere, J. Therm. Anal. 53 (1998) 533

[27] A. Sen, P. Pramanic, J. Mater. Synth. Process. 10 (2002) 3

[28] B. M. Abu-Zied, Colloids Surf. A 211(2002) 27

[29] I. Jendrzejewska, A. Waskowska, T. Mydlarz, J. Alloys Compd. 327 (2001) 73

[30] W. R. Moser, K. E.Connolly, J. Chem. Eng. 64 (1996) 239

[31] K. Du, J Xie, J. Wang, H. Zhang, J. Power Sources. 119 (2003) 130

[32] A.Verma, T. C. Goel, R. G. Mendiratta, R. G. Gupta, J. Magn. Magn. Mater. 192 (1999) 271

[33] E. E. Sileo, R. Rotelo, S. E. Jacobo, Physica B 320 (2002) 257

[34] W. H. Bragg, Philosophical Magazine 30 (1915) 305

[35] R. J. Hill, J. R. Craig, G. V.Gibbs, Phys.Chem. Miner. 4 (1979) 317

[36] H. Jagodzinski, "Crystallographic aspects of Non-stoichiometry of spinels", (Eds; A.Rabenau), North-Holland, Amsterdam, p.131

[37] E. J. W. Verwey, E. L. Heilmann, J. Chem. Phys. 15 (1947) 174

[38] T. F. W. Barth, E. Posankaj, Z. Krist, 84 (1952) 325

[39] R. K. Datta, K. Roy, Nature. 191 (1961) 169

[40] S. Hafner, F. Laves, Z. Krist. 115 (1961) 321

[41] E. J. W. Verwey, F. D. Boer, J. H. Van Santen, J. Chem. Phys. 16 (1948) 1091

[42] F. D. Boer, J. H. Van Santen, E. J. W. Verwey, J. Chem. Phys. 18 (1950) 1032

[43] F. C. Romeijn, Phil.Res.Rep. 8 (1953) 304

[44] J. D. Dunitz, L. E. Orgel, Phys. Chem. Solids. 3 (1957) 318

[45] D. S. Mc Clare, Phys. Chem. Solids, 3 (1957) 311

[46] G. Blasse, Philips Res. Repts. Supplement. 3 (1964) 40

[47] R. J. Rennard, W. L. Khel, J. Catal. 21 (1971) 282

[48] S. Berkman, C. Jacque Morrel, G. Egloff, Catalysis: Organic and Inorganic, New York 1940

[49] B. M. Abu-Zied, Appl. Catal. A 198 (2000) 139

[50] S. Ohyama, H. Kishida, Appl. Catal. A 172 (1998) 241

[51] B. J. Liaw, Y. Z. Chen, Appl. Catal. A 199 (2000) 196

[52] G. Xanthopoulo, G. Vekinis, Appl. Catal. A 199 (2000) 227

[53] M. Wojciechowska, J. haber, S. Lomicki, J. Stoch, J. Mol. Catal. A. 141 (1999) 155

[54] J. Sloczynski, J. Janas, T. Machej, J. Rynkowski, J. Stoch. Appl. Catal. B 24 (2000) 45

[55] A. M. E. Awad, B. M. Abu-Zied, J. Mol. Catal. A 176 (2001) 213

[56] B.Grzybowska, J. Sloczynski, R.Grabowski, K.Wcilo, A. Kozlowska, J. Stoch, J. Zielinski, J. Catal. 178 (1998) 687

[57] D. W. Flick, M. C. Huff, Appl. Catal. A 187 (1999) 13

[58] J. H. Uhm, M. Y. Shin, J. Zhidong, J.S.Chung, Appl. Catal. B 22 (1999) 293

[59] H.G. El- Shobaky, A. M. Ghozza, G. A. El- Shobaky, G. M. Mohamed, Colloids Surf. A. 152 (1999) 315

[60] B. M. Weckhuysen, R. A. Schoonheydt, Catal. Today 51 (1999) 215

[61] R. B. Fahim, M. I. Zaki, A. M. El- Roudi, A. M. A. Hassaan J. Colloid. Inter. Sci. 82 (1982) 163

[62] R. B. Fahim, R. M. Gabr, M.I. Zaki, S. A. A. Mansour, J. Colloid. Inter. Sci. 81 (1981) 468

[63] N. J. Jebarathinam, M. Eswaramoorthy, V. Krishnasamy, Appl. Catal. A 145 (1996) 57

[64] T. Mathew, S. Malwadkar, Shivanand Pai, C. P. Sebastian, C. V. Satyanarayana, V. V. Bokade, Catal.Lett. 91 (2003) 217

[65] I. Wang, W. H. Chang, R. J. Shiau, J. C. Wu, C. S. Chung, J. Catal 83 (1983) 438

[66] A. Krause, Sci.Pharm.38 (1970) 266

[67] J. A. T. Antonio, N. Nava, M. Martinez, X. Bokhimi, Appl. Catal. A 234 (2002) 137

[68] J. Sloczynski, J. Ziolkowski, B.Grzybowska, R.Grabowski, D. Jachewicz, K. Wcislo, I. Gengembre, J. Catal. 187 (1999) 410

[69] W.S. Epling, G. B. Hoflund, W.M. Hart, D.M. Minjan, J. Catal. 169 (1997) 438

[70] W.S. Epling, G. B. Hoflund, W. M. Hart, D. M. Minhan, J. Catal. 172 (1997) 13

[71] W. S. Epling, G. B. Hoflund, D. M. Minhan, J. Catal. 175 (1998) 175

[72] D. M. Minhan W. S. Epling, G. B. Hoflund, J. Catal. 179 (1998) 241

[73] W. S. Epling, G. B. Hoflund, D. M. Minhan, Appl.Catal. A 183 (1999) 335

[74] G. B. Hoflund W. S. Epling, D. M. Minhan, Catal. Today. 52 (1999) 99

[75] X. Sun, G. W. Roberts, Appl.Catal.A 247 (2003) 133

[76] A. M. Abu-Zied, A. M. El-Awad, J. Mol.Catal.A 176 (2001) 227

[77] B. M. Abu-Zied, Appl.Catal.A. 198 (2000) 139

[78] E. H. Shreiber, G. W. Roberts, Appl.Catal.B 26 (2000) 119

[79] W. F. Shanggun, Y. Teraoka, Kagawa, Appl. Catal. A 8 (1996) 217

[80] W. F. Shanggun, Y. Teraoka, Kagawa, Appl.Catal.16 (1998) 149

[81] J. Sloczynski, J. Janas, T. Machej, J. Rynkowski, J. Stoch, Appl. Catal. B 24 (2000) 45

[82] A. B. Lamb, W. C. Bray, J. C. Frazer, J. Ind. Eng. Chem. 12 (1920)

[83] S. Paldey, S. Gedevanishvili, W. Zhang, S. Rasouli, Appl. Catal. B 56 (2006) 241

[84] J. Ghose, K. S. R. C. Murthy, J. Catal. 162 (1996) 359

[85] K. S. R. C. Murthy, J. Ghose, J. Catal. 147 (1994) 171

[86] M. M. Rashad, O. A. Fouad, Mat.Chem and Phy. 94 (2005) 365

[87] D. Mehandjiev, A. Naydenov, G. Ivanov, Appl.Catal.A 206 (2001) 13

[88] P. Thormahlen, E. Fridell, N. Cruise, M. Skoglundh, A. Palmqvist, Appl. Catal. B 31(2001) 1

[89] K. Sreekumar, T. Jyothy, C. G. Ramankutty, B. S. Rao, S. Sugunan, React. Kinet. Catal. Lett. 70 (2000) 161

[90] K. Sreekumar, T. Mathew, S. P. Mirajkar, S. Sugunan, B.S. Rao, Appl. Catal. A 201(2000) 1

[91] K. Sreekumar, S. Sugunan, Appl. Catal. A 230 (2002) 245

[92] S. P. Ghorpade, V. S. Darshane, S. G. Dixit, Appl. Catal. A 166 (1998) 135

[93] V. R.Choudhary, S. K. Jana, V. S. Narkade, Catal.Commu. 2 (2001) 331

[94] H. Grabowska, W. Mista, J. Trawczynski, J. Wrzyszcz, M. Zawadzki, Appl.Catal.A 220 (2001) 207

[95] T. Yamaguchi, Y. Nakano, K. Tanabe, Chem Lett. (1976) 677

[96] J. Klinowshi, Chem.Rev.91 (1991) 1459

[97] B. K. Hodnett, J. B. Moffat, J.Catal. 88 (1984) 253

[98] S. Gomez, L. J. Garces, J. Villegas, R. Ghosh, O. Giraldo, S. L. Suib, J. Catal.

233 (2005) 60

[99] W. E. Farneth, R. J. Gorte, Chem. Rev. (1995) 615

[100] H. G. Karge, V. Dondur, J. Phys. Chem. 94 (1990) 765

[101] H. G. Karge, V. Dondur, J. Weitkamp, J. Phys. Chem. 95 (1991) 283

[102] M. C. Abella, A. P. Velasco, M. F. Goniez, J. B. Riyarola, Langmuir. 13 (1997) 2596

[103] H. Matsuhashi, H Motoj, K. Arata, Catal.Lett. 26 (1994) 325

[104] S. B. Sharma, B. I. Mayers, D. T. Chem, A. Dunisie, Appl.Catal. A 102 (1993) 253

[105] N. Y. Topsoc, K. Pederson, E. G. derouane, J. Catal.70 (1981) 41

[106] C. V. Hidalago, H. Itoh, T. Hattori, M. Niwa, Y. Hurakami, J. Catal. 85 (1984) 362

[107] W. Reschetilowski, K. P. Wendlandt, J. Chem. Soc. Faraday Trans. I, 85 (1989) 2941

[108] G. I. Kapustin, T. R. Brueva, A. L. Klyachko, B. Wiehterlova, Appl. Catal. 42 (1988) 239

[109] K. Chao, B. H. Chiou, C. C. Cho, S. Y. Jeng, Zeolites. 4 (1984) 2

[110] F. Arena, R. Dario, A. Parmaliana, Appl Catal. 170 (1988) 127

[111] M. Haneda, E. Joubert, M. Daturi, N. Bion, H. Hamada, Phys. Chem. Chem. Phys. 3 (2001) 1366

[112] M. Ilyas, Ikramullah, Catal. Commun. 5 (2004) 1

[113] M. A. Aramendia, V. Borau, C. Jimenez, J. M. Marinas, F. J. Romero, J. Catal.151 (1995) 44

[114] R. Jothirmalingam, B. Viswanathan, T. K.Varadarajan, Catal. Commun. 6(2005) 41

[115] S. Zhai, J. Zheng, J. Li, D. Wu, Y. Sun, F. Deng. Microporous Mesoporous Mater. 83 (2005) 10

[116] C. S. Narasimhan, C. S. Swami, Appl.Catal. A 2 (1982) 315

[117] M. P. Rosynek, R. J. Koprovski, G. N. Dellisante, J. Catal. 122 (1990) 80

[118] C. Bezouhanava, M. A. Al-Zihari, Catal.Lett.11 (1991) 245

[119] N. J. Jebarathinam, V. Krishnaswamy, "Catalysis:Modern Trends", (Eds., N.M.Gupta and D.K.Chakrabarthy) 1995,Narosa Publishing house, New Delhi, India

[120] N. J. Jebarathinam, V.Krishnaswamy; "Catalysis: Present and Future", (Eds., P.Kantha Rao and B.S.Benwal) Publication and Information Directorate, New Delhi, P-288

[121] M. V. Joshi, S. G. Oak, V. S. Darshane, "Catalysis: Modern Trends" (Eds., N. M. Gupta and D. K. Chakrabarthy) 1995, Narosa Publishing house, New Delhi, India

[122] T. Mishra, K. M. Parida, S. B. Rao, Appl.Catal.A 166 (1998) 115

[123] M. Hino, M. Kurashige, K. Arata, Catal. Commun.5 (2004) 107

[124] K. M. Parida, S. K. Samantaray, H. K. Mishra, J. Colloid Interface Sci. 216 (1999) 127

[125] K. Wada, K. Tada, N. Itayama, T. Kondo, T. Mitsudo, J. Catal. 228 (2004) 374

[126] M. S. Rana, S. K. Maity, J. Ancheyta, G. M. Dhar, T. S. R. P. Rao, Appl.Catal.A 258 (2004) 215

[127] A. C. B. D. Santos, W. B. Kover, A. C. Faro, Appl.Catal. A153 (1997) 83

[128] A. Gedeon, A. Lassoued, J. L. Bonardet, J. Fraissard, Microporous Mesoporous Mater. 44 (2001) 801

[129] S. P. Asprey, B. W. Wojciechowski, J.Catal.159 (1996) 246

[130] H. Onoda, H. Nariari, A. Moriwaki, H. Maki, I. Motooka, J.Mater.Chem. 12 (2002) 1754

[131] D. B. Dadyburjor, A. Bellare, J. Catal. 126 (1990) 261

[132] R. A. Sheldon. I.W.C.E. Arends, A. Dijksman, Catal.Today. 57 (2000) 157

[133] D. Guin, B. Baruwati, S. V. Manorama, J. Mol. Catal. A 242 (2005) 26

[134] L. Zhou, J. Xu, H. Miao, F. Wang, X. Li, Appl.Catal.A 292 (2005) 223

[135] K. Weissermel, H. J. Arpe, Industrial Organic Chemistry, second ed., VCH Press, Weinheim, 1993

[136] V. R. Choudhary, J. R. Indurkar, V. S. Narkade, R. Jha, J. Catal. 227 (2004) 257

[137] R. A. Shelden, Chem.Tech. (1991) 566

[138] R. A. Shelden, J. Mol. Catal. 107 (1996) 75

[139] P. Thormahlen, E. Fridell, N. Cruise, M. Skoglundh, A. Palmqvist Appl. Catal. B 31(2001) 1

[140] L. C. A. Oliveira, J. D. Fabris, R. R. V. A. Rios, W. N. Mussel, R. M. Lago, Appl. Catal. A 259 (2004) 253

****

CHAPTER 2

MATERIALS AND METHODS

Abstract

The development and preparation of heterogeneous catalysts are considered more as alchemy than science with the predominance of trial and error experiments. A minute change in conditions occurring during catalyst preparation can change the quality of catalysts. Hence they must be thoroughly characterized before use. In this chapter, the experimental methods used for the catalyst preparation, the characterization techniques and catalytic activity measurements are discussed in detail. The physico-chemical characterizations of the catalysts were done by techniques such as Powder XRD, EDX, FT-IR, SEM, TG-DTA analysis and BET surface are and pore volume measurements. The surface acidity of the catalysts was measured by TPD of ammonia and test reactions such as cumene cracking and cyclohexanol decomposition reactions to know acid site distribution. Liquid phase oxidation of benzyl alcohol, styrene, cyclohexane and ethylbenzene were performed over the prepared catalysts. Oxidative dehydrogenation of ethylbenzene and carbon monoxide oxidation reactions were carried out in gas phase to evaluate the activity of the prepared spinel catalysts.

2.1 Introduction

In heterogeneous catalysis, the reaction occurs at the surface. Catalysis and catalytic surfaces, hence, need to be characterized by reference to their physical properties and by their actual performance as a catalyst. The most important physical properties are those relating to the surface because catalyst performance is determined by surface parameters. Any characterization of a catalyst must start with knowledge of the chemical composition of the same. We can broadly divide for convenience characterization of a catalyst into two categories. These are related to the structural and textural properties of the catalyst. The structural characterization invariably means the geometry, the long-range order and so on of a solid. For condensed materials like perovskites and spinels structural properties provide a wealth of information about the catalyst. In oxide catalysts, the surface area is largely contained within a porous structure, which often provides the rate-determining step in a reaction. The properties associated with such a porous catalyst or influenced by the porous nature of a support material are broadly termed as the texture of a catalyst.

Numerous instrumental techniques are known today for the characterization of solid acid catalysts viz. EDX, XRD, TGA/DTA, FT-IR, SEM, TPD and TPR to name a few. The physical characterization provides an insight into the structure of different species and its interaction while chemical characterization leads to an insight into reactivity for the application of the catalysts in an industrial point of view.

2.2 Catalyst Preparation

2.2.1 Chemicals for catalyst preparation

The chemicals used for the preparation of catalysts are listed below in table 2.1.

Table 2.1: Chemicals used for the preparation of catalysts

Sl. No.	Chemicals	Company
1.	$Cr(NO_3)_3.9H_2O$	Merck
2.	$Mn(NO_3)_2.4H_2O$	Merck
3.	$Fe(NO_3)_3.9H_2O$	Merck
4.	$Co(NO_3)_2.6H_2O$	Merck
5.	$Ni(NO_3)_2.6H_2O$	Merck
6.	$Cu(NO_3)_2.3H_2O$	Merck
7.	$Zn(NO_3)_2.6H_2O$	Merck
8.	Ammonia solution	Qualigens fine chemicals

2.2.2 Preparation of different compositions of chromites

Five series of spinel systems with compositions $CuCr_{2-x}Fe_xO_4$ (x = 0.5, 1.0, 1.5, 2.0) and $Cu_{1-x}M_xCr_2O_4$ (M is a metal cation like Co, Ni, Mn or Zn and x= 0, 0.25, 0.5, 0.75 and 1.0) were prepared by co-precipitation method[1-3]. Initially calculated amounts of each metal nitrate were dissolved in distilled water and the precipitation of the hydroxides was carried out at a controlled pH of 6.5-8 using 15% ammonia solution at a temperature of 70-80^{0}C. The precipitate was maintained at this temperature for two hours and aged for one day. The precipitate was filtered and washed with distilled water to remove nitrate ions. The compounds were dried in an air oven at 80^{0}C for 24 hours and then calcined at 650^{0}C for 8 hours. The formation of single spinel phase was ascertained by XRD.

2.2.3 Catalysts Prepared

The catalysts prepared for the present work with its symbols are listed in table 2.2.

Table 2.2: Notation of the catalysts prepared

Sl. No.	Catalyst Composition	Catalyst labeling
1.	$CuCr_2O_4$	CCr
2.	$CuFe_{0.5}Cr_{1.5}O_4$	CFCr-1
3.	$CuFeCrO_4$	CFCr-2
4.	$CuFe_{1.5}Cr_{0.5}O_4$	CFCr-3
5.	$CuFe_2O_4$	CF
6.	$Cu_{0.75}Mn_{0.25}Cr_2O_4$	CMCr-1
7.	$Cu_{0.5}Mn_{0.5}Cr_2O_4$	CMCr-2
8.	$Cu_{0.25}Mn_{0.75}Cr_2O_4$	CMCr-3
9.	$MnCr_2O_4$	MCr
10.	$Cu_{0.75}Co_{0.25}Cr_2O_4$	CCoCr-1
11.	$Cu_{0.5}Co_{0.5}Cr_2O_4$	CCoCr-2
12.	$Cu_{0.25}Co_{0.75}Cr_2O_4$	CCoCr-3
13.	$CoCr_2O_4$	CoCr
14.	$Cu_{0.75}Ni_{0.25}Cr_2O_4$	CNCr-1
15.	$Cu_{0.5}Ni_{0.5}Cr_2O_4$	CNCr-2
16.	$Cu_{0.25}Ni_{0.75}Cr_2O_4$	CNCr-3
17.	$NiCr_2O_4$	NCr
18.	$Cu_{0.75}Zn_{0.25}Cr_2O_4$	CZCr-1
19.	$Cu_{0.5}Zn_{0.5}Cr_2O_4$	CZCr-2
20.	$Cu_{0.25}Zn_{0.75}Cr_2O_4$	CZCr-3
21.	$ZnCr_2O_4$	ZCr

2.3 Catalyst Characterization

To investigate the fundamental relations between the state of a catalyst and its catalytic properties several approaches can be adopted. By using the appropriate combination of analysis techniques, the desired characterization on the atomic as well as bulk scale is certainly possible. Various techniques adopted for the characterization are presented in table 2.3.

Table 2.3: Techniques applied for catalysts characterization

Technique	In	Out	Information
X-ray Diffraction	X-ray	X-ray	Bulk structure, Particle Size
Energy Dispersive X-ray	e-	X-ray	Composition
Infrared Spectroscopy	Photon	Photon	Molecular Vibrations
Scanning Electron Microscopy	e-	e-	Morphology
Temperature Programmed Desorption	Heat + Gas	Gas	Mechanism of Surface and Bulk Reactions

Chemicals used for the physico-chemical characterization of catalysts are listed in table 2.4.

Table 2.4: Chemicals used for physico-chemical characterizations

Sl. No.	Chemicals	Company
1.	Conc. H_2SO_4	s.d Fine Chem. Ltd.
2.	Sodium hydroxide	Merck
3.	Cyclohexanol	Central Drug House P. Ltd.
4.	Cumene	Sigma Aldrich P. Ltd.
5.	Liquid Nitrogen	STIC, CUSAT
6.	Potassium bromide	Merck

2.3.1 Powder X-Ray Diffraction

Powder X-ray Diffraction (XRD) is one of the primary techniques used by solid state chemists to characterize materials[4,5]. Powder XRD can provide information about crystalline structure in a sample even when the crystallite size is too small for single crystal X-ray diffraction, purity of the substance, transition to different phases, lattice constants and presence of foreign atoms in crystal lattice. The XRD method involves the interaction between monochromatic X-rays (like Cu K_α or Mo K_α) with family planes (identified by a system of Miller indices, hkl) in the polycrystalline materials. For every set of crystal planes, by chance, one or more crystals will be in the correct orientation to give the correct Bragg angle to satisfy the Bragg's equation,

$$n\lambda = 2d \sin\theta$$

where λ is the X-ray wave length, n is an integer called order of reflection, d is the inter planar distance and θ is the scattering angle.

The mean crystallite size of a material can also be determined from the broadening of an X-ray diffraction peak, which is inversely proportional to crystallite size and this can be achieved by following the Scherrer method using the formula,

$$t = 0.9\lambda / \beta\cos\theta$$

This is derived from Bragg's equation. 't' is the thickness of the crystal and β is the FWHM (half the width of the peak with maximum intensity).

The XRD patterns of the catalyst samples were taken using Rigaku D-max C X-ray diffractometer using Ni filtered Cu K_α radiation source (λ=1.5406A^0) and a movable detector, which measures the intensity of diffracted radiation as a function of 2θ are the main parts of the instrument.

2.3.2 Energy Dispersive X-Ray Analysis

Energy Dispersive X-ray analysis (EDX), also referred to as EDS or EDAX analysis is a technique used for identifying the elemental composition of the specimen, or an area of interest thereof[6]. The EDX analysis system works as an integrated feature of a scanning electron microscope (SEM), and cannot operate on its own without the latter.

During EDX analysis, the specimen is bombarded with an electron beam inside the scanning electron microscope. The bombarding electrons collide with the specimen atoms' own electrons, knocking some of them off in the process. A position vacated by an ejected inner shell electron is eventually occupied by a higher-energy electron from an outer shell. To be able to do so, however, the transferring outer electron must give up some of its energy by emitting an X-ray. The amount of energy released by the transferring electron depends on which shell it is transferring from, as well as which shell it is transferring to. Furthermore, the atom of every element releases X-rays with unique amounts of energy during the transferring process. Thus, by measuring the amounts of energy present in the X-rays being released by a specimen during electron beam bombardment, the identity of the atom from which the X-ray was emitted can be established. The output of an EDX analysis is an EDX spectrum. The EDX spectrum is just a plot of how frequently an X-ray is received for each energy level. An EDX spectrum normally displays peaks corresponding to the energy levels for which the most X-rays had been received. Each of these peaks is unique to an atom, and therefore corresponds to a single element. The higher a peak in a spectrum, the more concentrated the element is in the specimen.

The chemical compositions of catalysts were obtained from Stereoscan 440 Cambridge, UK energy dispersive X-ray analyzer used in conjunction with SEM.

2.3.3 BET Surface Area and Pore Volume

Stephen Brunauer, Paul Hugh Emmett and Edward Teller[7] developed the famous BET equation for the determination of the surface area of a solid in 1938. The concept of the theory is an extension of the Langmuir theory, which is for monolayer molecular adsorption, to multilayer adsorption with the following hypotheses: (a) gas molecules physically adsorb on a solid in layers infinitely; (b) there is no interaction between each adsorption layer; and (c) the Langmuir theory can be applied to each layer. The resulting BET equation is expressed by

$$p/V\,(p_0 - p) = 1/V_mC + (C-1)\,p/CV_m\,p_0)$$

p and p_0 are the equilibrium and the saturation pressure of adsorbates at the temperature of adsorption, V is the adsorbed gas quantity, and V_m is the monolayer adsorbed gas quantity. *C* is the BET constant, which is expressed by:

$$C = \exp^{(E1\text{-}EL)/RT}$$

E_1 is the heat of adsorption for the first layer, and E_L is that for the second and higher layers and is equal to the heat of liquefaction. BET plot is an adsorption isotherm and can be plotted as a straight line with $1/v\,[(p_0/p) - 1]$ on the y-axis and p/p_0 on the x-axis according to experimental results. The linear relationship of this equation is maintained only in the range of $0.05 < p/p_0 < 0.35$. The value of the slope and the y-intercept of the line are used to calculate the monolayer adsorbed gas quantity V_m and the BET constant C. The BET method is widely used in surface science for the calculation of surface areas of solids by physical adsorption of gas molecules. A total surface area S_{total} and a specific surface area S are evaluated by the following equations:

$$S_{total} = v_m Ns/M$$

$$S = S_{total}/a$$

N: Avogadro's number,
s: adsorption cross section,
M: molecular weight of adsorbate
a: weight of sample solid

For example, activated carbon, which is a strong adsorbate and usually has an adsorption cross section *s* of 0.16 nm^2 for nitrogen adsorption at liquid nitrogen temperature, is revealed from experimental data to have a large surface area around 3000 m^2 g^{-1}. Moreover, in the field of solid catalysis, the surface area of catalysts is an important factor in catalytic activity. Porous inorganic materials such as mesoporous silica and layered clay minerals have high surface areas of several hundred m^2g^{-1} calculated by the BET method, indicating the possibility of application for efficient catalytic materials.

BET surface areas and pore volume values of the catalysts were acquired by nitrogen adsorption and subsequent desorption at liquid nitrogen temperature (77 K) with a Micromeritics Gemini 2360 surface area analyzer. The catalyst was degassed at 623 K for 3 h in a Flow Prep-060 degas chamber prior to analysis.

2.3.4 Thermal Analysis

Thermal analysis (TG/DTA/DTG) includes a group of techniques in which specific physical properties of a material are measured as a function of temperature. Thermo gravimetric analysis, (TGA) in which the catalyst sample is subjected to a controlled heating to higher temperatures at a specified heating rate is a well-established technique in heterogeneous catalysis[8]. It finds widest application in the determination of drying range, calcinations temperature, phase composition, percentage weight loss and stability limits of a catalyst. In TGA, the loss of weight of a sample is being continuously recorded over a period of time under controlled heating rate. Changes in weight are due to the rupture and/or formation of various physical and chemical bonds at elevated temperatures, which lead to the evolution of volatile products or formation of heavier reaction products. From the thermogram, when we plot weight against temperature, information about dehydration, decomposition and various forms or products at various temperatures can be obtained. The first derivative of the thermogram (DTG) gives a better understanding of the weight loss and can also be used to determine the thermal stability of the samples.

In differential thermal analysis (DTA), the difference in temperature between the sample and a thermally inert reference material is measured as a function of temperature usually the sample temperature. Any transition that the sample undergoes results in liberation or absorption of energy by the sample with a corresponding deviation of its temperature from that of the reference. A plot of the differential temperature, ΔT versus the programmed temperature, T, indicates the transition temperatures and whether the transition is exothermic or endothermic. When an endothermic change occurs, the sample temperature lags behind the reference temperature because of the heat in the sample. Exothermic behavior is associated with the decrease in enthalpy of a phase or a chemical system. DTA and thermo gravimetric analyses are often run simultaneously on a single sample.

TGA/DTG/DTA were collected on a Perkin Elmer Pyris Diamond thermo gravimetric/differential thermal analyzer under nitrogen atmosphere at heating rate of 10°C/ min from room temperature to 800°C with samples mounted on an alumina sample holder.

2.3.5 Scanning Electron Microscopy

Scanning electron microscopy is used for inspecting topographies of specimens at very high magnifications using a piece of equipment called the scanning electron microscope[9]. SEM magnifications can go to more than 300,000 X but most semiconductor manufacturing applications require magnifications of less than 3,000 X only. SEM inspection is often used in the analysis of die/package cracks and fracture surfaces; bond failures, and physical defects on the die or package surface.

During SEM inspection, a beam of electrons is focused on a spot volume of the specimen, resulting in the transfer of energy to the spot. These bombarding electrons also referred to as primary electrons, dislodge electrons from the specimen itself. The dislodged electrons, also known as secondary electrons, are attracted and collected by a positively biased grid or detector, and then translated into a signal. To produce the SEM image, the electron beam is swept across the area being inspected, producing many such signals. These signals are then amplified, analyzed, and translated into images of the topography being inspected. Finally, the image is shown on a CRT. The energy of the primary electrons determines the quantity of secondary electrons collected during inspection. The emission of secondary electrons from the specimen increases as the energy of the primary electron beam increases, until a certain limit is reached. Beyond this limit, the collected secondary electrons diminish as the energy of the primary beam is increased, because the primary beam is already activating electrons deep below the surface of the specimen. Electrons coming from such depths usually recombine before reaching the surface for emission. Aside from secondary electrons, the primary electron beam results in the emission of backscattered (or reflected) electrons from the specimen. Backscattered electrons possess more energy than secondary electrons, and have a definite direction. As such, they cannot be collected by a secondary electron detector, unless the detector is directly in their path of travel. All emissions above 50 eV are considered to be backscattered electrons.

Backscattered electron imaging is useful in distinguishing one material from another, since the yield of the collected backscattered electrons increases monotonically with the specimen's atomic number. Backscatter imaging can distinguish elements with atomic number differences of at least 3, i.e., materials with atomic number differences of at least 3 would appear with good contrast on the image. For example, inspecting the remaining Au on an Al bond pad after its Au ball bond has lifted off would be easier using backscatter imaging, since the Au islets would stand out from the Al background. The SEM pictures of the catalysts were recorded on a Stereoscan 440 Cambridge, UK SEM analyzer used in conjunction with energy dispersive X-ray analyzer.

2.3.6 Fourier Transform Infrared Spectroscopy

FTIR (Fourier Transform Infrared) Spectroscopy is an analytical technique that provides information about the chemical bonding or molecular structure of materials, whether organic or inorganic[10]. The technique works on the fact that bonds and groups of bonds vibrate at characteristic frequencies. A molecule that is exposed to infrared rays absorbs infrared energy at frequencies, which are characteristic to that molecule. During FTIR analysis, a spot on the specimen is subjected to a modulated IR beam. The specimen's transmittance and reflectance of the infrared rays at different frequencies is translated into an IR absorption plot consisting of reverse peaks. The resulting FTIR spectral pattern is then analyzed and matched with known signatures of identified materials in the FTIR library. FTIR spectroscopy does not require a vacuum, since neither oxygen nor nitrogen absorbs infrared rays. FTIR analysis can be applied to minute quantities of materials, whether solid, liquid, or gaseous. When the library of FTIR spectral patterns does not provide an acceptable match, individual peaks in the FTIR plot may be used to yield partial information about the specimen. Single fibers or particles are sufficient enough for material identification through FTIR analysis. Organic contaminants in solvents may also be analyzed by first separating the mixture into its components by gas chromatography, and then analyzing each component by FTIR.

FT-IR spectra were recorded with KBr pellets on AVATAR 370 Thermo-Nicolet FT-IR spectrometer in the range 400-4000 cm^{-1}.

2.3.7. Temperature Programmed Desorption-NH_3

Temperature programmed desorption of basic molecules such as ammonia, pyridine, n-butyl amine etc. is a well-known method for the determination of acidity as well as acid strength of solid heterogeneous catalysts. In this, an inert gas is passed over a catalyst bed pre adsorbed with the base, while the temperature is increased. A TPD profile is obtained by monitoring the gases, which are desorbed from the surface as the temperature is increased. The temperature of desorption is an indication of the strength of binding of the adsorbate[11].

Acidity measurements were performed by temperature programmed desorption of ammonia (TPD-NH_3) using a conventional flow apparatus. In a typical experiment, about 500 mg of catalyst was activated at 773 K for 1 h and kept in a tube. The sample was pretreated by passage of nitrogen at 573 K for 1 h. Subsequently it was cooled to room temperature and saturated with pure anhydrous ammonia gas and the system was allowed to attain equilibrium. After 30 min, the excess and physisorbed ammonia was subsequently flushed with flowing nitrogen. TPD analysis was then carried out by desorption of ammonia from 373 K to 873 K at a heating rate of 20 K/min in nitrogen atmosphere. The amount of ammonia desorbed was calculated by volumetrically.

2.3.8. Cyclohexanol Decomposition

Alcohols are amphoteric in nature and this permits its interaction with both acidic and basic centers. As a result, dehydration and dehydrogenation are catalyzed by the oxide system resulting in the formation of cyclohexene and cyclohexanone respectively[12-14]. Alcohol decomposition has been widely studied because it is a simple model reaction to determine the functionality of an oxide catalyst. Decomposition of cyclohexanol and that of isopropanol are the most widely studied reactions in this category. Dehydration activity is linked to the acidic property and dehydrogenation activity to the combined effect of acidic and basic properties of the catalyst. Studies on cyclohexanol decomposition on spinel oxide have been reported[15-18]. Bezouhanova and Al-Zihari[19] have recommended the dehydration of cyclohexanol conversion as a simple test to measure the Bronsted acid sites in a metal oxide. Cyclohexanol dehydrogenation was more favorable than dehydration of cyclohexanol on cerium ion incorporated OMS-2 catalyst[20].

The vapour-phase cyclohexanol decomposition experiments were performed at atmospheric pressure in a fixed bed, vertical, down flow, quartz reactor of 2 cm I.D and 30 cm length placed inside a double zone furnace. 0.5 g of the activated catalyst was positioned in the center of the reactor in such a way that the catalyst is sandwiched between the layers of inert silica beads. The upper portion of the reactor served as a vapouriser cum pre-heater. A syringe pump fed the liquid reactant mixture and temperature measurements were done using a temperature controller and a Cr-Al thermocouple placed at the center of the catalyst bed. The products of the reaction were analyzed by a Chemito 8610 G C with Flame Ionization Detector using FFAP column.

2.3.9. Cumene Cracking

Cumene cracking is one of the test reactions applied in heterogeneous catalysis for the acidity measurement of catalysts[21-23]. Generally cumene conversion gives dealkylation as well as dehydrogenation products on acidic catalysts. α-methyl styrene, the dehydrogenation product is attributed to the Lewis acidity of the catalyst and then dealkylation product benzene is formed by the Bronsted acid sites in the catalyst. Cracked products like ethylbenzene, styrene and toluene were also formed. Parida *et al* studied the cumene cracking on sulphated TiO_2-SiO_2 mixed oxide catalyst and found a good correlation between the cumene cracking and acidity of the catalysts[24].

Cumene cracking in vapour phase was conducted in a tubular, down flow reactor at atmospheric pressure as described earlier. Prior to the reaction, the catalyst was pretreated at 773 K for 2 h. The reaction products were collected and analyzed with a gas chromatograph equipped with a flame ionization detector.

2.4 Catalytic Activity Studies

The reactions studied for the present work can be put under two categories as liquid phase reactions and vapour phase reactions. Under the liquid phase reactions, oxidation of benzyl alcohol, styrene, cyclohexane and ethylbenzene and under vapour phase reactions, oxidative dehydrogenation of ethylbenzene and oxidation of carbon monoxide were carried out. The chemicals used for the catalytic activity studies of prepared catalysts are listed below in table 2.5 along with the company supplied.

Table 2.5: Chemicals used for catalytic activity study

Sl. No.	Chemicals	Company
1.	Benzyl alcohol	s.d Fine Chem. Ltd.
2.	Styrene	Lancaster
3.	Cyclohexane	Merck
4.	Ethylbenzene	s.d Fine Chem. Ltd.
5.	Hydrogen peroxide	s.d Fine Chem. Ltd.
6.	TBHP	Sigma Aldrich Pvt.Ltd
7.	Acetonitrile	Qualigens Fine Chemicals
8.	Dichloromethane	Qualigens Fine Chemicals

2.4.1 Liquid Phase Oxidation of Benzyl Alcohol, Styrene, Cyclohexane and Ethylbenzene

The liquid-phase oxidation of aromatics was carried out in a 50 ml round bottom flask. The flask connected with a water condenser was immersed in an oil bath in order to make the working temperature constant. In a typical run, catalyst, and substrate were added to the solvent. The oxidant, 30% H_2O_2 / 70% TBHP was added to the system after attaining the reaction temperature. The reaction mixture was stirred magnetically for the indicated reaction time. Then, the reaction products were analyzed by gas chromatography (flame ionization detector and with appropriate column). Conversion and selectivity were calculated based on the relative area of each of authentic samples with standard ones and the products were identified by GC-MS.

2.4.2 Oxidative Dehydrogenation of Ethylbenzene

The oxidative dehydrogenation of ethylbenzene was performed at atmospheric pressure in a fixed bed, vertical, down flow, quartz reactor of 2 cm I.D and 30 cm length placed inside a double zone furnace. Reaction was performed in presence of air as oxidant. 0.5 g of the activated catalyst was positioned in the center of the reactor in such a way that the catalyst is sandwiched between the layers of inert silica beads. The upper portion of the reactor served as a vapouriser cum pre-heater. A syringe pump fed the liquid reactant mixture and temperature measurements were done using a temperature controller and a Cr-Al thermocouple placed at the center of the catalyst bed. The mass balance was noted wherever necessary. The hydrocarbon products were collected to ice traps and analyzed with a gas chromatograph equipped with a flame ionization detector.

2.4.3 Oxidation of Carbon Monoxide

The carbon monoxide oxidation was performed in a glass micro reactor. About 0.5 g of powder sample was loaded to the reactor previously loaded with glass balls, which helped to minimize developing of inlet gas pressure. The reactor was fixed in the furnace and introduced nitrogen, oxygen and carbon monoxide of composition 1% carbon monoxide, 5% oxygen and the rest nitrogen (using control valves or Mass flow controllers, MFC). An outlet flow of ~15000 ml/hr was set so as to get the space velocity factor of 30 h^{-1}. Space velocity is the gas flow in litre per hour per volume of the catalyst. The experimental set up for the CO oxidation is given in figure 2.1.

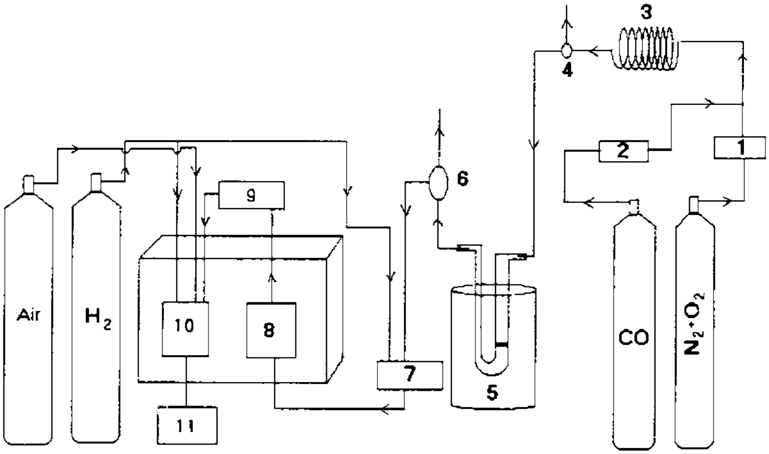

Figure 2.1. Flow diagram of the reactor and the analytical set up

1. Mass flow controller for N_2-O_2 mixture gas
2. Mass flow controller for CO
3. Loop for mixing gases
4. Sampling point for inlet analysis
5. U-Tube glass reactor in the electric furnace with PID controller
6. Outlet for measuring total gas flow
7. Gas Sample Injector
8. GC- column
9. Methanator with Ni based methenation catalyst
10. GC-FID detector
11. Data processor

The furnace temperature was raised slowly through the required temperature profile and analyzed the outlet gas sample for CO and CO_2 using GC with FID detector and Pouropack column. After separation at the column, CO and CO_2 were detected with FID by converting them to methane by passing through a Ni based catalyst kept at 400°C. From the amount of CO and CO_2, percentage conversion was calculated. Simultaneously, flow at different temperatures could also be measured through the valves provided.

Analysis conditions of various reactions are presented in table 2.6

Table 2.6: GC analysis conditions of various reactions

Reaction	Column	Temperature (°C)		
		Injector	Detector	Column - oven temperature
Cumene	SC-30	250	250	70-2 -10-280
Cyclohexanol	FFAP	175	200	60-2-10-250
Benzyl alcohol	Capillary BP-1	250	250	80-2-10-280
Styrene	FFAP	250	250	80-2-10-280
Cyclohexane	FFAP	175	200	60-2-10 -250
Ethylbenzene	Capillary BP-1	250	250	70-2-10-280
ODH of Ethylbenzene	FFAP	170	250	70-5-10-280
Carbon monoxide	Pouropack	-	-	-

References

[1] J. Sloczynski, J. Janas, T. Machej, J. Rynkowski, J. Stoch; Appl. Catal. B 24 (2000) 45

[2] N. J. Jebarathinam, M. Eswaramoorthy, V. Krishnasamy; Appl. Catal. A 145

(1996) 57

[3] K. E. Jeong, D. C. Kim, S. K. Ihm; Catal. Today. 87 (2003) 29

[4] C. Suryanarayana; M.G. Norton, X-ray Diffraction: A Practical Approach, New York (1998)

[5] C. whiston; "X-Ray Methods", (Eds., F.E.Prichard), ACOL, Thames Polytech, London, 1991

[6] J. Matta, D. Courcot, E. Abi-Aad, A. Aboukais; Chem. Mater. 14 (2002) 4118.

[7] S. Brunauer, P. H. Emmett, E. Teller; J. Am. Chem. Soc. 60 (1938) 309

[8] H. H. Willlared, L. L. Merrit Jr., J.A. Dean, F.A. Settle Jr., Instrumental Methods of Analysis 7th edn, CBS Publishers, New Delhi (1986).

[9] J. W. Niemantsverdriet; Spectroscopy in Catalysis: An Introduction, VCH Publisher, New York (1995) 165

[10] J.W. Niemantsverdriet; Spectroscopy in Catalysis: An Introduction, VCH Publisher, New York (1995) 200

[11] M. Bhaiyalakshmi, K. Shanmugapriya, M. Palanichamy, B. Arabindoo, V. Murugesan; Appl. Catal. A 267 (2004) 77

[12] M. Haneda, E. Joubert, M. Daturi, N. Bion, H. Hamada; Phys.Chem.Chem.Phys. 3(2001) 1366

[13] M. Ilyas, Ikramullah; Catal. Commun. 5(2004) 1

[14] M. A. Aramendia, V. Borau, C. Jimenez, J. M. Marinas, F.J. Romero; J. Catal.151 (1995) 44

[15] J. Babu, K. R. Sunajadevi, S. Sugunan; Indian J. Chem., Sect A 43 (2004) 473

[16] C. G. Ramankutty, S. Sugunan, B. Thomas; J. Mol. Catal. A 187 (2002) 105

[17] N. J. Jabarathinam, V. Krishnaswamy, P. Kanta Rao, R. S. Beniwal (Eds), Catalysis: Present and Future, Publication and information Directorate and Wiley Eastern Ltd., New Delhi, 1995, P-288

[18] M. V. Joshi, S. G. Oak, V. S. Darshane; "Catalysis:Modern Trends" (Eds., N. M. Gupta and D. K. Chakrabarthy)1995, Narosa Publishing house, New Delhi, India p-275

[19] C. Bezouhanava, M. A. Al-Zihari; Catal.Lett. 11(1991) 245

[20] R. Jothirmalingam, B.Viswanathan, T. K. Varadarajan; Catal. Commun. 6 (2005) 41

[21] T. Mishra, K. M. Parida, S. B. Rao; Appl.Catal.A 166 (1998) 115

[22] M. Hino, M. Kurashige, K. Arata; Catal. Commun.5 (2004) 107

[23] K. Wada, K. Tada, N. Itayama, T. Kondo, T. Mitsudo; J. Catal. 228 (2004) 374

[24] K. M. Parida, S. K. Samantaray, H. K. Mishra; J. Colloid Interface Sci.216 (1999) 127

****

CHAPTER 3

CHARACTERIZATION AND SURFACE PROPERTIES

Abstract

Characterization of catalyst surfaces plays an important role since the solid surface is a predominant factor in heterogeneous catalysis. The physico-chemical characterization of transition metal substituted copper chromite spinel catalysts were carried out and the results obtained are presented in this chapter. A detailed investigation was performed by different techniques such as powder X-ray diffraction analysis, Energy dispersive X-ray analysis, Surface area and pore volume measurements, TG-DTA analysis, FT-IR spectroscopy and Scanning electron microscopy. The surface acidity of the catalysts were evaluated by Temperature programmed desorption of ammonia. Test reactions such as cumene cracking and cyclohexanol decomposition reactions were carried out over the prepared catalysts to get an insight to the nature of surface acid site distribution.

3.1. Introduction

Catalysis is a mature field with extensive practical applications in today's society. Characterization of catalyst surface is of major importance in modern catalytic research since the solid surfaces play the decisive role in heterogeneous catalysis. Of particular importance are the composition, i.e., the distribution of elements in the catalyst, and the detection of phases and surface compounds. Also of interest are differences in composition between catalyst volume and catalyst surface, as well as interactions between active components and support materials and between the active components themselves. Relationships between the structures of material and the catalyst activity require high-resolution investigation of the microstructure of the catalyst. Catalyst surfaces, surface compounds, metals dispersed on supports and adsorbed molecules are investigated by X-ray techniques, electron and nuclear spectroscopes, analytical tools and other methods. Spinel chromites containing transition metals are attractive for many applications. This chapter deals with the results of various instrumental techniques used to characterize the spinels.

3.1.1 Powder X-ray Diffraction

Powder X-Ray Diffraction is an important tool for the determination of crystalline structure, phase, purity and the presence of foreign atom in the crystal lattice. Powder X-ray diffraction patterns were collected for all catalysts after calcination at the temperature of 650°C. The corresponding diffraction patterns of the spinel oxides are presented in figure 3.1.

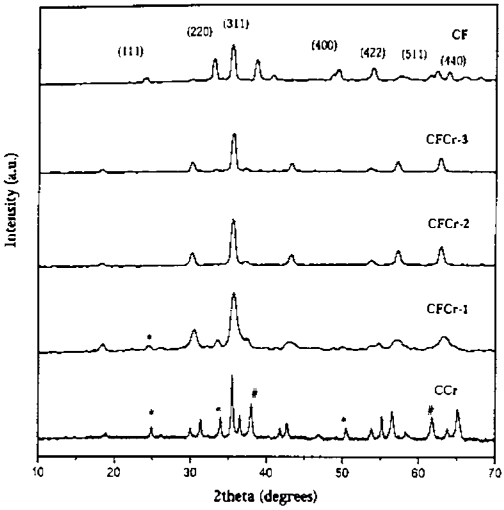
(111)
(220)
(311)
(400)
(422)
(511)
(440)
CF
CFCr-3
CFCr-2
CFCr-1
CCr
*
#
Intensity (a.u.)
10
20
30
40
50
60
70
2theta (degrees)

(a)

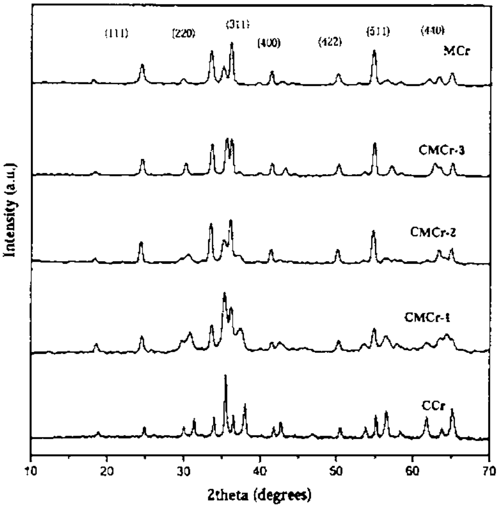
(111)
(220)
(311)
(400)
(422)
(511)
(440)
MCr
CMCr-3
CMCr-2
CMCr-1
CCr
Intensity (a.u.)
10
20
30
40
50
60
70
2theta (degrees)

(b)

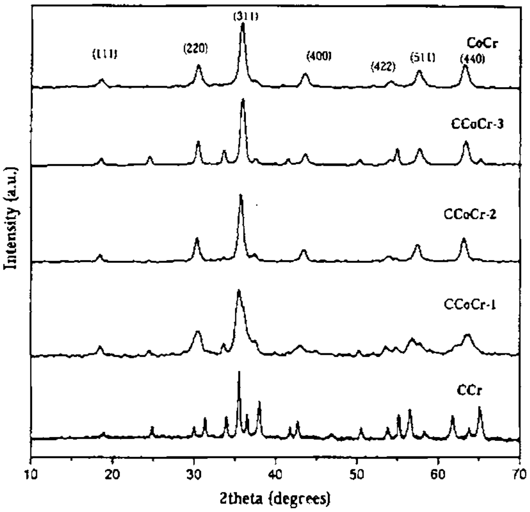
(111)
(220)
(311)
(400)
(422)
(511)
(440)
CoCr
CCoCr-3
CCoCr-2
CCoCr-1
CCr
Intensity (a.u.)
10
20
30
40
50
60
70
2theta (degrees)

(c)

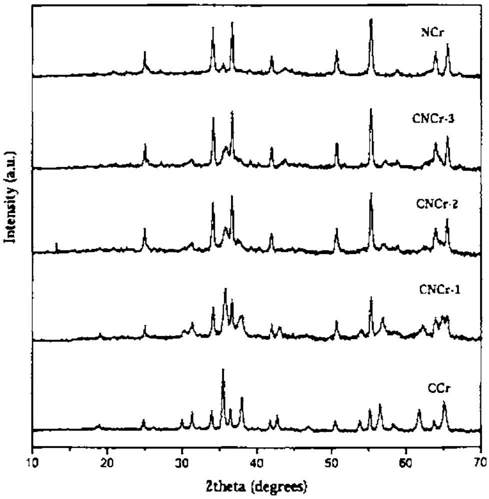
NCr
CNCr-3
CNCr-2
CNCr-1
CCr
Intensity (a.u.)
10
20
30
40
50
60
70
2theta (degrees)

(d)

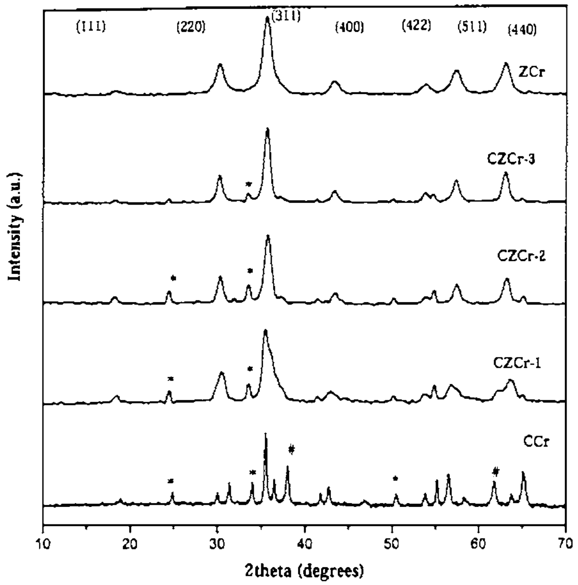

(e)

Figure 3.1: XRD Profiles of: - (a) $CuCr_{2-x}Fe_xCr_2O_4$ series, (b) $Cu_{1-x}Mn_xCr_2O_4$ series, (c) $Cu_{1-x}Co_xCr_2O_4$ series, (d) $Cu_{1-x}Ni_xCr_2O_4$ series, (e) $Cu_{1-x}Zn_xCr_2O_2$ series

From XRD patterns, we can notice that the peaks are sharper and are crystalline in nature. The theoretical and experimental d_{hkl} values for simple spinels are well coordinated. Interestingly, it was also observed that the mixed chromites of Cr-Fe, Cr-Mn, Cr-Co, Cr-Ni and Cr-Zn series gave much identical XRD patterns with those of the corresponding simple chromites. In the systems studied, the compositional differences are due to different proportion of the atoms Fe, Mn, Co, Ni and Zn in pure $CuCr_2O_4$. These atoms have close atomic numbers and so, much alike XRD patterns. In some cases, the peaks corresponding to the pure oxides are also observed. Star (*) indicates the peak corresponding to the chromia phase.

The average crystallite size of the samples can be determined from the Scherrer equation, $t = 0.9\ \lambda / \beta \cos\theta$; where, t - average particle size, λ- wavelength of the X-ray used, θ - glancing angle and β- FWHM (half the width of the peak with maximum intensity). The crystallite size of different series of chromite spinels is presented in table 3.1.

Table 3.1: Crystallite size calculated from XRD

Catalyst	Crystallite size (nm)	Catalyst	Crystallite size (nm)
CCr	39	CCoCr-3	16
CFCr-1	32	CoCr	15
CFCr-2	31	CNCr-1	22
CFCr-3	38	CNCr-2	41
CF	38	CNCr-3	49
CMCr-1	53	NCr	42
CMCr-2	51	CZCr-1	8
CMCr-3	40	CZCr-2	9
MCr	44	CZCr-3	16
CCoCr-1	16	ZCr	10
CCoCr-2	16		

3.1.2 Energy Dispersive X-Ray Analysis

The elemental compositions of the prepared catalytic systems were determined by EDX analysis and the results are presented in table 3.2. There was a good agreement between the experimentally obtained and the theoretically calculated values. Small deviation observed in the case of manganese systems were attributed to the leaching of metal ions during washing.

Table 3.2: Atom percentage from EDX analysis

Catalyst	Atom Percentage						
	Cu	Cr	Fe	Mn	Co	Ni	Zn
CCr	34.4	65.6	-	-	-	-	-
CFCr-1	33.4	52.0	14.6	-	-	-	-
CFCr-2	30.9	35.3	33.9	-	-	-	-
CFCr-3	32.3	19.3	48.4	-	-	-	-
CF	47.7 ~~49.8~~	-	53.1	-	-	-	-
CMCr-1	26.0	69.6	-	4.4	-	-	-
CMCr-2	21.1	69.8	-	9.0	-	-	-
CMCr-3	9.0	75.5	-	15.6	-	-	-
MCr	-	69.7	-	30.4	-	-	-
CCoCr-1	26.4	66.1	-	-	7.6	-	-
CCoCr-2	16.0	65.9	-	-	18.1	-	-
CCoCr-3	12.2	67.5	-	-	20.3	-	-
CoCr	-	67.2	-	-	32.8	-	
CNCr-1	24.5	69.4	-	-	-	6.1	-
CNCr-2	15.5	68.1	-	-	-	16.4	-
CNCr-3	7.2	71.9	-	-	-	20.9	-
NCr	-	68.8	-	-	-	31.2	-
CZCr-1	24.5	67.6	-	-	-	-	7.7
CZCr-2	14.1	64.7	-	-	-	-	21.2
CZCr-3	7.5	68.8	-	-	-	-	23.7
ZCr	-	67.6	-	-	-	-	32.4

3.1.3 BET Surface Area and Pore Volume

The BET and Langmuir surface areas and pore volume of the different compositions of the chromite samples calcined at 650°C were measured by nitrogen adsorption at liquid nitrogen temperature (Micromeritics Gemini 2360 Surface Area Analyzer). The data are shown in table 3.3.

Table 3.3: Surface area and pore volume of the catalysts

Catalyst	Surface area (m^2/g)		Pore volume
	BET	Langmuir	(cc/g)
CCr	6.0	8.7	0.02
CFCr-1	17.8	25.9	0.05
CFCr-2	20.8	30.6	0.05
CFCr-3	12.6	18.7	0.03
CF	6.6	10.2	0.01
CMCr-1	8.4	12.3	0.01
CMCr-2	6.2	9.0	0.01
CMCr-3	6.3	9.2	0.01
MCr	7.0	10.3	0.01
CCoCr-1	23.0	34.2	0.07
CCoCr-2	27.3	40.6	0.09
CCoCr-3	12.5	18.4	0.02
CoCr	65.1	98.0	0.15
CNCr-1	10.2	14.8	0.03
CNCr-2	8.9	13.1	0.03
CNCr-3	6.5	9.5	0.02
NCr	13.3	19.7	0.04
CZCr-1	16.0	23.6	0.05
CZCr-2	21.8	31.9	0.07
CZCr-3	35.3	52.3	0.13
ZCr	74.4	112.9	0.14

It was observed that $ZnCr_2O_4$ was having the highest surface area among the spinels studied followed by $CoCr_2O_4$. The incorporation of metal cations such as Fe^{3+}, Mn^{2+}, Co^{2+}, Ni^{2+} and Zn^{2+} increased the surface area to small extent.

3.1.4 Thermal Analysis

The thermal stability of the catalysts was examined by TG-DTA analysis. This analysis was carried out on the catalyst samples which were dried at 80°C before calcination at 650°C. TG-DTA curves for representative samples are given in figure 3.2.

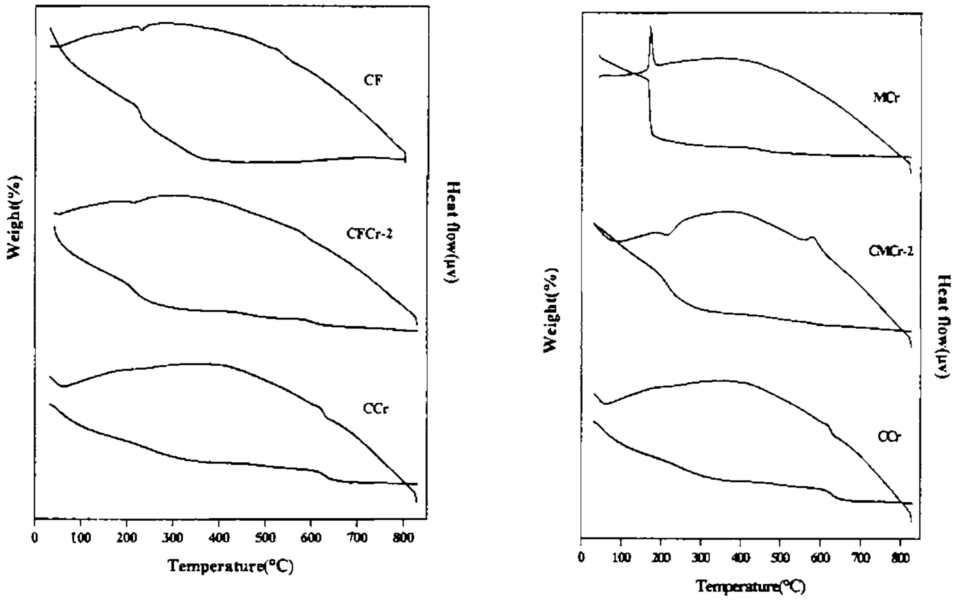

(a) (b)

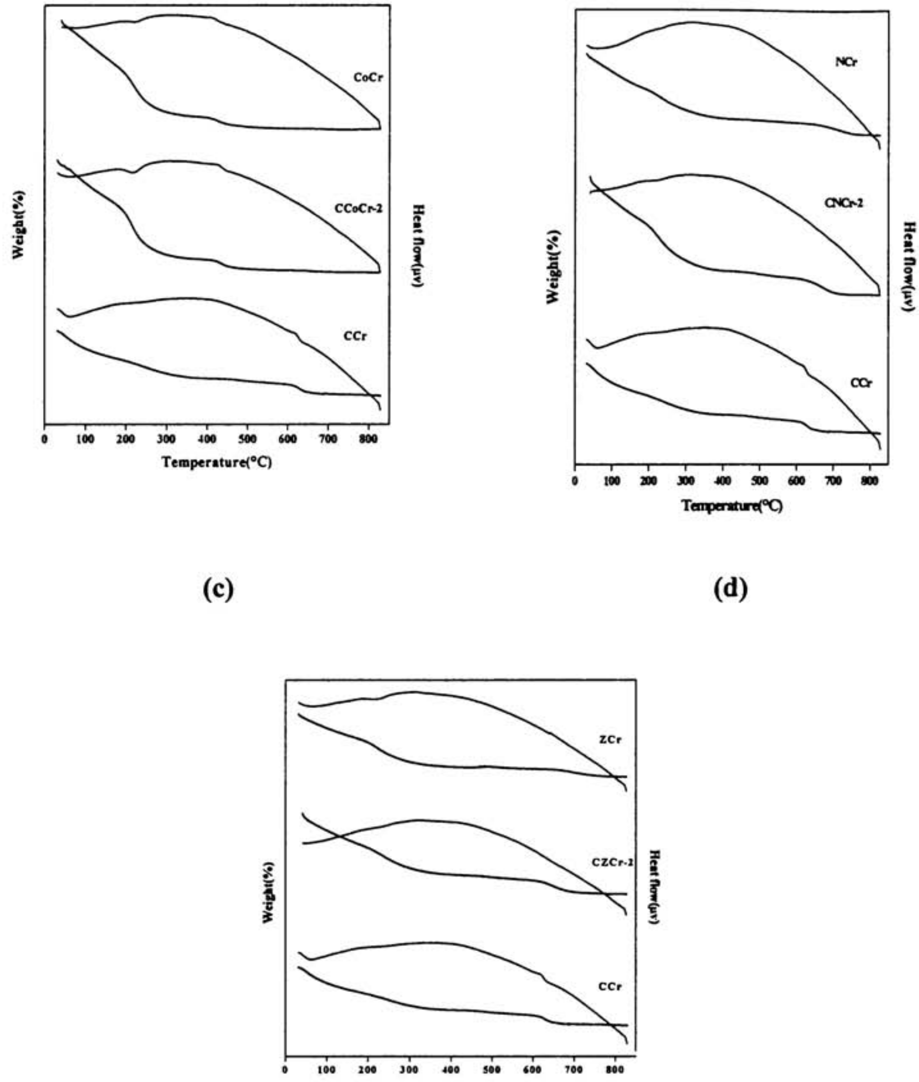

(c)

(d)

(e)

Figure 3.2: TG-DTA curves of: - (a) $CuCr_{2-x}Fe_xCr_2O_4$ series, (b) $Cu_{1-x}Mn_xCr_2O_4$ series, (c) $Cu_{1-x}Co_xCr_2O_4$ series, (d) $Cu_{1-x}Ni_xCr_2O_4$ series, (e) $Cu_{1-x}Zn_xCr_2O_2$ series

In the samples prepared by co-precipitation method, the weight loss of the samples is characterized by three events. The first weight loss around 100°C is associated with the removal of adsorbed water. The second event between 200-300°C is observed. Since the samples are precipitated from the respective nitrate solutions, some amount of the nitrate may present in the adsorbed form and the decomposition of nitrate is responsible for the weight loss around this temperature region. The last one, over 650°C is associated with the thermal decomposition of the catalysts. In $CuCr_2O_4$, the thermal decomposition is due to the phase transition of $CuCr_2O_4$ to $Cu_2Cr_2O_4$[1].

3.1.5. Scanning Electron Microscopy

Scanning electron micrographs (SEM) were recorded to get the surface morphology of the catalysts. SEM micrographs of the representative catalysts are presented in figure 3.3. Figure shows samples are aggregates without shape definition.

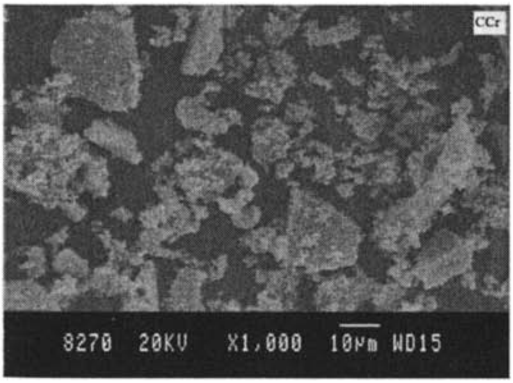

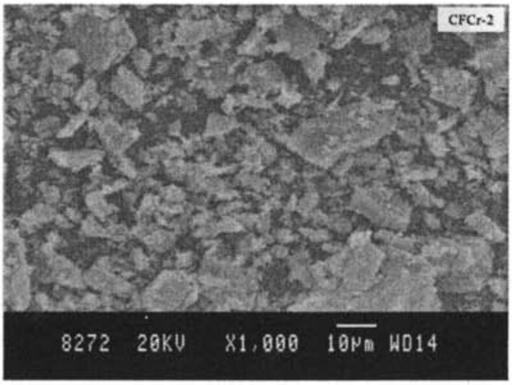

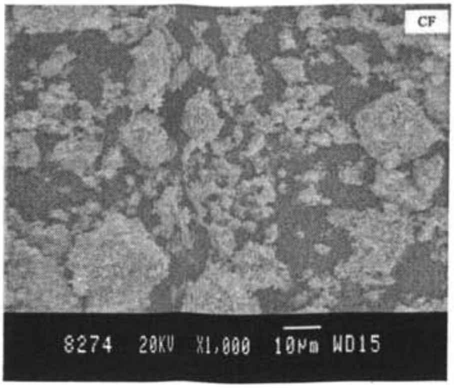
CF
8274 20KV X1,000 10µm WD15

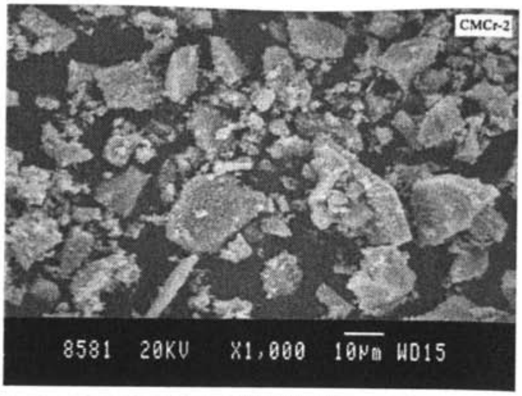
CMCr-2
8581 20KV X1,000 10µm WD15

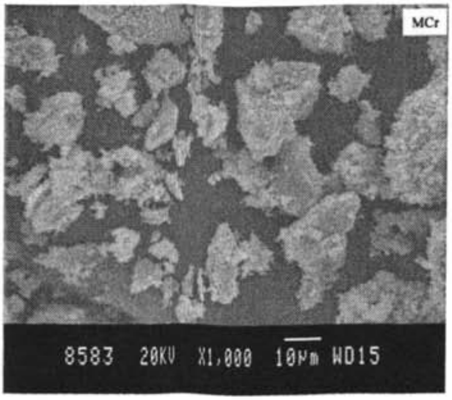
MCr
8583 20KV X1,000 10µm WD15

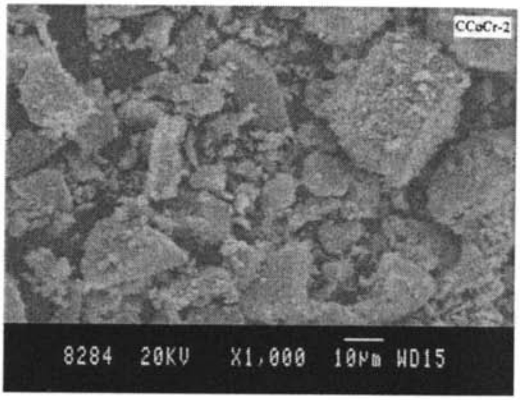
CCoCr-2
8284 20KV X1,000 10µm WD15

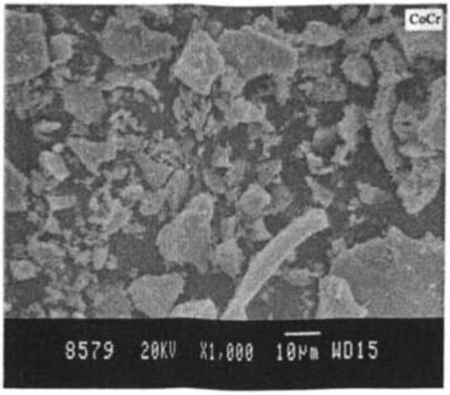
CoCr
8579 20KV X1,000 10µm WD15

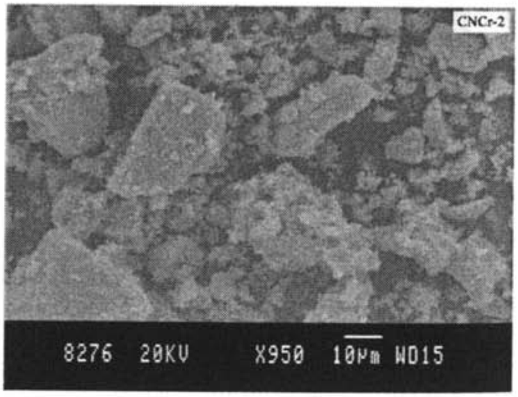
CNCr-2
8276 20KV X950 10µm WD15

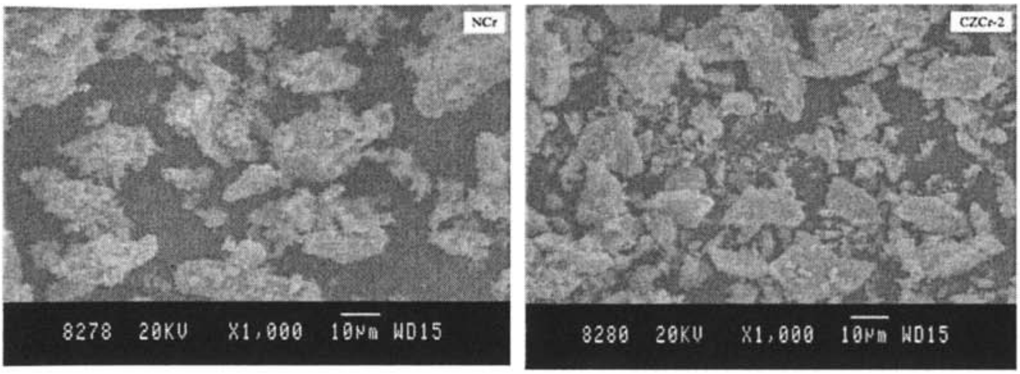

Figure 3.3: SEM pictures of representative catalysts

3.1.6 Fourier Transform Infrared Spectroscopy

FT-IR spectra of the catalysts were taken by KBr pellet method and the spectra of the representative samples are presented in figure 3.4.

The spectra of all the samples showed two strong absorption bands characteristic of spinels at around 620 and 510 cm^{-1}. The band at higher and lower wavelength regions was assigned by Yur'eva et al.[2] to the vibrations of tetrahedral metal-oxygen bond and octahedral metal-oxygen bond respectively. The spectra of all samples showed a characteristic absorption band at 1620 cm^{-1} corresponding to the bending vibrations of adsorbed water molecule and the peak at 3450 cm^{-1} corresponds to the stretching vibrations of OH groups[3].

Group theory calculations have indicated that spinel oxides should exhibit four IR bands[4,5]. However, most of the work done on spinel oxides has shown that in addition to the four expected bands some more bands are present and various explanations have been given to account for these additional bands[6-9].

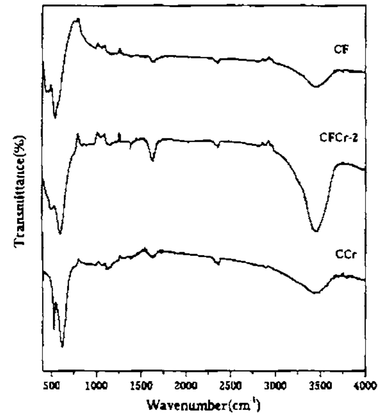
CF
CFCr-2
CCr
Transmittance(%)
500
1000
1500
2000
2500
3000
3500
4000
Wavenumber(cm-1)

(a)

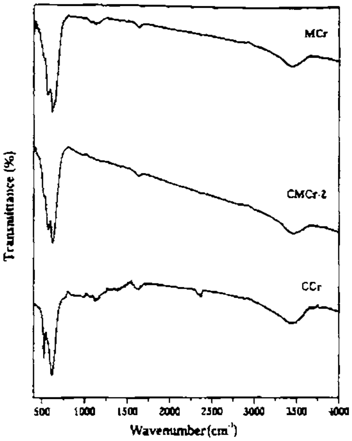
MCr
CMCr-2
CCr
Transmittance (%)
500
1000
1500
2000
2500
3000
3500
4000
Wavenumber(cm-1)

(b)

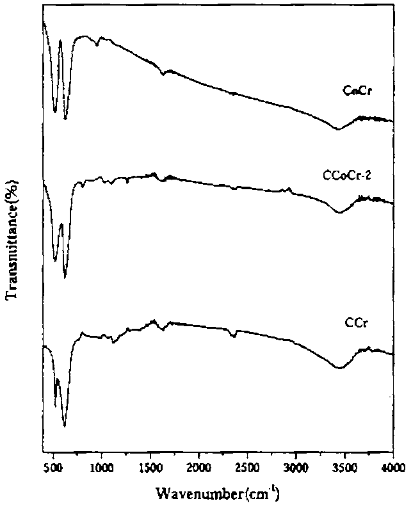
CoCr
CCoCr-2
CCr
Transmittance(%)
500
1000
1500
2000
2500
3000
3500
4000
Wavenumber(cm-1)

(c)

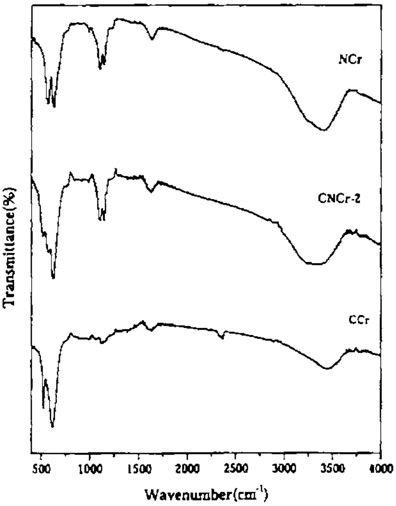
NCr
CNCr-2
CCr
Transmittance(%)
500
1000
1500
2000
2500
3000
3500
4000
Wavenumber(cm-1)

(d)

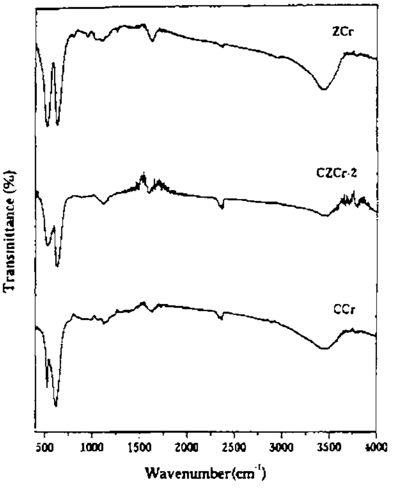

(e)

Figure 3.4: FT-IR spectra of:- (a) $CuCr_{2-x}Fe_xCr_2O_4$ series, (b) $Cu_{1-x}Mn_xCr_2O_4$ series, (c) $Cu_{1-x}Co_xCr_2O_4$ series, (d) $Cu_{1-x}Ni_xCr_2O_4$ series, (e) $Cu_{1-x}Zn_xCr_2O_2$ series

A large amount of work has been done by Preudhomme and Tarte on the IR studies of the spinels[9-11]. From these studies on normal II-III spinel, they concluded that υ_1 and υ_2 (the high frequency bands) in the IR spectrum are nearly insensitive to a modification of the bivalent cation, whereas υ_3, (the low frequency band) depends on the mass of the bivalent cation[9]. Thus it is expected that when Cu^{2+} of $CuCr_2O_4$ is substituted by another bivalent cation, the IR spectrum should not show much change in the υ_1 and υ_2 bands.

$CuCr_2O_4$ is a normal spinel, where all the Cr^{3+} ions are on the octahedral sites and, as it has a strong preference for this site, substitution of the tetrahedral Cu^{2+} ions by any bivalent cation does not alters the cation distribution of these spinel oxides. Thus any change in the IR patterns of the Cu^{2+} substituted $CuCr_2O_4$ spinel compounds will only be due to a change in the tetrahedral cation. With the presence of more than one type of cation on either side of the spinel lattice, all three bands were broadened. The broadening of the bands could be due to the presence of more than one type of cation, leading to two different tetrahedra. Any change in the band position of υ_1 attributes to a change in the degree of tetragonality, and its intensity depends on the degree of inversion. According to J.Ghose[12], υ_1 depends on the degree of tetragonality of the spinel oxides and in cubic samples, no shift in υ_1 occurs. However, υ_2 do not seem to have any dependence on the degree of tetragonality.

According to Lutz[13], in the case of chromite spinels MCr_2O_4, due to the presence of triagonal distortion[8], the true space group becomes $F4^{-}{}_{3m}$ instead of $Fd^{-}{}_{3m}$ which implies that the site symmetry of the octahedrally coordinated metals, i.e., the chromium ions, is C_{3v}, compared to D_{3d} for space group $Fd^{-}{}_{3m}$.This reduction in symmetry probably give rise to more than four bands or sometimes broader bands in the IR spectra of the chromite spinels.

In a normal spinel oxide, irrespective of substitution of the tetrahedral bivalent cation or the octahedral trivalent cation, the broadening mainly occurs in υ_2 and υ_3. while υ_1 shows a shift in its band position. Any shift in the band position of υ_2 and υ_3 could not be recorded accurately due to much more broadening of υ_2 and υ_3 than υ_1. This is however, not true when substitution leads to a change in cation distribution as observed in the IR spectra of $CuCr_{2-x}Al_xO_4$ compounds[14]. When Cu^{2+} ions were replaced by Al^{3+} ions in $CuCr_2O_4$, De et al.[15] have shown that the cation distribution changes from normal ($CuCr_2O_4$) to partially inverse ($CuAl_2O_4$) and the IR spectra of the Al^{3+} substituted compounds show the broadening of υ_1 is much more than υ_2 which suggests that the intensity of υ_1 probably depend on the degree of inversion in the spinel lattice.

In their IR studies on spinels, Preudhomme and Tarte[11] had suggested that since the spinel lattice was constituted of "isolated" tetrahedra and "condensed" octahedra, the possibilities of vibrational interactions between: (1) identical tetrahedra; (2) different tetrahedra; (3) identical octahedra; (4) different octahedra; (5) tetrahedra and octahedra should be considered when analyzing their IR spectra. From the results of five solid solution series, compounds in the present studies, it appears that υ_1 is due to the interactions (1)-(5) and so with more than one type of bivalent cations, i.e., Cu^{2+} and $Mn^{2+}/Co^{2+}/Ni^{2+}/Zn^{2+}$ on the tetrahedron and trivalent cations, i.e., Cr^{3+} and Fe^{3+} on the octahedron.

3.1.7 Surface acidity measurements

Solid acid catalysts are the backbone of major processes of refining and of petrochemical industry. In reactions occurring by acid catalysts, the activity, selectivity, and stability of the solid acids are obviously determined to a large extent by their surface acidity[16] (i.e. the number, nature, strength and density of their acid sites). The rate and selectivity of reactions that do not occur by acid catalysis can also be affected by acidity. This has been shown in the case of oxidation of hydrocarbons on transition metal oxides. According to many authors[17-24], whatever is the type of spinel; the octahedral sites are exposed almost exclusively at the catalyst surface of the spinel oxides and so the catalytic performance greatly depends on the composition of the octahedral sites. Hence, the relative acid property of the cations present in the octahedral site is relevant in determining the acidity of the systems.

To determine the surface acidity, three independent methods were implemented- (1) Temperature programmed desorption of ammonia, (2) vapour-phase cumene cracking reaction and (3) vapour-phase decomposition of cyclohexanol.

3.1.7.1 Temperature Programmed Desorption-NH_3

Temperature Programmed Desorption (TPD) analysis permits to identify the strength, the number and the type of active sites that are available on the catalyst surface. The NH_3-TPD is an easy, rapid and quantitative method, widely employed in characterizing the acidity of solid catalysts. The technique consists in desorbing, by a linear temperature rate, a reactive gas such as ammonia previously chemisorbed on the surface. This method permits the determination of both protonic and cationic acidities.

Owing to the smaller size and strong basicity, ammonia can get adsorbed on acidic sites of any strength and type. The surface OH groups (Bronsted type) and exposed cations (Lewis type) are responsible for the acidity generation in a solid acid catalyst surface[25]. Ammonia can be adsorbed on an oxide surface through hydrogen bonds or through dipolar interaction yielding the total acidity (Bronsted and Lewis type) of the system[26]. Acidity values obtained by NH_3-TPD of spinel catalysts are given in table 3.4.

Table 3.4: Surface acidity measured by ammonia TPD method

Catalyst	Acidity distribution (m mol/g)			Total acidity
	Weak (RT-200°C)	Medium (201-400°C)	Strong (401-600°C)	
CCr	0.23	0.02	0.00	0.25
CFCr-1	0.24	0.11	0.05	0.40
CFCr-2	0.26	0.15	0.07	0.48
CFCr-3	0.27	0.17	0.13	0.57
CF	0.27	0.23	0.17	0.67
CMCr-1	0.16	0.11	0.01	0.28
CMCr-2	0.20	0.11	0.02	0.33
CMCr-3	0.30	0.18	0.12	0.60
MCr	0.13	0.09	0.04	0.26
CCoCr-1	0.17	0.08	0.04	0.29
CCoCr-2	0.30	0.12	0.01	0.43

CCoCr-3	0.24	0.14	0.06	0.44
CoCr	0.26	0.06	0.01	0.33
CNCr-1	0.33	0.13	0.03	0.49
CNCr-2	0.36	0.11	0.01	0.48
CNCr-3	0.23	0.14	0.05	0.42
NCr	0.39	0.15	0.03	0.57
CZCr-1	0.29	0.04	0.01	0.34
CZCr-2	0.29	0.14	0.05	0.48
CZCr-3	0.28	0.15	0.04	0.47
ZCr	0.17	0.07	0.03	0.27

From the results it was clear that solid solutions possessed more acidity than the simple chromites. On iron substitution, more Fe^{3+} is exposed to the octahedral sites and hence increases in acidity and maximum acidity was shown by $CuFe_2O_4$.

3.1.7.2 Cumene Cracking

Model reactions constitute an efficient means for measuring the surface acidity of the solids especially in terms of the nature, strength and density of the acid sites. Cumene cracking reaction is a test reaction for the simultaneous determination of Bronsted as well as Lewis acidity. The major reactions occurring during cumene conversion may be grouped into dealkylation (cracking) and dehydrogenation. Dealkylation of cumene yields benzene whereas dehydrogenation gives α-methyl styrene[27]. Lewis acid sites are responsible for dehydrogenation and dealkylation take place at the Bronsted acid sites. Another possibility is the cracking of the alkyl chain to give ethylbenzene, which on dehydrogenation to give styrene. The reaction conditions were optimized in terms of reaction temperature and flow rate. All the reactions were performed over CFCr-2 catalyst. The cumene conversion could be correlated with the surface acidity calculated from ammonia TPD.

(a) Effect of Temperature

Figure 3.5 shows the influence of reaction temperature on cumene conversion and product selectivity. The reactions were carried out in a temperature range from 350-500°C at a flow rate of 4ml/h. The enhancement in catalytic activity with temperature was observed. The selectivity to α-methyl styrene decreased with temperature correspondingly increases in amount of benzene. At high temperatures, there is a possibility for cracking of the alkyl chain and products like ethylbenzene and styrene were observed. Considering the cumene conversion, the optimum temperature selected for further studies is 500°C.

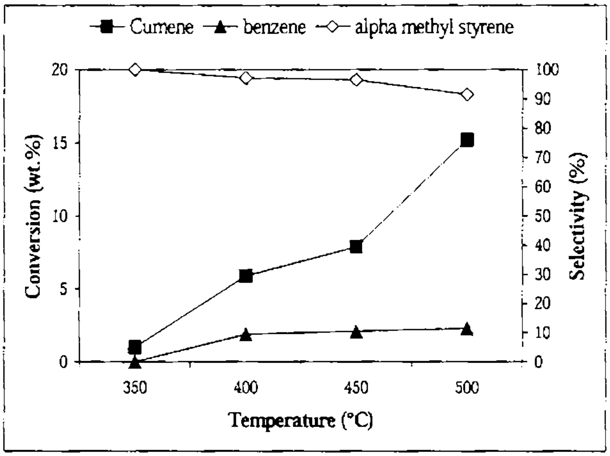

Reaction conditions: Catalyst-CFCr-2, Flow rate- 4 ml/h, Catalyst weight-0.5 g, Time- 2 h

Figure 3.5: Effect of Temperature on cumene cracking

(b) Effect of Flow rate

The effect of flow rate on cumene conversion is presented in figure 3.6. The reactions were carried out in different flow rates from 3-6 ml/h. The conversion depends on the residing time of the reactant on the catalyst surface. Increase in flow rate decreased the residing time and hence decrease in conversion. Cumene conversion decreased from 16.7 to 10.3 % on increasing the flow rate from 3 to 6 ml/h. An optimum flow rate of 4 ml/h was selected for further studies since moderate cumene conversion and selectivity to α-methyl styrene was achieved at this condition. At 6 ml/h, only α-methyl styrene and benzene were observed, not any dealkylated products.

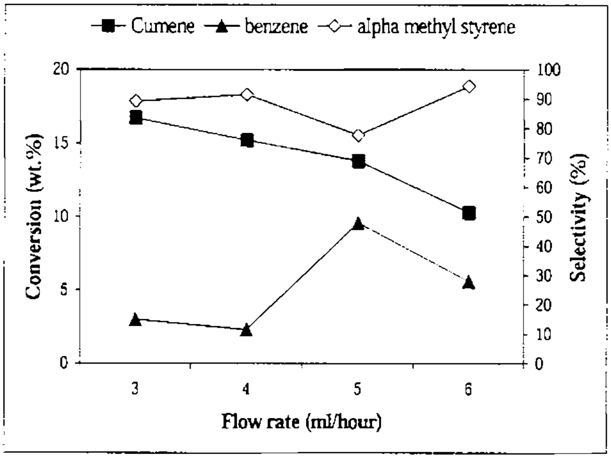

Reaction conditions: Catalyst-CFCr-2, Time- 2 h
Temperature-500°C, Catalyst weight-0.5 g,

Figure 3.6: Effect of flow rate on cumene cracking

The above observations revealed that reaction parameters play a decisive role in cumene conversion and product selectivity. The reaction was carried out over all the catalysts with the reaction conditions given in table 3.5.

Table 3.5: Optimized conditions for cumene cracking

Reaction Parameters		Selected condition
Temperature	:	500°C
Flow rate		4 ml/h
Time		2 h
Catalyst weight	:	0.5 g

(c) Effect of time on stream

To study the effect of time on cumene conversion, the reaction was carried out for eight hours continuously over the prepared catalysts and the product analysis was carried out at a regular interval of 1h. The results obtained on the samples CFCr-1, CMCr-1, CCoCr-1, CNCr-1 and CZCr-1 is presented in figure 3.7.

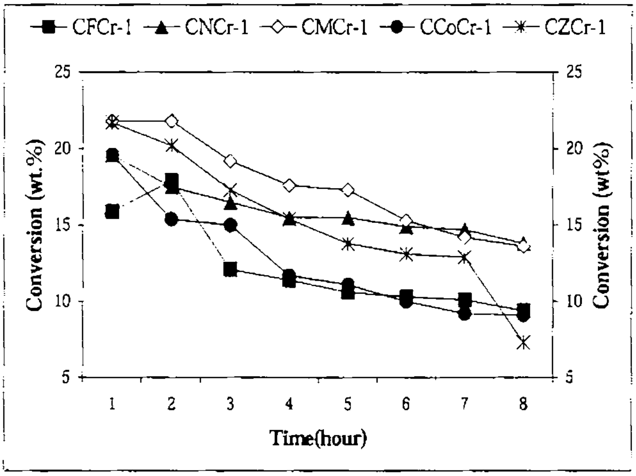

Reaction conditions: Temperature-500°C, Flow rate-4 ml/h, Catalyst weight-0.5g

Figure 3.7: Effect of time on stream on cumene cracking

From the results obtained, it was clear that the catalytic activity declined gradually with reaction time. The decrease in overall conversion was associated with a rapid decrease in the amount of benzene produced and must result from poisoning of active acidic sites on the surface by polymerization of propene produced by cumene alkylation[28]. The decrease of catalytic activity may also be due to coke formation during the reaction[29].

(d) Cumene conversion over prepared catalysts

The reaction was carried out over all the catalysts prepared and the results obtained are presented in table 3.6.

Table 3.6: Cumene cracking over the prepared catalysts

Catalyst	Cumene conversion (wt %)	Product selectivity (%)		
		α-methyl styrene	Benzene	Others
CCr	12.2	85.0	4.0	11.0
CFCr-1	14.9	89.1	2.4	8.5
CFCr-2	16.8	91.5	2.3	6.1
CFCr-3	21.4	88.8	2.9	8.3
CF	22.1	80.7	5.4	13.9
CMCr-1	12.2	88.3	3.1	8.7
CMCr-2	15.8	85.4	3.9	10.7
CMCr-3	17.5	82.5	1.1	16.3
MCr	12.1	85.1	5.3	9.9
CCoCr-1	15.4	89.8	2.5	7.8
CCoCr-2	24.2	84.2	3.4	12.4
CCoCr-3	23.9	90.8	0.9	8.4
CoCr	20.7	89.3	2.4	8.3
CNCr-1	17.5	88.3	3.0	8.6
CNCr-2	12.1	82.8	5.0	12.4
CNCr-3	10.2	82.1	5.5	12.4
NCr	13.7	87.7	3.7	8.6
CZCr-1	12.8	87.9	2.9	9.0
CZCr-2	20.2	88.9	3.2	7.9
CZCr-3	20.1	89.9	2.8	7.3
ZCr	11.9	88.9	3.0	8.1

Among all the catalytic systems, $CuFe_2O_4$ showed least selectivity to α-methyl styrene. Copper ferrite is an inverse spinel with the Lewis center; Fe distributed between the tetrahedral and octahedral sites and hence decreases in selectivity. A correlation was found between cumene conversion and total acidity from ammonia TPD and is presented in figure 3.8.

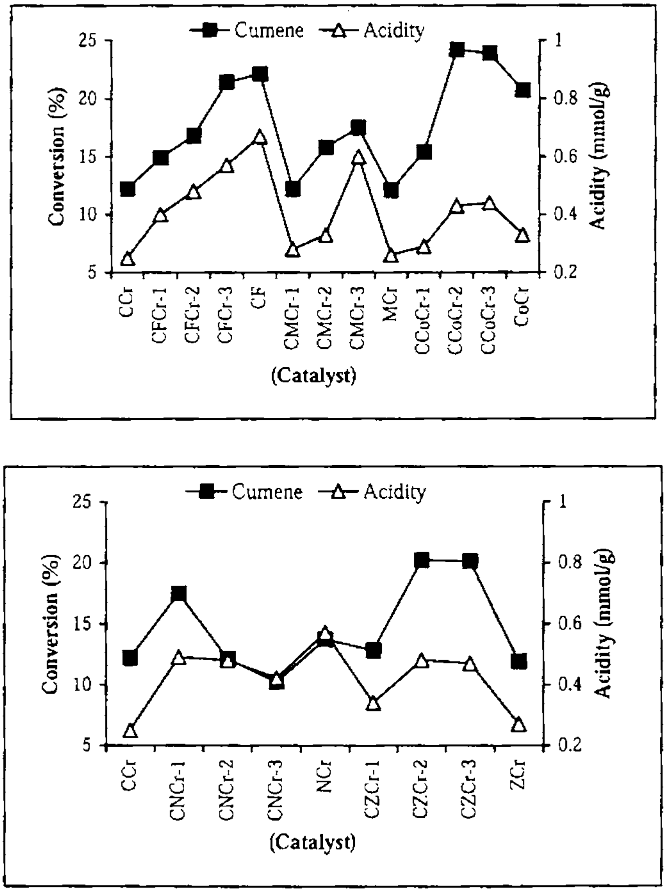

Figure: 3.8: Correlation between total acidity from NH_3 TPD and cumene conversion

(e) Mechanism of the reaction

A Friedel Crafts mechanism, involving initial protonation of aromatic ring followed by the cleavage of the ring side chain bond, is generally accepted for the cumene dealkylation over acidic catalysts[30]. This mechanism provides a route to the poisoning of the catalyst through coke formation, since the cracked side chain may polymerize on the acidic surface. Cracking of cumene to benzene is generally attributed to the action of Bronsted sites by a carbonium ion mechanism while dehydrogenation of cumene yields α-methyl styrene as the major product, the formation of which has been ascribed to the Lewis acid sites. A plausible mechanism of cumene conversion reaction is represented in scheme 3.1.

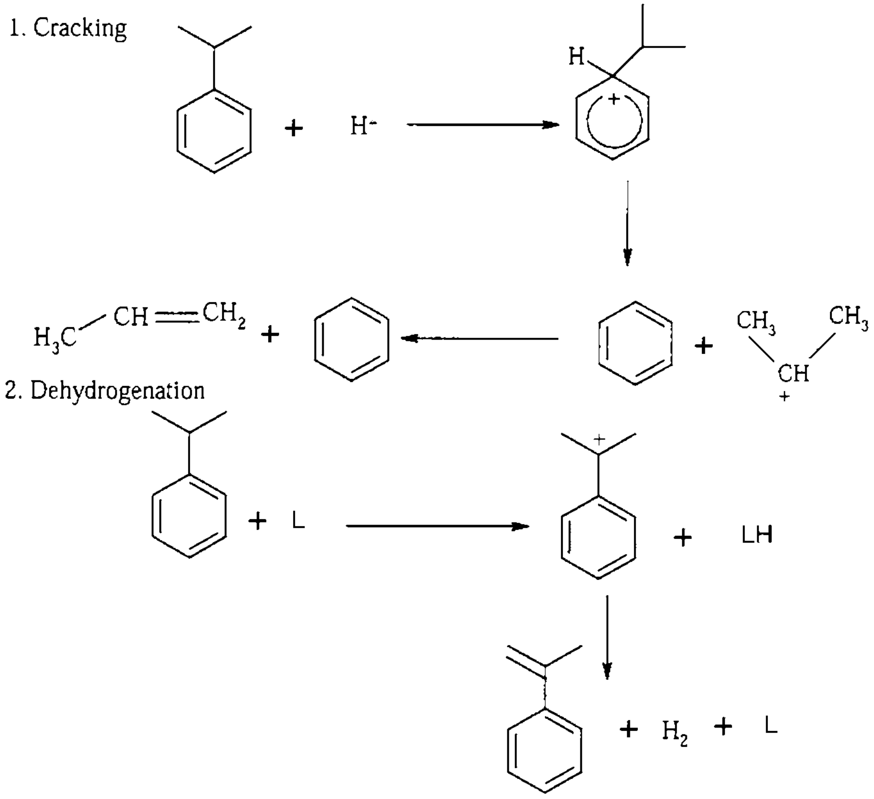

Scheme 3.1: Mechanism of cumene cracking reaction

3.1.7.3 Cyclohexanol Decomposition

Cyclohexanol decomposition is widely used as a probe reaction to characterize the acid-base properties of the catalysts[31]. The amphoteric nature of the alcohol permits its interaction with both acidic and basic centers[32,33]. The acid sites on the catalyst surface are responsible for dehydration and dehydrogenation is take place by the action of basic sites on the catalyst surface. The dehydrogenation reaction resulting in the ketone usually competes with the dehydration reaction. The dehydrogenation and dehydration result in the formation of cyclohexanone and cyclohexene respectively[34]. Methyl cyclopentane, benzene, cyclohexane and phenol are the other possible products of this reaction. The optimum conditions for the reactions were determined by carrying out the reaction at various temperatures and flow rates over CZCr-2 catalyst.

(a) Effect of Temperature

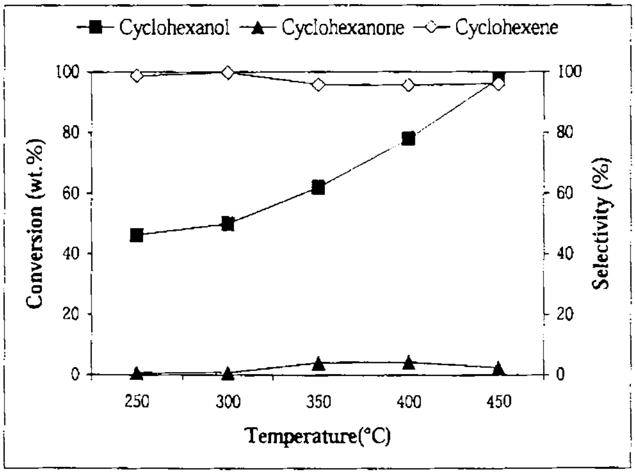

Reaction conditions: Catalyst-CZCr-2, Flow rate- 4 ml/h, Catalyst weight-0.5 g, Time- 2 h

Figure 3.9: Effect of temperature on cyclohexanol decomposition

The effect of reaction temperature on cyclohexanol decomposition was studied by varying the temperature from 250°C to 450°C. The results obtained are presented in figure 3.9. The percentage cyclohexanol conversion increased with increase in temperature. The percentage selectivity of cyclohexene decreased with temperature while that of cyclohexanone increased. Moderate cyclohexanol conversion and product selectivity was observed at 350°C and was selected as the optimum temperature for further studies.

(b) Effect of Flow rate

The effect of flow rate on cyclohexanol decomposition was investigated and the results are presented in figure 3.10.

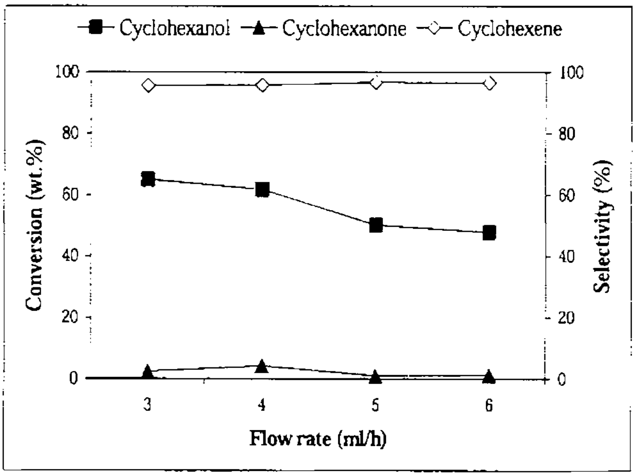

Reaction conditions: Catalyst-CZCr-2, Temperature-350°C, Catalyst weight-0.5 g, Time- 2 h

Figure 3.10: Effect of flow rate on cyclohexanol decomposition

The reaction was carried out at 350°C over CZCr-2 catalyst. The percentage conversion decreased with increasing flow rate. A reduction of conversion from 65.1% to 47.8% was observed when flow rate increased from 3 to 6 ml/h. The drastic reduction in the percentage cyclohexanol conversion was due to the decrease in contact time between the catalyst surface and the reactant. Percentage selectivity of cyclohexene is almost constant up to 4 ml/h and gradually increased. A flow rate of 4 ml/h was selected as the optimum condition for further studies.

From the above observations it was clear that reaction conditions play an important role in cyclohexanol conversion and product selectivity. The reaction was carried out over all the catalysts with the reaction conditions given in table 3.7.

Table 3.7: Optimized conditions for cyclohexanol decomposition

Reaction Parameters		Selected condition
Temperature	:	350°C
Flow rate		4 ml/h
Time		2 h
Catalyst weight	:	0.5g

(c) Effect of time on stream

Figure 3.11 illustrates the time on stream stability of the representative prepared catalysts at a reaction temperature of 350°C and at a flow rate of 4ml/h. Good catalytic activity was shown by all the catalysts. Deactivation was observed in all the catalysts with increase in time. The deactivation of the catalyst was due to the presence of surface oligomers resulting from poly condensation of cyclohexanone[35]. The cyclohexene produced in this reaction was also ascribed to have a capacity for deactivating the catalysts on account of the ease with which they can give rise to surface carbonaceous compounds.

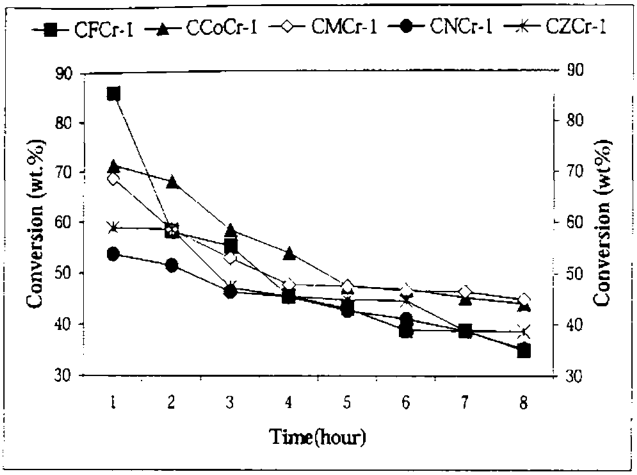

Reaction conditions: Temperature-350°C, Flow rate-4 ml/h, Catalyst weight-0.5 g

Figure 3.11: Effect of time on cyclohexanol decomposition

(d) Cyclohexanol decomposition over the prepared catalysts

The reaction was carried out over all the catalysts prepared and the results obtained are presented in table 3.8. Selectivity of only cyclohexene and cyclohexanone are given in the table.

Table 3.8: Cyclohexanol decomposition over the prepared catalysts

Catalyst	Cyclohexanol conversion (wt %)	Product selectivity (%)	
		Cyclohexene	Cyclohexanone
CCr	51.3	95.5	3.9
CFCr-1	58.1	94.1	3.6
CFCr-2	60.1	93.9	5.3
CFCr-3	83.5	95.1	3.9
CF	85.2	94.4	4.6
CMCr-1	58.5	92.7	5.9

CMCr-2	59.8	96.5	2.0
CMCr-3	65.4	95.6	3.2
MCr	47.5	94.7	3.7
CCoCr-1	68.0	95.5	2.7
CCoCr-2	69.8	93.1	5.9
CCoCr-3	62.8	92.6	5.9
CoCr	51.3	94.9	4.8
CNCr-1	57.9	97.4	1.2
CNCr-2	57.1	98.3	0.6
CNCr-3	56.2	98.3	0.8
NCr	77.4	94.8	0.9
CZCr-1	58.9	98.5	1.1
CZCr-2	60.0	92.0	4.9
CZCr-3	59.4	97.1	1.9
ZCr	56.9	91.9	2.9

A correlation was found between cyclohexanol decomposition rate and total acidity of the catalysts calculated from NH_3 TPD and is presented in figure 3.12.

(e) Mechanism of the reaction

It is generally accepted that the highest activities in dehydration of cyclohexanol to cyclohexene is related to acid sites, while dehydrogenation to cyclohexanone is generally associated to basic/redox sites[36-40]. Bronsted acid sites are directly involved in the alcohol dehydration mechanism. It is similar to the E-1 elimination in which the reaction proceeds through initial formation of carbocation. The elimination reaction on the basic site is carried out after the adsorption of cyclohexanol through the hydrogen atom in the α-carbon, which develops a carbenium character to some degree. The strongest basic sites could be able to carry out the adsorption of the hydrogen atom of the hydroxyl group, generating an oxygen anion, thus promoting the dehydrogenation reaction[41,42]. The general mechanism of cyclohexanol decomposition over metal oxides is given in scheme 3.2.

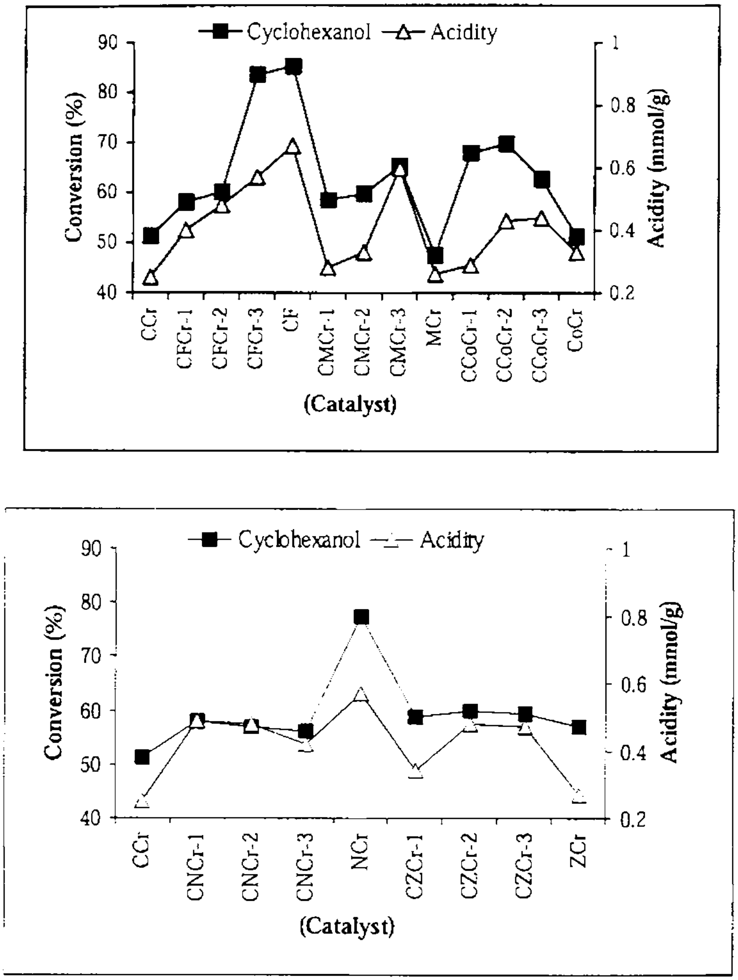

Figure: 3.12: Correlation between total acidity from NH$_3$ TPD and cyclohexanol decomposition rate

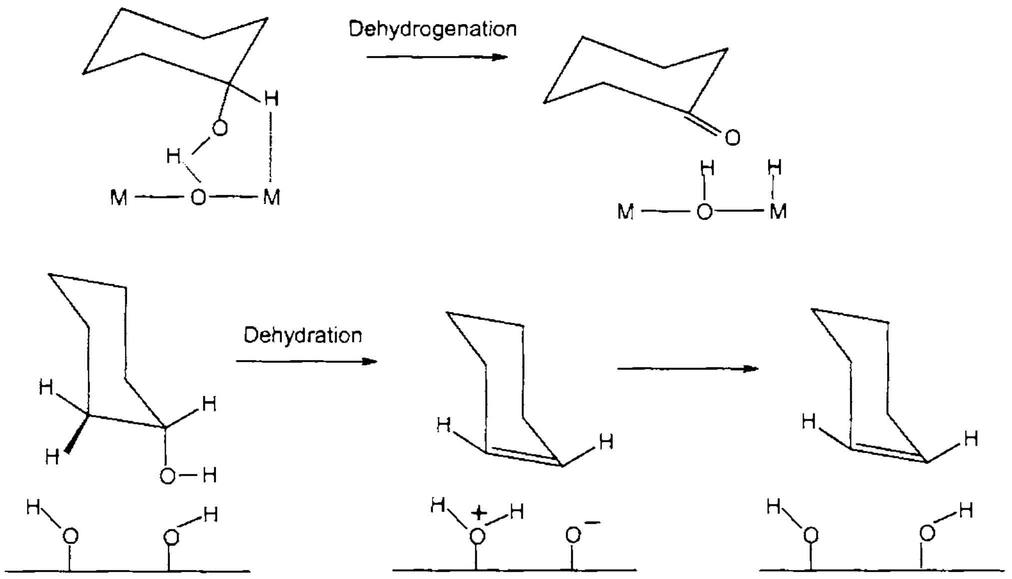

Scheme 3.2: Mechanism of dehydrogenation and dehydration of cyclohexanol on oxide surface

3.2 Conclusions

The conclusions from the present results can be summarized as follows.

- ✓ Modification of copper chromite spinel by transition metals showed improvement in the physico- chemical characteristics.
- ✓ XRD patterns of the prepared systems revealed the characteristic peaks of spinels. The spinel phase formation was again confirmed by the appearance of two bands at 620 and 510cm^{-1} in the FT-IR spectra.
- ✓ Chemical composition of the catalysts obtained from EDX analysis was in agreement with the theoretical values indicated the correct stoichiometry.

- ✓ Enhancement in surface area, pore volume and total acidity was observed in all the transition metal substituted copper chromite spinels.
- ✓ Scanning electron microscopy of the catalysts gave an idea about the surface morphology of the catalysts.
- ✓ The general observation that acid sites favor dehydration and both acidic and basic sites favor dehydrogenation was confirmed by the cyclohexanol decomposition reaction carried out over different spinel systems.
- ✓ Cumene conversion reaction gave α-methyl styrene as the major product indicated the presence of more Lewis acid sites in the catalyst.

References

[1] G. Plesch, F. Hanic, K. Putyera, Thermochimica Acta 176 (1999) 267

[2] T. M. Yur'eva, G. K. Boreskov, V. I. Zharkov, L. G. Karakchivev, V. V. Popovskii, V. A. Chigrina, Kinet. Katal. 9 (1968) 1063

[3] N. J. Jebarathinam, M. Eswaramoorthy, V. Krishnasamy, Appl. Catal. A 145 (1996) 57

[4] W. B. White, B. A. De Angelis, Spectrochim. Acta 23 A 985 (1967)

[5] H. D. Lutz, Z. Naturforsch, Spectrochim. Acta 24 A (1969) 1417

[6] V. A. M. Brabers, Phys. Stat. Sol. 33, (1969) 563

[7] K. Siratori, Y. Aiyama, J. Phys. Soc. Jpn. 20 (1965) 1962

[8] N. W. Grimes, A. J. Collett, Phys. Stat. Sol. B 43 (1971) 591

[9] J. Preudhomme, P. Tarte, Spectrochim. Acta 27 A (1971) 1817

[10] J. Preudhomme, P. Tarte, Spectrochim. Acta 28 A (1972) 69

[11] J. Preudhomme, P. Tarte, Spectrochim. Acta 27 A (1971) 845

[12] D. Basak, J. Ghose, Spectrochim. Acta 50 A (1994) 713

[13] H. D. Lutz, B. Muller, H. J. Steiner, J. Solid State Chem. 90 (1991) 54

[14] N. Padmanaban, Ph.D. Thesis. I.I.T. Kharagpur, India (1990)

[15] K. S. De, J. Ghose, K. S. R. C. Murthy, J. Solid State Chem. 47 (1983) 264

[16] M. R. Guisnet, Acc. Chem. Res. 23 (1990) 392

[17] H. Knozinger, P. Ratnaswami, Catal. Rev. - Sci. Eng. 17 (1979) 31

[18] J. P. Beaufils, Y. Barbaux, J. Chem. Phys. 78 (1981) 347

[19] J. P. Beaufils, Y. Barbaux, J. Appl. Crystallogr. 15 (1982) 301

[20] J. P. Jacobs, A. Maltha, J. G. H. Reintjes, J. Drimal, V. Ponec, H. H. Brongersma, J. Catal. 147 (1994) 294

[21] J. Ziolkowski, Y. Barbaux, J. Mol. Catal. 67 (1991) 199

[22] B. C. Lippens, J. J. Steggerda, "Physical and Chemical Aspects of Adsorbents and Catalysts", (Eds, B. G. Linsen), Academic Press, New York, 1970, P-171

[23] H. C. Yao, M. Shelef, J. Phys. Chem. 78 (1974) 2490

[24] M. Shelef, M. A. Z. Wheeler, H. C. Yao, Surf. Sci. 47 (1975) 697

[25] H. A. Benesi, J. Am. Chem. Soc. 78 (1956) 5490

[26] S. Sugunan, N. K. Renuka, Bull. Chem. Soc. Jpn. 75 (2002) 463.

[27] S. M. Bradley, R. A. Kydd, J. Catal. 141 (1993) 239

[28] J. M. Lewis, R. A. Kydd, P.M. Boorman, J. Catal. 120 (1989) 413

[29] P. Wu, T. Komatsu, T. Yashima, Microporous Mesoporous Mater. 22 (1998) 343

[30] N. Y. Chen, W. W. Kaeding, F. H. Dwyer, J. Am. Chem. Soc. 101 (1979) 6783

[31] M. Ai, Bull. Chem. Soc. Jpn. 50 (1997) 2579

[32] M. M. C. C. Costa, L. F. Hodson, R. A. W. Johnstone, J. Y. Liu, D Whitaker,

J. Mol. Catal. 142 (1999) 349

[33] D. Martin, Duprez, J. Mol. Catal. 118 (1997) 113

[34] M. Ai, Bull. Chem. Soc. Jpn. 50 (1977) 2587

[35] Y.M. Lin and I. Wang, Appl. Catal. A 41 (1988) 53

[36] R. A. W. Jonstone, J. Liu, D. Whittaker, J. Chem. Soc. Perkin Trans. 1 (1998) 1287

[37] R.A.W. Jonstone, J. Liu, D. Whittaker, J. Mol. Catal. A 174 (2001) 159

[38] Y. Shinohara, T. Nakajima, S. Suzuki, J. Mol. Struct. (Theochem) 460 (1999) 231

[39] V. Z. Fridman, A. A. Davydov, J. Catal. 195 (2000) 20

[40] F. M. Bautista, J. M. Campelo, A. Garcia, D. Leina, J. M. Marinas, R. A. Quiros, A. A. Romero, Appl. Catal. A 243 (2003) 93

[41] L. Nodek, J. Sedlaceck, J. Catal. 40 (1975) 34

[42] M. Bowker, R.W. Petits, K. C. Waugh, J. Catal. 99 (1986) 53

****

CHAPTER 4

OXIDATION OF HYDROCARBONS

Abstract

The development of heterogeneous catalysts for selective oxidation of hydrocarbons is a current challenge and has been studied extensively in recent years. Due to environmental and economic concerns, the development of highly efficient catalytic processes, which minimize the formation of side products and residues, is quite desirable. Oxidations using environmentally friendly oxidants such as molecular oxygen, hydrogen peroxide and t-butyl hydroperoxide are more desirable these days. Catalytic oxidation offers the advantage that volatile organic compounds can be removed from aerial effluents to very low levels. In this chapter, the liquid-phase oxidation reactions of four hydrocarbons over chromite spinel catalysts are analyzed in detail. They are the oxidations of benzyl alcohol, styrene, cyclohexane, and ethylbenzene. The influence of various reaction parameters was investigated thoroughly. Possible reaction pathways involved in each oxidation were proposed.

SECTION: A

4.1. OXIDATION OF BENZYL ALCOHOL

4.1.1. Introduction

Catalytic conversion of primary alcohols to aldehydes is essential for the preparation of fragrances and food additives as well as many organic intermediates[1]. Traditional methods for the synthesis of aldehydes generally involve the use of stoichiometric amounts of inorganic oxidants such as, Cr^{VI}, and generate large quantities of waste. Hence the development of effective and environmentally benign heterogeneously catalyzed oxidation of alcohols is an important challenge. Metal catalyzed reactions using molecular oxygen instead of mineral oxidizing agents, are particularly attractive for environmental reasons. Pd and Pt metals supported on alumina are among the widely used metal catalysts in the selective oxidation of alcohols. Such systems, however, tend to deactivate quickly due to the strongly adsorbed products or by-products formed during the reaction[2].

Metal oxides were found to be effective in the catalytic oxidation of benzyl alcohol. Stuchinskaya and Kozhevnikov[3] have reported heterogeneous oxidation of benzyl alcohol to benzaldehyde by O_2 in liquid phase at 100°C and ambient pressure using hydrous binary Pd^{II}-metal oxides as catalysts. Modification of Pd (II) oxides with transition metal cations generally improved the catalytic activity and selectivity to aldehyde, Co (III) and Fe (III) being the most effective promoters. The oxidation of alcohols on Pd-M oxide catalyst was accompanied by transfer hydrogenation and decarbonylation side reactions, which were similar to the oxidation on the Pd metal. This indicated that the oxidation of alcohol on Pd-M oxide catalysts occurred via a dehydrogenation mechanism with hydrogen being present on the catalyst surface.

Nano sized NiO_2 powder was applied as a catalyst for benzyl alcohol oxidation by Ji et al.[4]. Liotta et al.[5] reported the structural and surface characterization of chromia on silica and zirconia oxides and its catalytic performance towards benzyl alcohol oxidation. A correlation was found between the benzyl alcohol conversion and the amount of chromia reduced obtained from TPR of used samples.

MCM-41 supported hydroxo-bridged dicupric-phenanthroline complex were found to be efficient catalyst for the oxidation of benzyl alcohol with TBHP[6]. Ganeshan and Viswanathan synthesized μ-oxo bridged dinuclear iron 1,10-phenanthroline complex encapsulated in MCM-41 and compared benzyl alcohol oxidation in both neat and encapsulated complexes[7]. In neat complex, Fe-O-Fe bridge was cleaved during oxidation while in encapsulated system, it was stable. Farukawa et al. studied gas phase catalytic oxidation of benzyl alcohol over various zeolites catalysts. They have reported the effect of alkali metal doping to supported La/ZSM-5 catalysts on the catalytic activity of gas-phase oxidation of benzyl alcohol[8] and a promotion scheme for the alkali metal added to the La/NaZSM-5 catalyst was performed. Also the effect of alkali promotion on Cu-Na-ZSM-5 catalysts[9], Co (II) NaY[10] zeolites and copper exchanged Y-type zeolites[11] for benzyl alcohol oxidation were reported.

This section presents an exhaustive investigation on the liquid phase oxidation of benzyl alcohol with H_2O_2 over the prepared catalytic systems. The general scheme of the reaction represented in scheme 4.1.1. The main reaction product is benzaldehyde, which is then oxidized to benzoic acid. All the catalytic systems showed considerable activity towards the oxidation with high selectivity towards benzaldehyde.

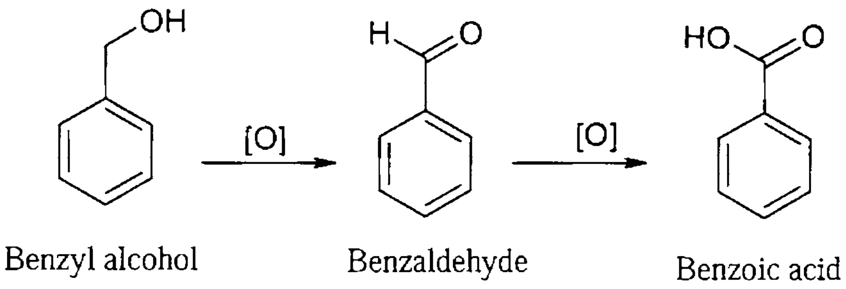

Scheme 4.1.1: Reaction scheme of benzyl alcohol oxidation

H_2O_2 has many advantages as oxidant because water is the only expected side product and it is easy to be dealt with after reactions. Meanwhile, dilute aqueous H_2O_2 (concentration less than 60%) solution is safe, non-toxic, and low cost. However, aqueous H_2O_2 is a moderate inorganic oxidant, and it does not form a homogeneous solution with most organics. The other problem of aqueous H_2O_2 as oxidant rises from its poor stability because it is liable to decompose while heated or in the presence of many metal ions, non-metal ions and finely ground particles. Therefore there is a competition between the decomposition reaction and oxidation reaction. The above disadvantages of aqueous H_2O_2 limit its application in organic oxidation reactions. Accordingly, the key problem of relevant research is to look for efficient catalyst that can activate but not decompose H_2O_2.

4.1.2 Influence of Reaction Conditions

Influence of reaction conditions is essential for a chemical reaction to occur with high percentage conversion and selectivity for products. The influence of different reaction parameters was analyzed in order to maximize the product yield and selectivity. Effect of reaction conditions for benzyl alcohol oxidation with H_2O_2 was initially assayed in non-optimized conditions with CCoCr-2 as the catalyst.

4.1.2.1 Effect of Time

The influence of reaction time on benzyl alcohol oxidation is illustrated in figure 4.1.1.

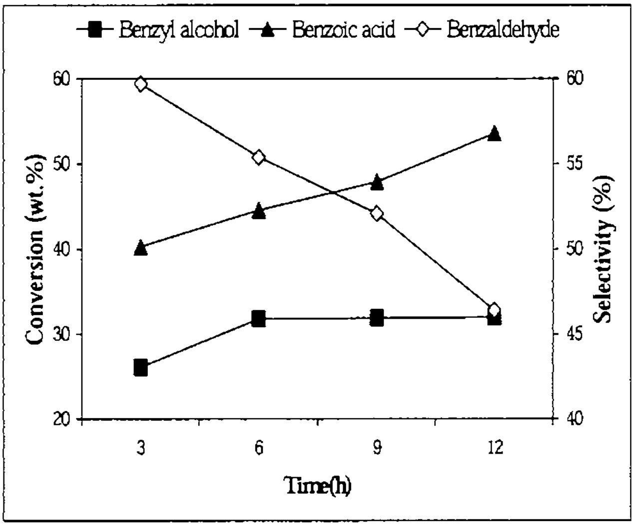

Reaction conditions: Catalyst-CCoCr-2, Temperature-80°C, Benzyl alcohol: H_2O_2 =1:4, Catalyst weight-0.1g, Solvent-10ml Acetonitrile

Figure 4.1.1: Effect of time on benzyl alcohol oxidation

After a 6 h run, a benzyl alcohol conversion of 32% was attained and this value remained steady throughout. Selectivity towards benzaldehyde decreased continuously while the reverse occurred for benzoic acid. This may be because consecutive oxidation of product benzaldehyde was favored with increasing time. A time on stream of 6 h was selected for further studies.

4.1.2.2 Effect of Temperature

The effect of temperature on benzyl alcohol oxidation was studied in a temperature range of 25-80°C while all other parameters were kept constant. Results are presented in figure 4.1.2.

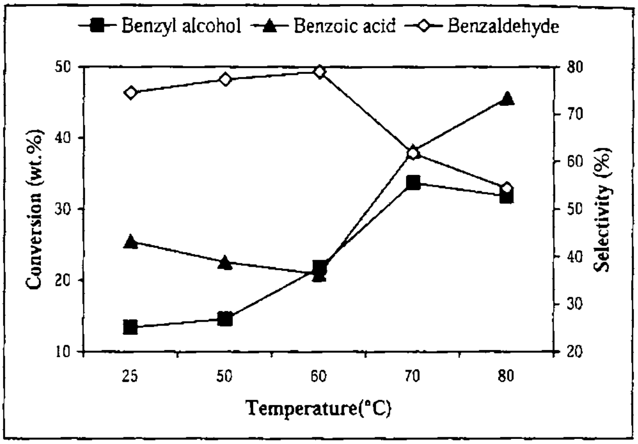

Reaction conditions: Catalyst-CCoCr-2, Time-6 h, Benzyl alcohol: H_2O_2 =1: 4, Catalyst weight-0.1g, Solvent-10ml Acetonitrile

Figure 4.1.2: Effect of temperature on benzyl alcohol oxidation

As temperature increased, benzyl alcohol conversion also increased till 70°C and later a decrease was observed. This decrease may be attributed to enhanced decomposition of H_2O_2, which was facilitated at higher temperature. Benzaldehyde selectivity increased up to 60°C. At higher temperatures, benzoic acid selectivity increased at the expense of benzaldehyde selectivity. This may be related to the activation energies for the reaction; higher temperature favor reactions with higher activation energy. Higher temperature also favors the successive steps in consecutive reactions. A temperature of 60°C was selected for further studies so that higher benzaldehyde selectivity was obtained.

4.1.2.3 Effect of Reactant Mole Ratio

Figure 4.1.3 summarizes the influence of molar ratio of benzyl alcohol to H_2O_2 in the oxidation over CCoCr-2 catalyst.

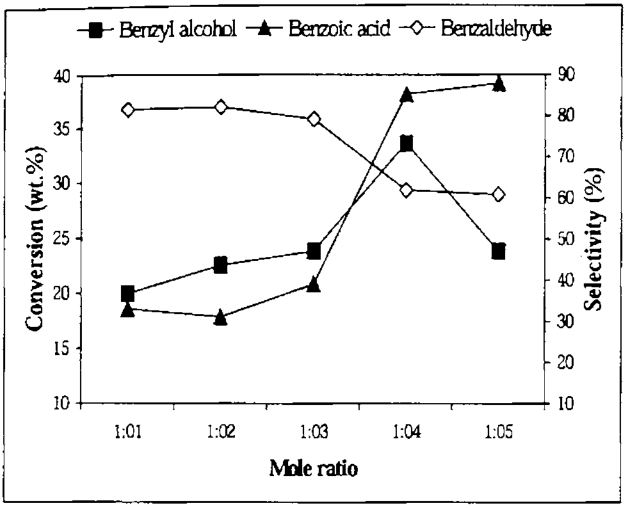

Reaction conditions: Catalyst-CCoCr-2, Time-6 h, Temperature-70°C, Catalyst weight-0.1g, Solvent-10 ml Acetonitrile

Figure 4.13: Effect of mole ratio on benzyl alcohol oxidation

Benzyl alcohol conversion increased up to a mole ratio of 1:4 after which a decrease was observed. This may be due to an enhancement of self-decomposition of oxidant at higher concentration. Formation of benzoic acid was promoted with increasing amount of oxidant. The presence of excess oxidant favored further oxidation of initially favored product, benzaldehyde. A mole ratio of 1:2 was selected.

4.1.2.4 Effect of Catalyst Weight

The activities for benzyl alcohol oxidation over CCoCr-2 with different catalyst amount are presented in figure 4.1.4.

Benzyl alcohol conversion remained steady initially and later showed a moderate decrease. This was because a large amount of the catalyst hastened the decomposition of H_2O_2. An amount of 0.1g of catalyst was selected.

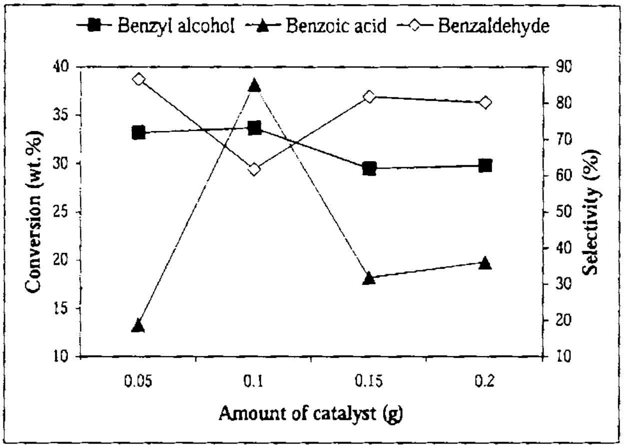

Reaction conditions: Catalyst-CCoCr-2, Time-6 h, Temperature-70°C, Mole ratio- 1:4, Solvent-10ml Acetonitrile

Figure 4.1.4: Effect of catalyst weight on benzyl alcohol oxidation

4.1.2.5 Effect of Solvent

To investigate the role of solvent on the oxidation of benzyl alcohol, reaction was carried out in methanol, dichloromethane, benzene and acetonitrile. The influence of these solvents on benzyl alcohol conversion is shown in figure 4.1.5.

The enhanced activity and moderate selectivity of the catalysts in acetonitrile could be explained on the basis of polarity of these solvents. In organic solvent the reaction is initiated by electron transfer at the interface leading to the radical cation of the substrate and super oxide anion while in the aqueous solution, the actual active species are assumed to be hydroxyl radicals formed by oxidation of solvent. Acetonitrile is an aprotic solvent. The activity of the catalysts was found to increase with the solvent polarity and acetonitrile having more polar nature always enhanced the activity. In this solvent, the phase separation between the aromatic substrate and the aqueous oxidant was greatly decreased thereby allows an easy transport of the active oxygen species for the oxidation.

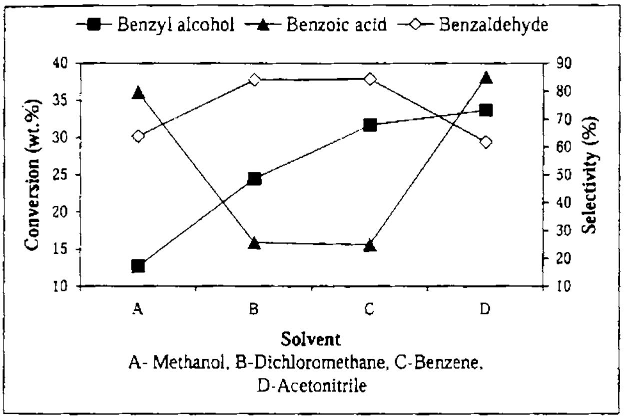

Reaction conditions: Catalyst-CCoCr-2, Time-6 h, Temperature-70°C, Mole ratio- 1:4, Catalyst weight-0.1g, Solvent volume-10ml

Figure 4.1.5:Effect of solvents on benzyl alcohol oxidation

4.1.3 Benzyl Alcohol Oxidation over the Prepared Catalysts

The oxidation of benzyl alcohol reaction was carried out over all the prepared catalysts under the selected reaction conditions (table 4.1.1) with the aim to produce benzaldehyde more selectively.

Table 4.1.1: Optimized reaction conditions for benzyl alcohol oxidation

Reaction Parameters		Selected condition
Temperature	:	60°C
Time		6 h
Benzyl alcohol: H_2O_2 ratio		1:2
Catalyst weight		0.1 g
Solvent	:	Acetonitrile 10 ml

The activity for benzyl alcohol oxidation over the five series of chromite spinel catalysts is presented in table 4.1.2.

Table 4.1.2: Catalytic activity of spinels in benzyl alcohol oxidation

Catalyst	Benzyl alcohol conversion (wt %)	Selectivity (%)	
		Benzaldehyde	Benzoic acid
CCr	20.3	84.2	15.8
CFCr-1	24.0	78.7	21.3
CFCr-2	24.3	90.7	9.3
CFCr-3	30.2	73.6	26.4
CF	21.2	73.9	26.1
CMCr-1	26.5	72.4	27.6
CMCr-2	27.2	68.1	31.9
CMCr-3	26.8	61.5	38.5
MCr	15.9	58.9	41.0
CCoCr-1	26.6	80.6	19.4
CCoCr-2	27.3	76.4	23.6
CCoCr-3	24.1	67.1	32.9
CoCr	27.1	65.9	34.1
CNCr-1	21.9	86.7	13.3
CNCr-2	26.2	60.5	39.5
CNCr-3	26.1	66.6	33.4
NCr	15.9	73.9	26.1
CZCr-1	21.6	85.6	14.4
CZCr-2	27.4	67.1	32.9
CZCr-3	19.6	80.2	19.8
ZCr	15.1	73.1	26.9

4.1.4 Regeneration and Stability

To study the stability of the catalysts, recycling experiments with regenerated catalysts were carried out. The procedure adopted was as follows. After 6 h reaction, the catalyst was recovered by hot filtration, washed several times with acetone, dried at 80°C overnight and calcined for 8 h at 650°C. The recovered catalysts were reused for benzyl alcohol oxidation under the same reaction conditions. The result obtained with regenerated catalysts is presented in table 4.1.3.

Table 4.1.3: Activity of regenerated catalysts

Catalyst	Cycle	Benzyl alcohol conversion (wt %)	Product selectivity (%)	
			Benzaldehyde	Benzoic acid
CNCr-2	1	26.2	60.5	39.5
	2	25.9	65.3	34.7
	3	22.9	76.6	23.4
	4	19.5	74.8	25.2

Benzyl alcohol conversion remained almost constant for the first two cycles and showed a decrease for the third and fourth cycle. There was a significant variation in benzaldehyde selectivity up to the third cycle, after which it remained nearly constant.

4.1.5 Discussions

The oxidation of benzyl alcohol to benzaldehyde was carried out over copper chromite and transition metal substituted copper chromite spinel catalysts. In almost all catalysts, above 20% benzyl alcohol conversion was achieved along with more than 60% selectivity towards benzaldehyde. It was observed that the product benzaldehyde had a tendency to oxidize to benzoic acid under the same reaction conditions. Another observation was that simple chromites were less active than mixed chromite systems.

Iron substitution lead to an enhancement in the catalytic activity of copper chromite. On iron substitution, benzyl alcohol conversion increased whereas copper ferrite showed less activity than the solid solutions. In spinel catalysts, octahedral metal ions are exposed to the surface and are more active in catalytic reactions. In solid solutions containing both chromium and iron in octahedral position are exposed to surface and they showed higher activity. Among these systems, CFCr-3 showed maximum benzyl alcohol conversion and moderate selectivity to benzaldehyde.

Substitution of copper by manganese in copper chromite spinel improved the catalytic activity. Among manganese containing solid solutions, the catalyst with composition $Cu_{0.5}Mn_{0.5}Cr_2O_4$ showed maximum conversion (copper and manganese are in 1:1 ratio in the tetrahedral position). Though the catalytic activities of spinels depend mainly on the octahedral metal ion, tetrahedral metal ions may have some influence. Manganese chromite exhibited the lowest activity in this series of spinel catalysts.

Cobalt substitution increased the catalytic activity of copper chromite spinel. Benzaldehyde selectivity was lowered upon cobalt substitution. This may be because cobalt enhanced the successive oxidation of benzaldehyde.

Nickel substituted copper chromites were more active than the parent spinel. A higher conversion was achieved with the catalyst $Cu_{0.5}Ni_{0.5}Cr_2O_4$. Nickel chromite showed the least activity. There was a significant improvement in benzaldehyde selectivity also. Similarly, zinc substitution enhanced the catalytic activity of copper chromite. A greater alcohol conversion was achieved with $Cu_{0.5}Zn_{0.5}Cr_2O_4$. Zinc chromite showed the least activity.

4.1.6. Mechanism of the reaction

Different mechanisms have been suggested by various authors for the oxidation of benzyl alcohol with hydrogen peroxide. Zbigniew has reported the mechanism and kinetics of epoxidation of allyl alcohol by H_2O_2 with tungstic acid as a catalyst[12]. A peroxo complex formed from the tungstic acid and H_2O_2 acts as an oxidizing agent. Venturello and Ricci have proposed that the oxidative cleavage of 1, 2-diols to carboxylic acids by H_2O_2 in the presence of tungstate and phosphate (or arsenate) ions proceeds via formation of peroxo intermediate[13]. Jacobson et al.[14] have proposed a similar mechanism for the oxidation of monohydric alcohols catalyzed by oxodiperoxo tungstate (VI).

A plausible mechanism for the oxidation of benzyl alcohol with H_2O_2 is described below. At first, a peroxo complex is formed by the reaction between H_2O_2 and the catalyst. In the second stage, the peroxo complex and benzyl alcohol react to give an intermediate. This intermediate, on loss of water molecule, gives benzaldehyde and the regenerated catalyst.

4.1.7. Conclusions

The summary of the results of the various studies is presented below:

- Copper chromite and transition metal substituted copper chromites effectively catalyzed the oxidation of benzyl alcohol with hydrogen peroxide.
- The reaction always gave benzaldehyde as the oxidation product and benzoic acid was formed by the oxidation of benzaldehyde.
- Reaction variables such as reaction time, temperature of the reaction, benzyl alcohol to hydrogen peroxide ratio, catalyst weight and solvent used are the indispensable factors influencing the catalytic activity of the systems.

- Regeneration and stability of the catalysts were studied and the results proved that they are stable up to four reaction cycles.
- Mixed solid solutions exhibited improved activity.

****

SECTION: B

4.2. OXIDATION OF STYRENE

4.2.1. Introduction

The oxidative conversion of olefins to aldehydes and ketones is important in chemical industry. The current practices can be divided into three categories: (i) the cleavage of C=C bond over materials such as osmium tetroxide and ruthenium tetroxide in stoichiometric amount[1-3], (ii) the ozonolysis of olefins to ozonides and the subsequent conversion to aldehydes or ketones in reductive workup conditions[3,4] and (iii) the oxidation of olefins by hydrogen peroxide[5,6].

Styrene oxidation is of considerable commercial and academic interest for the synthesis of important products such as benzaldehyde, styrene oxide and phenyl acetaldehyde. Two major reactions take place during styrene oxidation depending on the nature of the catalyst and the reaction conditions. They are the oxidative C=C cleavage into benzaldehyde and epoxidation followed by isomerisation into phenyl acetaldehyde. The reaction pathways involved in the styrene oxidation is shown in scheme 4.2.1.

A number of workers investigated styrene oxidation on various catalysts. In spinel catalysts, the major reaction taking place is the oxidative C=C cleavage into benzaldehyde. Ma et al.[7] studied styrene oxidation over nanosized spinel type $Mg_xFe_{3-x}O_4$ complex oxides prepared by co precipitation and citrate gel method. Their results predicted that catalysts obtained by citrate gel method are more active for oxidation of styrene with H_2O_2 as oxidant, due to their higher dispersity and smaller particle size. The presence of highly dispersed α-Fe_2O_3 in the spinel matrix was probably the cause for the increased activity of the non-stoichiometric catalysts. Manorama and co-workers reported styrene oxidation with H_2O_2 over Ni, Fe and Zn ferrites and a plausible mechanism involved in the catalytic reaction was proposed[8]. Their observations showed that, among all complex ferrites, Fe_3O_4, synthesized at around pH 7 was found to be most effective for styrene oxidation to benzaldehyde. This may be due to a large number of oxygen vacancies on the surface.

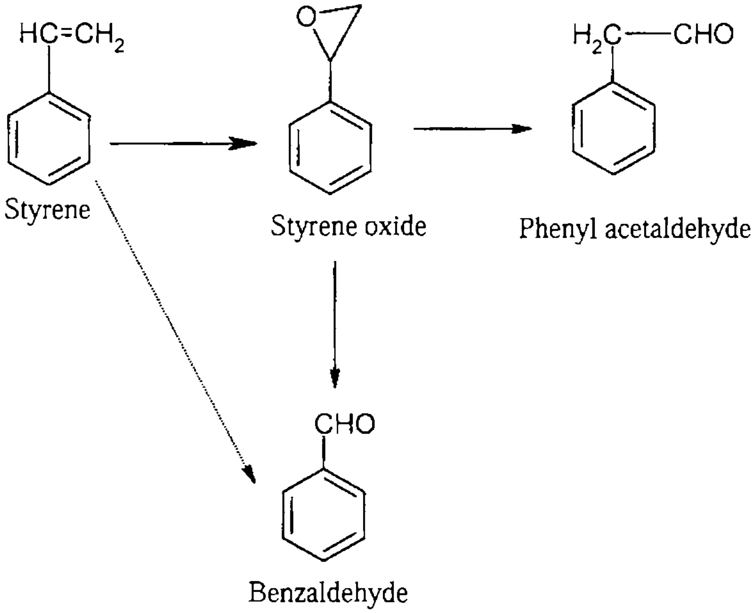

Scheme: 4.2.1: Reaction scheme of styrene oxidation

Styrene oxidation by manganese schiff base complexes in zeolite structures was studied by Silva et al.[9] They predicted that both neat and encapsulated Mn (III) complexes were active in oxidation and the catalytic activity pattern did not change upon encapsulation. The major product was benzaldehyde followed by styrene oxide. The effect of catalysts such as iron porphyrins[10], 'salen-type' Mn (III) catalysts derived from D-glucose[11] and metalloporphyrins[12] in the oxidation of styrene with various oxidants have been investigated and discussed by some workers.

Functionalized mesoporous silica was found to be better catalysts in styrene oxidation. Luo and Lin synthesized Co (II) salen functionalized MCM-41 type hybrid mesoporous silica and they are applied as catalysts for styrene oxidation with H_2O_2[13]. The silica framework kept the active sites dispersed resulting in the formation of active heterogenized catalysts for the liquid phase oxidation of styrene with excellent stability against leaching. Transition metal incorporated (Mn, V and Cr) MCM-48 materials were found to be very active in oxidation of styrene[14] and their activity depend on the nature of the transition metal used. Titanium substituted SBA-15 mesoporous molecular sieves[15,16], mesoporous nickel silicate membranes on porous alumina supports[17] and titanium silicalite zeolites[18] were found to be act as catalysts in styrene oxidation.

In this section, a detailed investigation of the prepared spinel catalysts for styrene oxidation with TBHP as oxidant has been carried out. In addition, the influence of reaction parameters such as reaction time, temperature, styrene: TBHP mole ratio, catalyst weight and effect of solvent have also been discussed.

4.2.2. Influence of Reaction Conditions

Influence of reaction conditions is essential for a chemical reaction to occur with high percentage conversion and selectivity for products. The influence of different reaction parameters was analyzed in order to maximize the product yield and selectivity. Effect of reaction conditions for styrene oxidation with TBHP was initially assayed in non-optimized conditions with CCoCr-2 as the catalyst.

4.2.2.1. Effect of Time

In heterogeneous catalysis the formation and selectivity of products always depends upon the reaction time. Effect of time on styrene oxidation is shown in figure 4.2.1.

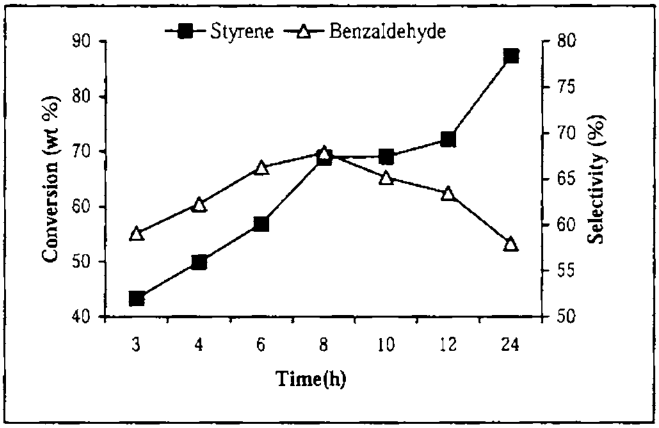

Reaction conditions: Catalyst-CCoCr-2, Temperature-70°C, Styrene: TBHP=1:2, Catalyst weight-0.1g, Solvent-10ml Acetonitrile

Figure: 4.2.1: Effect of time on styrene oxidation

Styrene conversion increased with reaction time. Benzaldehyde selectivity increased steadily up to 8 h and later declined. As time progressed, formation of other side products increased, resulting in reduced benzaldehyde selectivity. A time on stream of 8 h was selected in order to get maximum selectivity to benzaldehyde.

4.2.2.2. Effect of Temperature

The dependence of reaction temperature on benzaldehyde production was studied by varying the temperature between 50 and 80°C while other parameters were kept constant. Results are presented in figure 4.2.2.

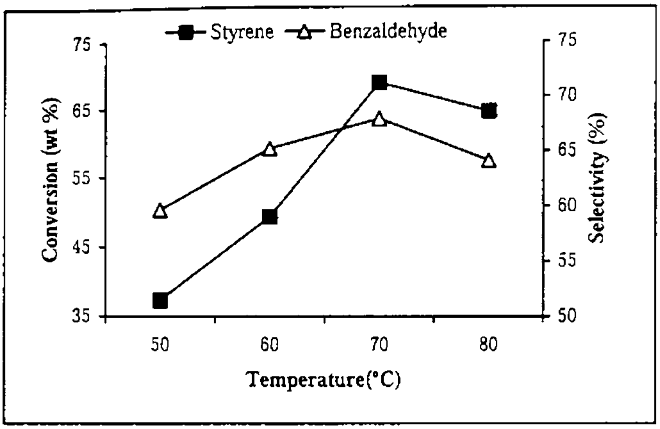

Reaction conditions: Catalyst-CCoCr-2, Time-8 h, Styrene: TBHP= 1:2, Catalyst weight-0.1g, Solvent-10ml Acetonitrile

Figure: 4.2.2: Effect of temperature on styrene oxidation

When reaction temperature was raised, styrene conversion improved dramatically up to 70°C after which a decrease was observed. Higher temperature favored C=C bond cleavage which explained the increase in conversion. Benzaldehyde selectivity showed a similar behavior but with a moderate increase only. Above 70°C, self-decomposition of TBHP proceeded faster and it did not participate effectively in the oxidation process. Similarly, formation of styrene polymers was observed and hence a decreased selectivity towards benzaldehyde occurred. A temperature of 70°C was selected for further studies.

4.2.2.3. Effect of Reactant Mole Ratio

The effect of the styrene to TBHP mole ratio on the oxidation was investigated and the results are shown in figure 4.2.3.

Styrene conversion increased dramatically with increased concentration of TBHP and the value touched 100% at a mole ratio of 1:5. Selectivity to benzaldehyde showed a marginal variation only. Moderate conversion and maximum selectivity was achieved with a mole ratio of 1:2 and this concentration was selected for the further studies of the reaction.

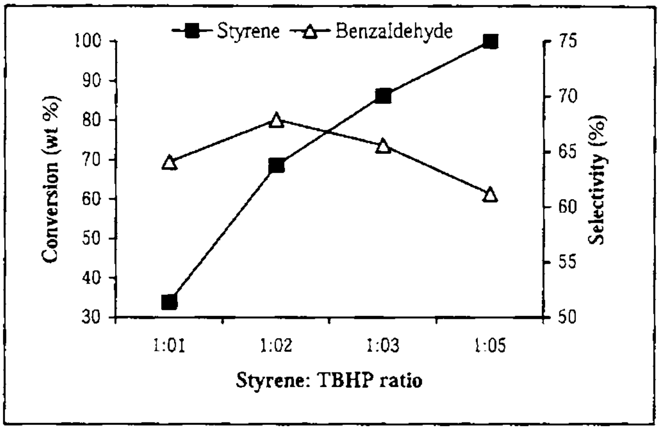

Reaction conditions: Catalyst-CCoCr-2, Temperature-70°C, Time-8 h, Catalyst weight-0.1g, Solvent-10ml Acetonitrile

Figure: 4.2.3. Effect of mole ratio on styrene oxidation

4.2.2.4. Effect of Catalyst weight

The dependence of the amount of the catalyst on the production of benzaldehyde is presented in figure 4.2.4.

When the amount of catalyst was increased to 0.1g, styrene conversion increased significantly. Later it showed a marginal decrease with higher catalyst amounts. Selectivity towards benzaldehyde was nearly constant initially and showed a moderate decrease at higher amounts of catalyst. The dependence of product formation on catalyst concentration suggested that the reaction proceeded in a purely heterogeneous fashion. The catalyst amount selected was 0.1g.

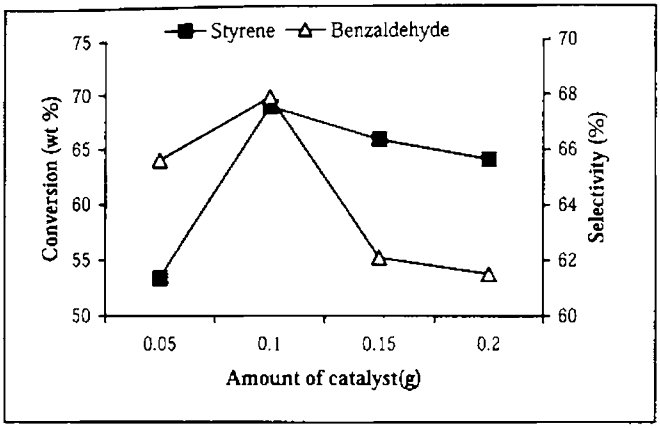

Reaction conditions: Catalyst-CCoCr-2, Temperature-70°C, Time-8h, Styrene: TBHP ratio-1: 2, Solvent-10ml Acetonitrile

Figure: 4.2.4. Effect of catalyst weight on styrene oxidation

4.2.2.5. Effect of Solvent

In order to investigate the role of solvent, the oxidation of styrene was carried out in propan-2-ol, benzene, methanol and acetonitrile. The influence of these solvents on styrene conversion is shown in figure 4.2.5.

The reaction media had a strong influence on the activity of the catalysts. Acetonitrile was found to be the best solvent in terms of both conversion and selectivity. The enhanced activity and selectivity of the catalysts in acetonitrile could be explained on the basis of polarity of these solvents. In organic solvent, the reaction was initiated by electron transfer at the interface leading to the radical cation of the substrate and super oxide anion while in the aqueous solution, the actual active species were assumed to be hydroxyl radicals formed by oxidation of solvent. The activity of the catalysts was found to increase with the solvent polarity. Acetonitrile, an aprotic solvent had more polarity which explained the enhanced activity. In this solvent, the phase separation between the aromatic substrate and the aqueous oxidant was greatly decreased thereby an easy transport of the active oxygen species took place.

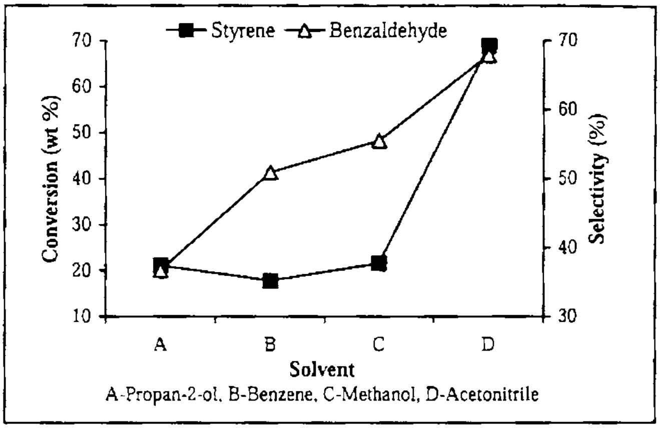

Reaction conditions: Catalyst-CCoCr-2, Temperature-70°C, Time-8 h, Catalyst weight-0.1g, Solvent volume-10ml

Figure: 4.2.5. Effect of solvent on styrene oxidation

4.2.3. Styrene Oxidation over the Prepared Catalysts

The oxidation of styrene was carried out over all the prepared catalysts under the selected reaction conditions (table 4.2.1). Improved selectivity to benzaldehyde was the major concern.

Table 4.2.1: Optimized reaction conditions for styrene oxidation

Reaction Parameters		Selected condition
Temperature	:	70°C
Time		8 h
Styrene: TBHP ratio		1:2
Catalyst weight		0.1 g
Solvent	:	10 ml Acetonitrile

Table 4.2.2 shows the activity for styrene oxidation over the five series of chromite spinel catalysts.

Table 4.2.2: Catalytic activity of spinels in styrene oxidation

Catalyst	Styrene conversion (wt %)	Benzaldehyde (%)
CCr	49.5	76.7
CFCr-1	50.7	62.9
CFCr-2	66.9	70.9
CFCr-3	50.8	74.1
CF	46.4	75.6
CMCr-1	48.7	59.3
CMCr-2	48.9	65.0
CMCr-3	30.9	61.5
MCr	28.4	54.6
CCoCr-1	61.1	70.4
CCoCr-2	68.9	67.9
CCoCr-3	47.8	69.9
CoCr	29.5	64.1
CNCr-1	58.1	72.4
CNCr-2	65.4	71.5
CNCr-3	52.4	74.2
NCr	16.2	62.0
CZCr-1	44.6	65.6
CZCr-2	62.4	64.6
CZCr-3	52.5	69.6
ZCr	31.6	72.1

4.2.4. Regeneration and Stability

The stability of the catalysts was tested by recycling experiments with regenerated catalysts. They were carried out as follows. After 8 h reaction, the catalyst was recovered by hot filtration, washed several times with acetone, dried at 80°C overnight and calcined for 8 h at 650°C. The recovered catalysts were reused for styrene oxidation under the same reaction conditions. The result obtained with regenerated catalysts is presented in table 4.2.3.

Table 4.2.3. Activity of regenerated catalysts

Catalyst	Cycle	Styrene conversion (wt %)	Benzaldehyde (%)
CZCr-2	1	62.4	64.6
	2	64.2	66.6
	3	63.8	68.5
	4	61.1	67.5

There was no significant change in styrene conversion and benzaldehyde selectivity during all cycles. The catalyst demonstrated good reusability and regenerability.

4.2.5. Discussions

Styrene oxidation was carried out over all the catalysts using TBHP as oxidant. Moderate styrene conversion and good selectivity to benzaldehyde were obtained in all the catalysts. Copper chromite showed about 50% styrene conversion. Iron substitution had an enhanced effect on the activity of copper chromite. Among the iron systems, CFCr-2 showed maximum conversion of 77% and had a benzaldehyde selectivity of 71%. Spinel solid solutions were more active than simple spinels. Iron and chromium on the octahedral site of the spinel had improved activity since the catalytic activity of spinels mainly depends on the metal ion on the octahedral position. Copper ferrite was least active among this series of spinel catalysts.

Manganese substitution led to a decrease in activity of copper chromite spinel. All the manganese-substituted spinels were less active than copper chromite and manganese chromite was the least active catalyst among that series. CMCr-2 showed maximum conversion of about 50%. Among cobalt substituted copper chromites, cobalt substitution first increased the catalytic activity and at higher composition of cobalt, the activity decreased. In this case too, the activity of cobalt chromite was low compared to the solid solutions.

Nickel substitution had also improved the activity of copper chromite towards styrene oxidation. Among nickel-substituted series, CNCr-2 with equal ratio of nickel and copper in the tetrahedral position exhibited maximum activity towards styrene oxidation. Nickel chromite was the least active catalyst among all the systems studied. CZCr-2 was found to be the most active in the zinc substituted copper chromite spinels. It gave a styrene conversion of 62.4% with 64.6% selectivity to benzaldehyde.

From all the above observations, it was concluded that copper chromite and transition metal substituted copper chromites were active in the oxidation of styrene with TBHP and simple chromites were less active than the spinel solid solutions.

4.2.6. Mechanism of the reaction

Two reaction pathways are involved in the oxidation of styrene. They are the oxidative double bond cleavage on styrene to benzaldehyde and epoxidation of styrene to styrene oxide and further isomerisation to phenyl acetaldehyde. A proposed mechanism for the oxidation of styrene to benzaldehyde was described in scheme 4.2.2. A radical chain reaction (one electron transferred), leading to benzaldehyde, in which the TBHP molecularity is two is proposed.

$$2\ C(CH_3)_3OOH \longrightarrow C(CH_3)_3O^{\cdot} + C(CH_3)_3OO^{\cdot} + H_2O$$

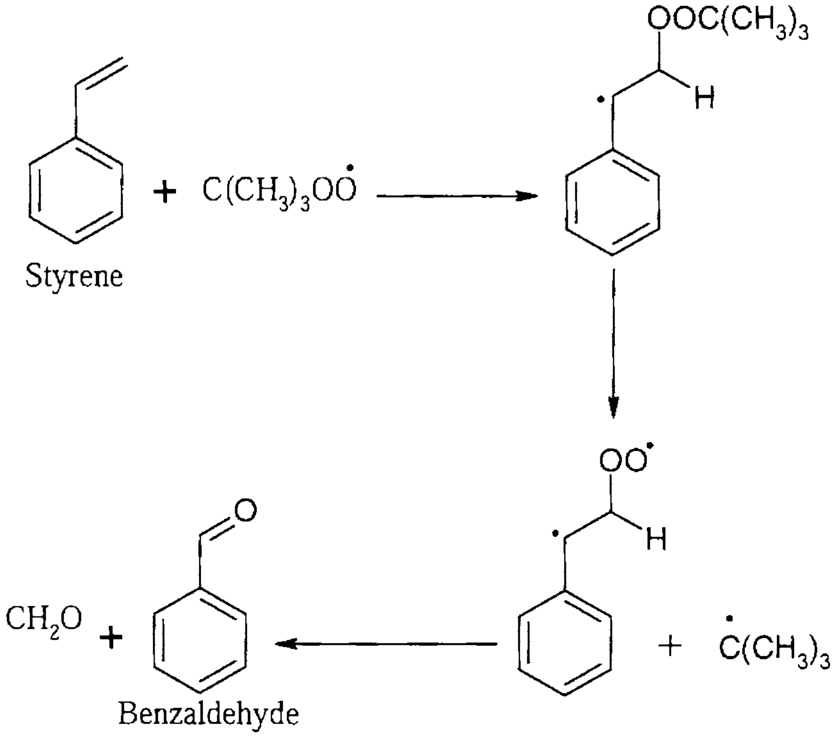

Scheme 4.2.2: Proposed mechanism for oxidation of styrene in the presence of TBHP

4.2.7. Conclusions

The summary of the results of styrene oxidation reaction is given below.

- ✓ Copper chromite and transition metal substituted copper chromite catalysts effectively catalyzed styrene oxidation with TBHP.

- ✓ The reaction gave benzaldehyde as the major product formed by the oxidative cleavage of C=C of styrene.
- ✓ Reaction parameters such as time, temperature, styrene: TBHP ratio, catalyst weight and effect of solvents were studied in detail and reaction conditions were optimized.
- ✓ Regeneration and stability of the catalysts were also studied and found that the catalyst was stable up to the four cycles studied.
- ✓ A possible radical chain mechanism involving single electron transfer was proposed for the formation of benzaldehyde from styrene.

****

SECTION: C

4.3. OXIDATION OF CYCLOHEXANE

4.3.1. Introduction

The selective oxidation of cyclohexane is one of the most challenging and promising subjects from synthetic and industrial point of view[1,2], because this process produces an important K/A oil (a mixture of cyclohexanone and cyclohexanol) intermediate in the petroleum industrial chemistry. Such oil can be used for the production of adipic acid and ε- caprolactum, which are key materials for manufacturing nylon-6,6 and nylon-6 respectively[3]. More than 10^6 tonnes of cyclohexanone and cyclohexanol are produced world wide per annum[4]. Modern industrial methods usually require high pressure and temperature when using soluble cobalt as catalyst, which has led to the realization of high selectivity (about 80 %) for the sum of cyclohexanone and cyclohexanol only at a low conversion (1-4 mol %), since the products, cyclohexanone and cyclohexanol, are substantially more reactive than the cyclohexane reactant. Thus, it is difficult to receive high conversion and selectivity simultaneously under mild conditions. Commonly used oxidants are molecular oxygen, hydrogen peroxide and alkyl hydro peroxide. The reaction pathways involved in the cyclohexane oxidation is shown in scheme 4.3.1.

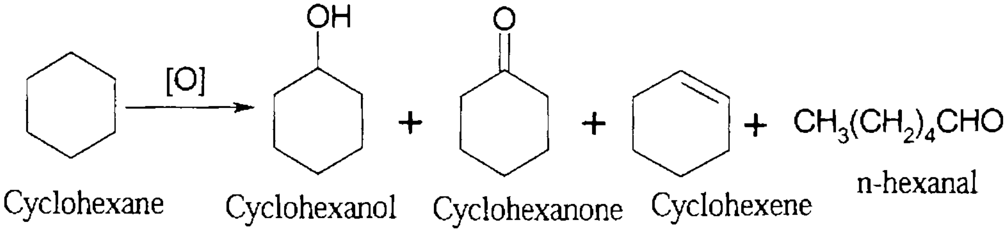

Scheme: 4.3.1. Reaction scheme of cyclohexane oxidation

Many efforts have been made to develop new catalysts to oxidize cyclohexane under mild conditions with high selectivity for the target products using different oxidizing agents[5,6]. A noteworthy development in this regard was the results by Thomas et al. in that their catalyst, FeAlPO-31, allowed for a clean, solvent free one step process, albeit with a significant co-production of adipic acid[7]. Zhou et al. prepared nanocrystals of Co_3O_4 and found it as an effective catalyst in cyclohexane oxidation to K/A oil with molecular oxygen as oxidant[8]. A better conversion of 7.6% conversion and 89.1% selectivity towards desired products was obtained for a reaction time of six hour and they proposed a free radical mechanism for cyclohexane oxidation. Redox metals such as Ti, Co, Fe and Cr were incorporated into the framework of TUD-1 by Maschmeyer and co-workers[9] and cyclohexane oxidation was studied over these catalysts. A conversion close to 3% was achieved with 85% selectivity towards the desired products over Fe and Ti-TUD-1. Bellifa et al. prepared 20 wt% V_2O_5-TiO_2 mixed oxides by sol-gel route and studied cyclohexane oxidation in the presence of acetic acid as solvent and acetone as initiator. The catalyst showed an appropriate 8% conversion with 76% selectivity towards K/A oil[10].

Metal containing mesoporous materials such as Ti-MCM-41, Cr-MCM-41, V-MCM-41, Bi-MCM-41 and V-MCM-48 were applied to catalyze the oxidation of cyclohexane[11-18]. Metal complexes and metal containing zeolites were also used as catalysts for this oxidation reaction[19-26]. Elements such as V, Sn, Cr, Zr and W could have been immobilized in crystalline or amorphous silica matrices[27-34]. The activity of these materials in liquid phase oxidation had generally been correlated with the redox properties of these elements.

4.3.2. Influence of Reaction Conditions

The influence of different reaction parameters was analyzed in order to maximize the product yield and selectivity. Effect of reaction conditions for cyclohexane oxidation with TBHP was initially assayed in non-optimized conditions with CNCr-2 as the catalyst.

4.3.2.1. Effect of Time

The influence of reaction time on cyclohexane conversion and product selectivity is shown in figure 4.3.1.

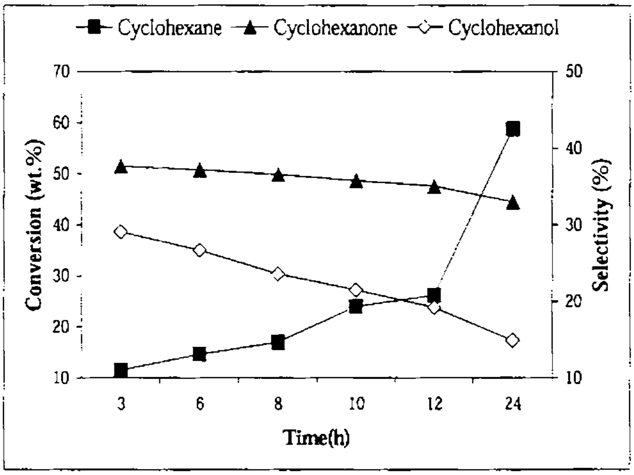

Reaction conditions: Catalyst-CNCr-2, Temperature-70°C, Cyclohexane: TBHP =1:2, Catalyst weight-0.1g, Solvent-10ml Acetonitrile

Figure 4.3.1: Effect of time on cyclohexane oxidation

Cyclohexane conversion increased with time. A high conversion of about 59% was achieved at 24 hours. The ketone selectivity was found to be increased with time correspondingly a decrease in selectivity of the alcohol was observed. The decrease in selectivity of cyclohexanol could be explained as follows. The catalyst was active and well promoted reaction with cyclohexanol, possibly the oxidation to form cyclohexanone. Also cyclohexanol was dehydrated to form cyclohexene.

Moderate cyclohexane conversion and K/A oil selectivity was obtained after 10 h reaction and this time was selected for further investigations.

4.3.2.2. Effect of Temperature

The dependence of reaction temperature on cyclohexane was studied by carrying out this reaction at various reaction temperatures from 60°C to 90°C and the results are given in figure 4.3.2.

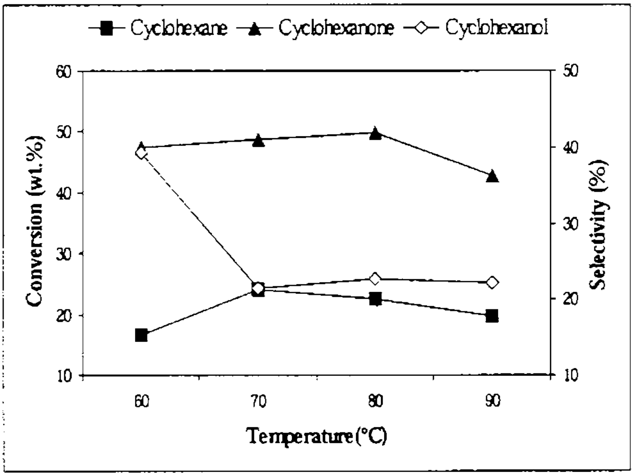

Reaction conditions: Catalyst-CNCr-2, Time-10 h, Cyclohexane: TBHP =1:2, Catalyst weight-0.1g, Solvent-10ml Acetonitrile

Figure 4.3.2: Effect of temperature on cyclohexane oxidation

Cyclohexane conversion reached about 24% when temperature reached 70°C with 71% selectivity to K/A oil. The percentage conversion was 16.6% when the temperature was 60°C. An increase in temperature increased the conversion rate up to 70°C and then decreased. From the results it could be concluded that the oxidation of cyclohexane proceeded with high activity and selectivity under gentle reaction temperature. The decomposition of TBHP to alcohol and oxygen will take place at higher temperatures and cannot be consumed during the reaction. An optimum temperature of 70°C was selected for further studies.

4.3.2.3. Effect of Mole Ratio

The effect of cyclohexane: TBHP ratio in the oxidation of cyclohexane is presented in figure 4.3.3.

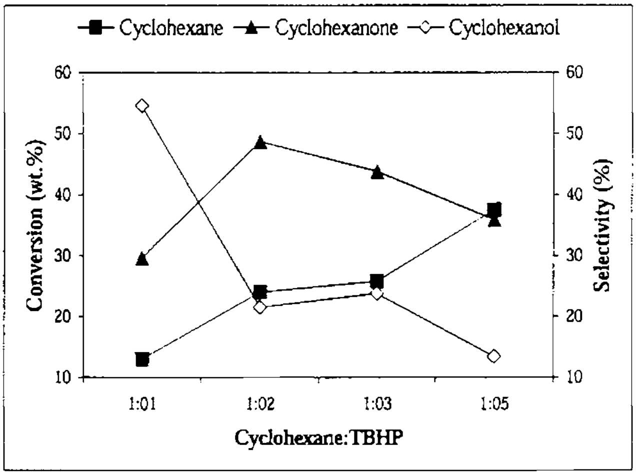

Reaction conditions: Catalyst-CNCr-2, Time-10 h, Temperature-70°C, Catalyst weight-0.1g, Solvent-10ml Acetonitrile

Figure 4.3.3: Effect of Cyclohexane: TBHP ratio on cyclohexane oxidation

Cyclohexane conversion increased with increase in volume of TBHP. Meanwhile, the selectivity of K/A oil decreased and the selectivity of cyclohexene, the dehydrated product of cyclohexanol was increased. About 50% cyclohexene was obtained at a cyclohexane: TBHP ratio of 1:5. Moderate conversion and selectivity to the desired products were obtained with a mole ratio of 1:2 and this was taken as the optimum ratio for further studies.

4.3.2.4. Effect of Catalyst weight

In heterogeneous catalysis, the amount of the catalyst plays an important role in determining the rate of the reaction. To study this, the catalyst weight was varied by taking different amount of CNCr-2 catalyst. Figure 4.3.4 shows the influence of catalyst weight on the cyclohexane oxidation reaction.

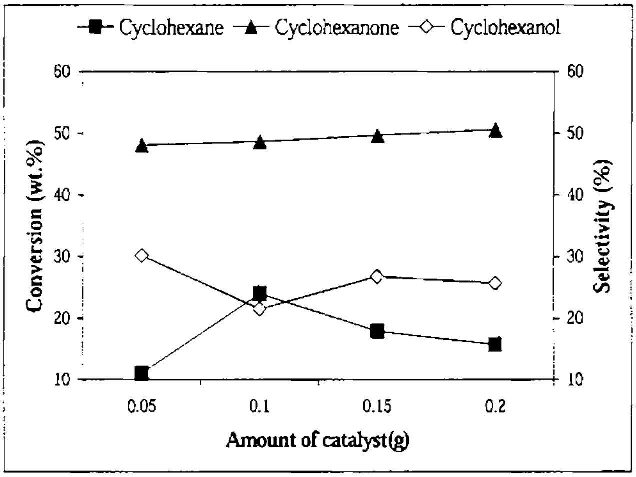

Reaction conditions: Catalyst-CNCr-2, Temperature-70°C, Time-10 h, Cyclohexane: TBHP-1: 2, Solvent-10 ml Acetonitrile

Figure 4.3.4: Effect of catalyst weight on cyclohexane oxidation

An initial sharp increase in percentage conversion was observed when the catalyst amount was increased to 0.1g. After that percentage conversion reduced and then remained almost constant. A gradual change in the product selectivity was also noticed with change in catalyst weight. An optimum catalyst weight of 0.1g was selected for the present reaction, considering the percentage conversion and product selectivity.

4.3.2.5. Effect of Solvent

Catalytic activity depends largely on the nature of the solvent used. So it is necessary to find out an ideal solvent for the oxidation of cyclohexane with TBHP as the oxidant. The influence of solvents like benzene, methanol, dichlorobenzene and acetonitrile on the oxidation is presented in figure 4.3.5.

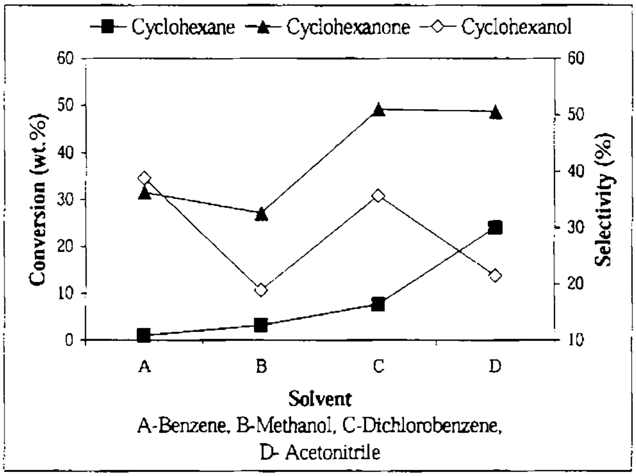

Reaction conditions: Catalyst-CNCr-2, Time-10 h, Temperature-70°C, Cyclohexane: TBHP-1:2, Catalyst weight-0.1g, Solvent volume-10ml

Figure 4.3.5: Effect of solvent on cyclohexane oxidation

No considerable conversion was obtained on solvents like benzene, dichlorobenzene and methanol. Acetonitrile was selected as the solvent for this reaction as moderate conversion and selectivity to desired products obtained with this solvent.

4.3.3 Cyclohexane Oxidation over the Prepared Catalysts

The above observations revealed that reaction parameters play an important role in determining the oxidation rate and product selectivity in the liquid-phase oxidation of cyclohexane using TBHP as oxidant. The oxidation of cyclohexane reaction was carried out over all the prepared catalysts under the selected reaction conditions (table 4.3.1) in order to produce the desired product K/A oil more selectively.

Table 4.3.1: Optimized reaction conditions for cyclohexane oxidation

Reaction Parameters		Selected condition
Temperature	:	70°C
Time		10 h
Cyclohexane: TBHP ratio		1:2
Catalyst weight		0.1 g
Solvent	:	Acetonitrile 10 ml

Table 4.3.2 shows the activity for cyclohexane oxidation over the five series of chromite spinel catalysts.

Table 4.3.2: Catalytic activity of spinels in cyclohexane oxidation

Catalyst	Cyclohexane conversion (wt%)	Product selectivity (%)		
		Cyclohexanol	Cyclohexanone	Cyclohexene
CCr	12.2	28.9	44.7	26.4
CFCr-1	14.2	34.5	43.4	22.1
CFCr-2	17.4	29.1	52.9	17.9
CFCr-3	19.0	24.9	47.6	27.5
CF	15.9	27.7	44.5	27.8
CMCr-1	18.5	23.9	47.5	28.6
CMCr-2	21.2	25.9	50.6	23.5
CMCr-3	18.6	26.4	44.4	29.2
MCr	16.5	28.5	44.5	27.0
CCoCr-1	22.1	19.2	45.5	35.3
CCoCr-2	20.8	21.2	49.9	28.9

CCoCr-3	20.9	20.5	45.5	34.0
CoCr	21.8	15.6	56.5	27.9
CNCr-1	15.7	26.9	46.0	27.1
CNCr-2	19.7	26.7	48.6	24.7
CNCr-3	14.9	25.1	48.2	26.7
NCr	5.4	32.9	41.4	25.6
CZCr-1	14.4	25.6	50.9	23.5
CZCr-2	16.8	23.6	52.1	24.3
CZCr-3	16.6	23.9	49.4	26.7
ZCr	23.3	12.3	64.4	23.3

4.3.4. Regeneration and Stability

To study the stability of the catalysts, recycling experiments were carried out with regenerated catalysts. The recycling experiments were carried out as follows. After 10 h reaction, the catalyst was recovered by hot filtration, washed several times with acetone, dried at 80°C overnight and calcined for 8 h at 650°C. The recovered catalysts were reused for cyclohexane oxidation under the same reaction conditions. The result obtained with regenerated catalysts is presented in table 4.3.3.

Table 4.3.3: Activity of regenerated catalysts

Catalyst	Cycle	Cyclohexane conversion (wt %)	Product selectivity (%)		
			Cyclohexanol	Cyclohexanone	Cyclohexene
CZCr-3	1	16.6	23.9	49.4	26.7
	2	18.8	22.9	45.3	31.8
	3	17.1	20.4	43.8	35.8
	4	18.4	20.1	47.5	32.4

It was observed that the activity of CZCr-3 did not decreased during the four runs. The catalytic performance remained stable, as proved by the similar conversion of cyclohexane and product selectivity for second third and fourth run. This showed that CZCr-3 was a highly active, selective and stable heterogeneous catalyst for the oxidation of cyclohexane.

4.3.5. Discussions

The liquid-phase oxidation of cyclohexane was performed over all the catalysts prepared at 70°C using TBHP as oxidant. The products obtained were cyclohexanol, cyclohexanone (K/A oil), cyclohexene and trace amount of n-hexanal. The percentage of n-hexanal was very low and was neglected. In all cases, cyclohexanone selectivity was higher than that of other two products. The reason for the higher selectivity of cyclohexanone was that, in the reaction medium, cyclohexanol formed had a tendency to oxidize to cyclohexanone. Cyclohexanol also underwent dehydration resulting in the formation of cyclohexene.

Cyclohexane oxidation over copper chromite catalyst resulted in 12.2% conversion with about 73% selectivity to K/A oil. Iron substitution had an enhanced activity towards cyclohexane oxidation and CFCr-3 gave a maximum conversion of 19%. Moderate cyclohexane conversion and good selectivity towards K/A oil was observed in all this catalyst series. Among manganese substituted copper chromites, CMCr-2 gave a maximum conversion of 21.2% with 76% selectivity to alcohol and ketone.

Cobalt substitution improved the catalytic activity of copper chromite towards cyclohexane oxidation. Cyclohexane conversion of more than 20% and good selectivity to K/A oil was observed in all cases. Though nickel substituted spinels exhibited higher conversion than copper chromite, these systems gave only below 20% conversion to cyclohexane. Among this series of spinels, CNCr-2 gave the maximum conversion of 19.7% and least activity by nickel chromite, only 5.4% conversion. Zinc substituted copper chromites were found to be the least active catalysts towards cyclohexane oxidation. Zinc chromite exhibited maximum activity with 23.3% conversion of cyclohexane.

4.3.6. Mechanism of the reaction

A proposed reaction mechanism for spinel catalyzed cyclohexane oxidation is depicted in scheme 4.3.2. TBHP is decomposed on the catalyst surface forming *t*-butoxy radicals with oxidized catalyst. These radicals abstract hydrogen from cyclohexane forming cyclohexyl radicals, which reacts with molecular oxygen from air. The cyclohexyl peroxy radicals thus formed can suffer a bimolecular Russell termination[35] to form cyclohexanone and cyclohexanol or abstract a hydrogen from cyclohexane to form cyclohexyl hydroperoxide. Hydroxy radical abstraction from cyclohexyl hydroperoxide by the catalysts forms cyclohexyloxy radicals which are in equilibrium with the open chain isomer, thus forming n-hexanal. The cyclohexyl radicals may suffer dehydrogenation to cyclohexene by reduction of the catalyst formed by the decomposition of TBHP, thus regenerating the active catalyst.

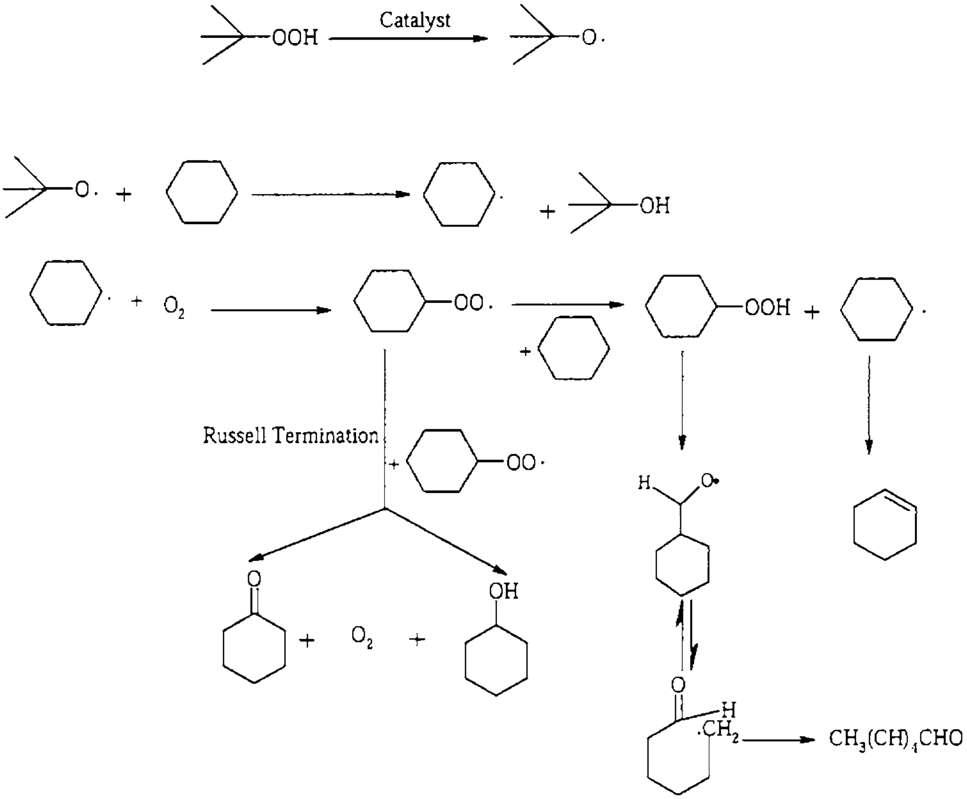

Scheme 4.3.2: Proposed mechanism for oxidation of cyclohexane

4.3.7. Conclusions

The important conclusions of the cyclohexane oxidation reaction are presented below.

- Cyclohexane was effectively oxidized by copper chromite and transition metal substituted copper chromite spinel catalysts in the presence of TBHP as oxidant.
- The major products obtained are cyclohexanol, cyclohexanone and cyclohexene. Trace amount of *n*-hexanal was also detected.

- Reaction conditions such as time, temperature, cyclohexane: TBHP ratio, catalyst weight and solvents were optimized in order to maximize the conversion and selectivity of products.
- Reusability study of the catalysts were carried out and found that the catalysts are stable up to four cycles of the reaction.
- A possible reaction mechanism involved in this oxidation was suggested.

****

SECTION: D

4.4. OXIDATION OF ETHYLBENZENE

4.4.1. Introduction

Effective utilization of ethylbenzene, available in the xylene stream of the petrochemical industry, for more value- added products is an interesting proposition. Oxidation of ethylbenzene is of much importance for the production of the aromatic ketone, acetophenone, one of the key products in the industries. It is used as a component of perfumes and as an intermediate for the manufacture of pharmaceuticals, resins, alcohols and tear gas (chloroacetophenone). The oxidation pathways of ethylbenzene are presented in scheme 4.4.1.

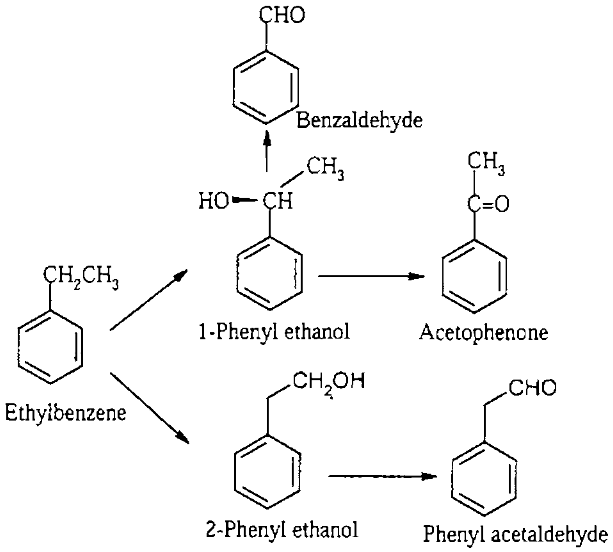

Scheme 4.4.1: Reaction scheme of ethylbenzene oxidation

Cobalt containing hexagonal mesoporous molecular sieves prepared by direct hydrothermal and post-synthesis method was found to be very effective in the oxidation of ethylbenzene to acetophenone[1]. The results showed that solvent had a negative impact over the performance of the cobalt-containing catalyst, which arouse from the blocking of active sites by the solvent molecules. Recently, Jana et al.[2] reported NiAl hydrotalcite to be an environmentally friendly solid catalyst for the liquid-phase selective oxidation of ethylbenzene to acetophenone with molecular oxygen. They have proposed a free radical mechanism in this case.

Most of the oxidations of alkyl aromatics were carried out in the slurry phase using sacrificial oxidants such as H_2O_2 and TBHP. Mal and Ramaswamy have used Ti, V and Sn containing silicates and obtained 62% product distribution of acetophenone in the low temperature region of 30-50°C under liquid phase reactions[3]. Vetrivel and Pandurangan used Mn-MCM-41 with various Si/Mn ratios and obtained 10-43% selectivity to acetophenone in the temperature range of 60-80°C with tert-butyl hydroperoxide as an oxidant[4]. Srinivas and workers have studied the catalytic effect of oxo-Mn-triazacyclononane complexes in the liquid phase oxidation of ethylbenzene[5]. The studies revealed that nuclearity and type of oxo-Mn speciation influence the catalytic activity. 1-phenylethanol and acetophenone were the benzylic oxidation products obtained along with a small amount of ortho- and para- ring hydroxylated compounds. Copper tri- and tetraaza macrocyclic complexes encapsulated in zeolite-Y exhibited good catalytic performance in the oxidation of ethylbenzene using TBHP as oxidant[6]. Acetophenone was the major product with small amounts of *o*- and *p*-hydroxyacetophenones indicating that C-H bond activation takes place both at benzylic and aromatic ring carbon atoms. Soluble acetylacetonate-nickel (II) complexes were used for ethylbenzene oxidation with quaternary ammonium salts and macrocyclic polyethers[7]. Ethylbenzene oxidation with TBHP by polynuclear Mn Schiff base complexes produced acetophenone and 1-phenyl ethanol with small amounts of peroxy compounds[8]. Selective oxidation of ethylbenzene with air produced 1-phenyl ethanol and acetophenone over dimeric metalloporphyrins[9]. According to Singh et al.[10], the redox behavior of MeAPO-11 had a potential influence on the catalytic activity during the oxidation of ethylbenzene with TBHP. Reddy and Varma[11] prepared Al_2O_3 supported V_2O_5 catalyst and the liquid phase oxidation of ethylbenzene to acetophenone was employed as a chemical probe reaction to examine the catalytic activity. Toribio et al.[12] reported the liquid-phase ethylbenzene oxidation to hydroperoxide with barium catalysts. Along with ethylbenzene hydroperoxide as the major product, small amounts of acetophenone and 1-phenyl ethanol were obtained indicating that C-H bond activation takes place only at the alkyl chain.

The oxidation of organic substrates using H_2O_2 as oxidant has been well documented[13-15]. According to Xavier et al.[16] Y- Zeolite encapsulated Co (II), Ni (II) and Cu (II) complexes gave acetophenone as the only partial oxidation product during ethylbenzene oxidation with H_2O_2. The catalytic activity was attributed to the geometry of encapsulated complexes. Titanosilicates mainly catalyze ring hydroxylation of arenes with H_2O_2; whereas vanadium and chromium substituted zeolites and an aluminophosphate molecular sieve have been known to favor side chain oxidation selectively[17]. Rebelo et al.[18] studied the oxidation of alkyl aromatics with H_2O_2 over Mn (III) porphyrins in the presence of ammonium acetate as co-catalyst. The catalysts produced acetophenone as the major product with 1-phenylethanol, 2-ethyl-1, 4-benzoquinone and styrene. Oxidation took place mainly in the benzylic positions with these catalysts. Products arising from further oxidation of acetophenone were not detected. The oxidation of alkyl benzenes with H_2O_2 over Cu (II) complexes took place selectively at the benzylic C-H bond without any oxidation in the remaining C-H bonds[19]. During liquid-phase oxidation of ethylbenzene with molecular oxygen over quaternary ammonium compounds ethylbenzene hydroperoxide was the main product[20,21].

A broad variety of catalytic systems have been described in the literature for vapour-phase oxidation of ethylbenzene with air. Vetrivel and Pandurangan have reported the catalytic behavior of Mn-MCM-41 mesoporous molecular sieves in the vapour-phase oxidation of ethylbenzene[22]. Acetophenone was obtained selectively than benzaldehyde and styrene. They have also reported this reaction over mesoporous MCM-41 and Al-MCM-41[23]. The catalytic oxidation of ethylbenzene to ethylbenzene hydroperoxide with air in liquid phase using Ni (II) complexes resulted mainly reaction byproducts as acetophenone and phenol[24]. μ-oxo dimeric metalloporphyrins[25], bis (acetylacetonate) nickel (II) and tetra-n-butyl ammonium tetrafluoro borate[26] were also employed as catalyst for this reaction.

4.4.2. Influence of Reaction Conditions

The influence of different reaction parameters was analyzed in order to maximize the product yield and selectivity since reaction conditions have a critical role in a chemical reaction. Effect of reaction conditions for ethylbenzene oxidation with TBHP was initially assayed in non-optimized conditions with CNCr-2 as the catalyst.

4.4.2.1. Effect of time

The effect of time on ethylbenzene oxidation reaction is depicted in figure 4.4.1. Ethylbenzene conversion was nearly steady up to 6 h and then increased significantly. Similarly, acetophenone selectivity, which was nearly steady, improved suddenly and then remained almost constant. Even though acetophenone was the major product of the reaction, 1-phenylethanol and a small amount of benzaldehyde were obtained as side products. Reaction time of 8 h was selected for further studies.

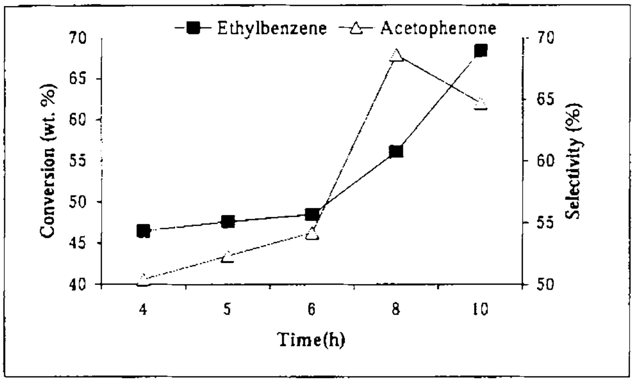

Reaction conditions: -Catalyst-CNCr-2, Temperature-70°C, EB: TBHP ratio- 1:2, Catalyst weight-0.1g, Solvent-10ml Acetonitrile

Figure 4.4.1: Effect of time on ethylbenzene oxidation

4.4.2.2. Effect of Temperature

Reaction temperature has an important role in conversion rate and product selectivity. The effect of temperature on ethylbenzene oxidation with TBHP is presented in figure 4.4. 2.

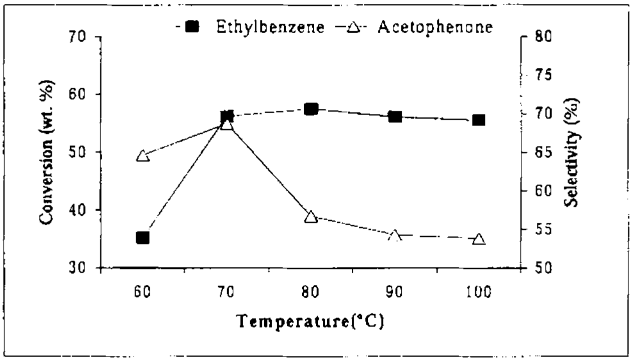

Reaction conditions: - Catalyst-CNCr-2, Time-8 h, EB: TBHP ratio- 1:2, Catalyst weight-0.1g, Solvent-10ml Acetonitrile

Figure 4.4. 2: Effect of temperature on ethylbenzene oxidation

As temperature was raised, the conversion of ethylbenzene increased initially and remained steady later. Selectivity towards acetophenone was nearly constant up to 70°C, decreased moderately at 80°C and was almost constant later on. A temperature of 70°C was selected for further studies.

4.4.2.3. Effect of reactant mole ratio

The effect of ethylbenzene: TBHP mole ratio on the oxidation of ethylbenzene is presented in figure 4.4.3.

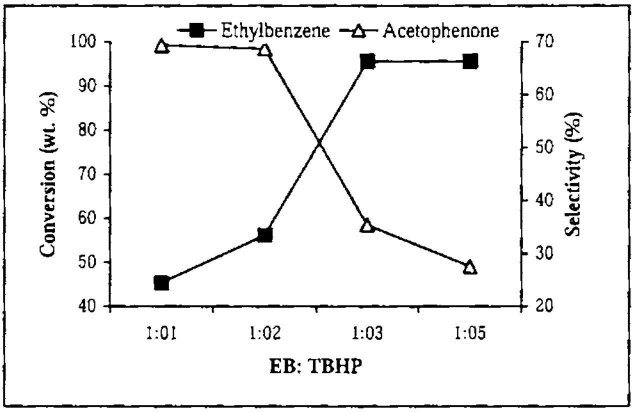

Reaction conditions: - Catalyst-CNCr-2, Time-8 h, Temperature-70°C, Catalyst weight-0.1g, Solvent-10ml Acetonitrile

Figure 4.4.3: Effect of mole ratio on ethylbenzene oxidation

A sharp increase in conversion was observed on increasing ethylbenzene: TBHP ratio up to 1:3 after which the conversion remained constant. Selectivity towards acetophenone showed the reverse trend. A higher concentration of TBHP increased the rate of conversion of 1-phenylethanol to benzaldehyde and hence a decrease in selectivity of ketone was observed. A mole ratio of 1: 2 was selected for the study.

4.4.2.4. Effect of catalyst weight

Figure 4.4.4 depicts the effect of catalyst weight on ethylbenzene oxidation.

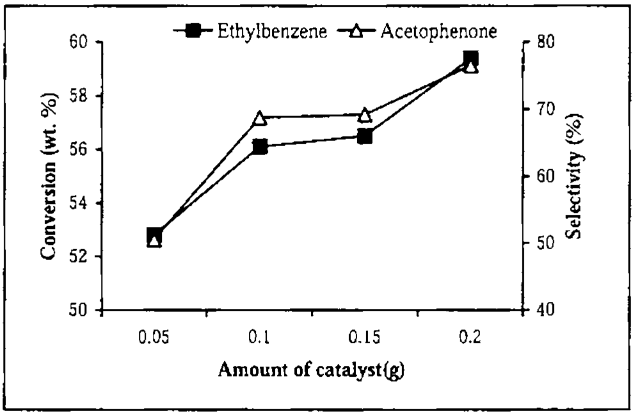

Reaction conditions: - Catalyst-CNCr-2, Time-8 h, Temperature-70°C, EB: TBHP- 1:2, Solvent-10 ml Acetonitrile

Figure 4.4.4: Effect of catalyst weight on ethylbenzene oxidation

Ethylbenzene conversion increased gradually with increasing catalyst amount. Change in acetonitrile selectivity was similar but with a more significant increase. A catalyst weight of 0.1 g was selected for further studies.

4.4.2.5. Effect of solvent

Solvents play a decisive role in liquid phase reactions in influencing both the conversion as well as product selectivity. Effect of solvents on ethylbenzene oxidation was studied and the results obtained are given in figure 4.4.5. The reaction was also carried out in the absence of solvent.

Maximum ethylbenzene conversion was observed when no solvent was used. Addition of solvent decreased the conversion. The decrease in conversion was attributed to the blocking of active sites by solvent molecules[1]. Even though maximum conversion was obtained without solvents, the reaction was carried out with 10 ml acetonitrile solvent.

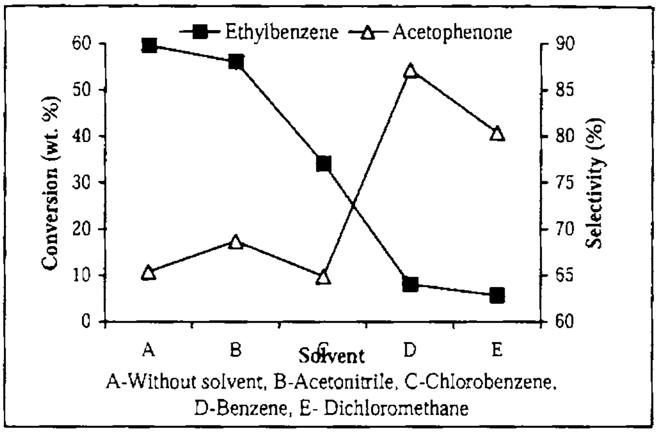

Reaction conditions: - Catalyst-CNCr-2, Time-8 h, Temperature-70°C, EB: TBHP- 1:2,Catalyst weight-0.1g, Solvent Volume-10ml

Figure 4.4.5: Effect of solvent on ethylbenzene oxidation

4.4.3. Ethylbenzene Oxidation over the Prepared Catalysts

The oxidation of ethylbenzene reaction was carried out over all the prepared catalysts under the selected reaction conditions (table 4.4.1) with an aim to produce acetophenone more selectively.

Table 4.4.1: Optimized reaction conditions for ethylbenzene oxidation

Reaction Parameters		Selected condition
Temperature	:	70°C
Time		8 h
Ethylbenzene: TBHP ratio		1:2
Catalyst weight		0.1 g
Solvent	:	Acetonitrile 10 ml

Table 4.4.2 shows the activity for ethylbenzene oxidation over the five series of chromite spinel catalysts.

Table 4.4.2: Catalytic activity of spinels in ethylbenzene oxidation

Catalyst	Ethylbenzene conversion (wt %)	Product selectivity (%)		
		Acetophenone	1-phenylethanol	Others
CCr	32.9	13.9	83.4	2.7
CFCr-1	43.3	39.1	52.6	8.3
CFCr-2	57.6	55.2	40.8	4.0
CFCr-3	60.2	55.6	26.3	18.1
CF	52.3	54.0	35.6	10.4
CMCr-1	52.7	53.8	35.7	10.5
CMCr-2	51.6	56.7	34.5	8.8
CMCr-3	52.9	62.6	27.8	9.6
MCr	37.7	52.4	35.1	12.5
CCoCr-1	50.4	65.0	29.5	5.5
CCoCr-2	52.9	65.9	28.3	5.8
CCoCr-3	55.3	61.8	36.3	2.9
CoCr	52.1	69.9	26.1	4.0
CNCr-1	44.7	51.9	46.4	1.7
CNCr-2	56.1	68.7	28.1	3.2
CNCr-3	55.5	55.6	39.6	4.8
NCr	20.2	59.1	19.4	21.5
CZCr-1	51.5	70.1	24.8	5.1
CZCr-2	53.7	57.5	33.5	9.0
CZCr-3	53.9	65.9	30.2	3.9
ZCr	49.4	66.4	30.0	3.6

4.4.4. Regeneration and Stability

To study the stability of the catalysts, recycling experiments were carried out with regenerated catalysts as follows. After 8 h reaction, the catalyst was recovered by hot filtration, washed several times with acetone, dried at 80°C overnight and calcined for 8 h at 650°C. The recovered catalysts were reused for ethylbenzene oxidation under the same reaction conditions. The result obtained with regenerated catalysts is presented in table 4.4.3.

Table 4.4.3: Activity of regenerated catalysts

Catalyst	Cycle	Ethylbenzene conversion (wt%)	Product selectivity (%)		
			Acetophenone	1-phenylethanol	Others
CZCr-3	1	53.9	65.9	30.2	3.9
	2	58.6	72.4	13.9	13.7
	3	54.9	72.8	12.7	14.5
	4	51.5	78.0	14.9	7.1

Ethylbenzene conversion remained almost constant over four catalytic runs. Acetophenone selectivity increased after first cycle and then remained nearly steady, while 1-phenylethanol selectivity decreased. It was concluded that the catalyst was stable up to four cycles.

4.4.5. Discussions

Ethylbenzene oxidation over all the prepared catalysts was carried out at 70°C in liquid phase using tertiary butyl hydro peroxide as the oxidizing agent. The major products obtained were 1-phenylethanol and acetophenone along with minor products such as phenyl acetaldehyde and benzaldehyde. These two minor products together were included in the others category. Ethylbenzene first reacted with TBHP to produce 1-phenylethanol, which was then oxidized to acetophenone, the major product.

Among the catalytic systems studied, copper chromite showed least selectivity to acetophenone. The conversion of 1-phenylethanol to acetophenone was very low in this case. Other products obtained are very less, below 3%. Iron substitution had a remarkable influence on the activity of copper chromite. About 60% conversion and 56% selectivity towards acetophenone was observed on CFCr-3 catalyst.

Manganese substituted copper chromite spinels were very active towards ethylbenzene oxidation. Above 50% ethylbenzene conversion and more than 50% selectivity towards acetophenone was observed in all the substituted catalysts. Meanwhile, manganese chromite showed the least activity among those catalytic systems.

Maximum selectivity towards acetophenone was observed on cobalt substituted copper chromite spinels. Above 60% selectivity to acetophenone was observed in all the systems along with more than 50% ethylbenzene conversion. Nickel substitution also had an enhanced efficiency in the oxidation of ethylbenzene. Among all the spinel systems studied, nickel chromite was least active. The selectivity towards 1-phenylethanol was also less and that of other products was more. Zinc substituted copper chromite spinels were also very active in ethylbenzene oxidation.

4.4.6. Mechanism of the reaction

A plausible mechanism for the oxidation of ethylbenzene is presented in scheme 4.4.2. TBHP was activated by co-ordinating with metal oxide. The activated distant oxygen of co-ordinated TBHP reacted with ethylbenzene to yield the products. 1-phenylethanol from ethylbenzene was produced by insertion of oxygen between carbon hydrogen bond of the methylene group. Abstraction of an alcoholic OH hydrogen and the CH hydrogen by the activated *t*-butylhydroperoxide oxygen yielded acetophenone. Similar abstraction of OH hydrogen of 1-phenylethanol by the activated *t*-butylhydroperoxide yielded benzaldehyde. The methyl group of ethylbenzene was also be attacked by activated *t*-butylhydroperoxide to yield 2-phenylethanol, which was very rapidly oxidized to phenyl acetaldehyde.

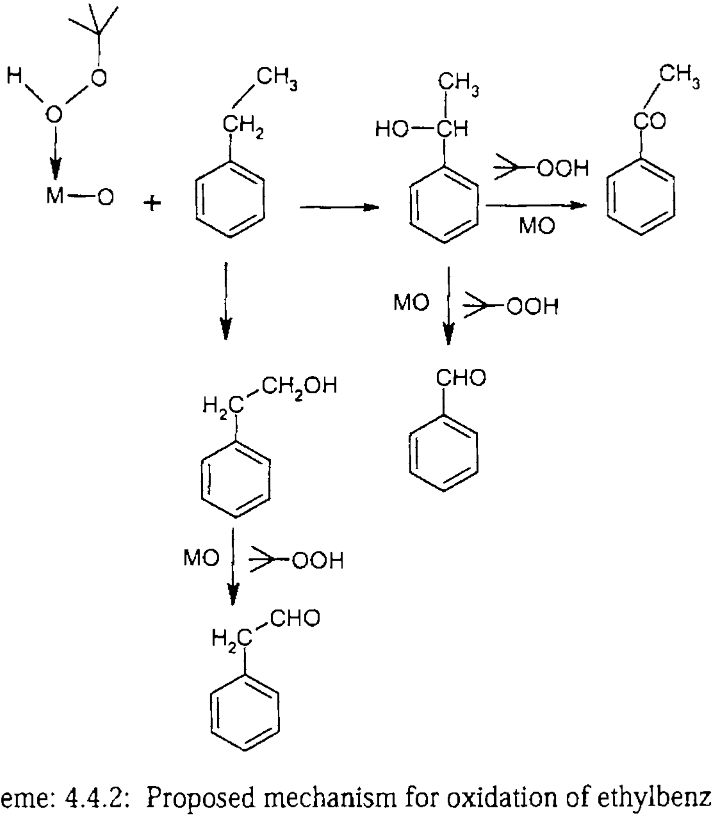

Scheme: 4.4.2: Proposed mechanism for oxidation of ethylbenzene

4.4.7. Conclusions

The following conclusions can be drawn from the present study.

- The oxidation of ethylbenzene with *t*-butylhydroperoxide over copper chromite and transition metal substituted copper chromites catalysts gave 1-phenylethanol and acetophenone as the major products. Trace amounts of benzaldehyde and phenyl acetaldehyde were also detected.
- The influence of reaction variables such as reaction time, temperature of the reaction, ethylbenzene to TBHP ratio, catalyst weight and solvent were studied and oxidation reaction was carried out under the optimized conditions.
- Regeneration and stability of the catalysts were studied and the results proved that they were stable up to four reaction cycles.
- A plausible mechanism involved in the oxidation of ethylbenzene was also proposed.

****

References

SECTION A

[1] R. A. Sheldon, I. W. C. E. Arends, A. Dijksman, Catal. Today 57 (2000) 157

[2] L. F. Liotta, A. M. Venezia, G. Deganello, A. Longo, A. Martorana, Z. Schay, L. Guczi, Catal. Today 66 (2001) 271

[3] T. L. Stuchinskaya, I. V. Kozhevnikov, Catal. Commun. 4 (2003) 417

[4] H. Ji, T. Wang, M. Zhang, Y. She, L. Wang, Appl. Catal. A. 282 (2005) 25

[5] L. F. Liotta, A. M. Venezia, G. Pantaleo, G. Deganello, M. Gruttadauria, R. Noto, Catal. Today 91(2004) 231

[6] S. T. Wong, C. H. Lee, T. S. Lin, C. Y. Mou, J. Catal. 228 (2004) 1

[7] G. Ganesan, B. Viswanathan, J. Mol. Catal. A 181(2002) 99

[8] M. Furukawa, Y. Nishikawa, S. Nishiyama, S. Tsuruya, J. Mol. Catal. A 211 (2004) 219

[9] H. Hayashibara, S. Nishiyama, S. Tsuruya, M. Masai, J. Catal. 153 (1995) 254

[10] S. Tsuruya, H. Miyamoto, T. Sakae, M. Masai, J. Catal. 64 (1980) 260

[11] S. Tsuruya, Y. Okamoto, T. Kuwada, J. Catal. 56 (1979) 52

[12] R. Zbigniew, J. Am. Chem. Soc. 82 (1960) 1267

[13] C. Venturello, M. Ricci, J. Org. Chem. 51 (1986) 1599

[14] S. E. Jacobson, D. A. Muccigrosso, F. Mares, J. Org. Chem. 44 (6) (1979) 921

SECTION B

[1] R. Pappo, D. S. Allen, R. U. Lemieux, W. S. Johnson, J.Am. Chem. Soc. 21 (1956) 478

[2] P. H. Carlsen, T. Katsuki, V. S. Martin, K.B. Sharpless, J. Org. Chem. 46 (1981) 3936

[3] B. S. Michael, Organic Synthesis, McGraw- Hill, 2nd ed., New York, 2002

[4] P. S. Bailey, Chem.Rev. 58 (1958) 925

[5] R. A. Sheldon, J. K. Kochi, Metal-catalyzed oxidations of organic compounds, Academic Press: New York 1981

[6] D. T. Sawyer, Oxygen Chemistry, Oxford University Press: New York 1981

[7] N. Ma, Y. Yue, W. Hua, Z. Gao, Appl. Catal. A. 251 (2003) 39

[8] D. Guin, B. Baruwati, S. V. Manorama, J. Mol. Catal. A 242 (2005) 26

[9] M. Silva, C. Freire, B. de Castro, J. L. Figueiredo, J. Mol. Catal. A 258 (2006) 327

[10] S. S. Kurek, P. Michorczyk, A. M. Balisz, J. Mol. Catal. A 194 (2003) 237

[11] C. Borriello, R. D. Litto, A. Panunzi, F. Ruffo, Inorg. Chem. Commun. 8 (2005) 717

[12] J. Y. Liu, X. F. Li, Y. Z. Li, W. B. Chang, A. J. Huang, J. Mol. Catal. A. 187 (2002) 163

[13] Y. Luo, J. Lin, Microporous Mesoporous Mater. 86 (2005) 23

[14] S. Gomez, L.J. Garces, J. Villegas, R. Ghosh, O. Giraldo, S. L. Suib, J. Catal. 233 (2005) 60

[15] V. Hulea, E. Dumitriu, Appl. Catal. A 277 (2004) 99

[16] Y. Chen, Y. Huang, J. Xiu, X. Han, X. Bao, Appl. Catal. A. 273 (2004) 185

[17] V. Parvulescu, C. Constantin, G. Popescu, B. L. Su, J. Mol. Catal. A 208 (2004) 253

[18] J. Zhuang, D. Ma, Z. Yan, X. Liu, X. Han, X. Bao, Y. Zhang, X. Guo, X. Wang, Appl. Catal. A 258 (2004) 1

SECTION C

[1] J. M. Thomas, R. Raja, G. Sankar, G. G. Bell, Nature 398 (1999) 227

[2] U. Schuchardt, D. Cardosa, R. Sercheli, R. Pereira, R. S. Cruz, M. C. Guerreiro, D.Mandelli, E.V. Spinace, E. L. Pires, Appl. Catal. A 211 (2001) 1

[3] R. A. Sheldon, I.W.C.E. Arends, H. E. B. Lempers, Catal. Today 41 (1998) 2319

[4] A. K. Suresh, T. Sridhar, Ind. Eng. Chem. Res. 39 (2000) 3589

[5] S. A. Chavan, D. Srinivas, P. Ratnasamy, J. Catal. 212 (2002) 39

[6] P. M. Reis, J. A. L. Silva, J. J. R. Frausto da Silva, A. J. L. Pombeiro, J. Mol. Catal. A 224 (2004) 189

[7] J. M. Thomas, R. Raja, G. Sankar, B. f. G. Johnson, D. W. Lewis, Chem. Eur. J. 7 (2001) 2972

[8] L. Zhou, J. Xu, H. Miao, F. Wang, X. Li, Appl. Catal. A 292 (2005) 223

[9] R. Anand, M. S. Hamdy, P. Ghourgkoulas, T. Maschemeyer, J. C. Jansen, U. Hanefeld, Catal. Today 117 (2006) 279

[10] A. Bellifa, D. Lahcene, Y. N. Tchenar, A.C. Braham, R. Bachir, S. Bedrane, C. Kappenstein, Appl. Catal. A 305 (2006) 1

[11] E. V. Spinace, H. O. Pastore, U. Schuchardt, J. Catal. 157 (1995) 631

[12] M. H. Zahedi- Niaki, M. P. Kapoor, S. Kaliaguine, J. Catal. 177 (1998) 2319

[13] N. Perkas, Y. Wang, Y. Koltypin, A. Gedanken, S. Chandrasekaran, Chem. Commun. (2001) 988

[14] A. Sakthivel, P. Selvam, J. Catal. 211 (2002) 134

[15] S. E. Dapurkar, A. Sakthivel, P. Selvam, J. Mol. Catal. A 223 (2004) 241

[16] P. Selvam, S. E. Dapurkar, J. Catal. 229 (2005) 64

[17] G. Qian, D. Gi, G. M. Lu, R. Zhao, Y. X. Qi, J. S. Suo, J. Catal. 232 (2005) 378

[18] P. Selvam, S. E. Dapurkar, Appl. Catal. A 278 (2004) 257

[19] G. S. Nunes, I. Mayer, H. E. Toma, K. Araki, J. Catal. 236 (2005) 55

[20] B. Moden, B. Z. Zhan, J. Dakka, J. G. Santiesteban, E. Iglesia, J. Catal. 239 (2006) 390

[21] H. X. Yuan, Q. H. Xia, H. J. Zhan, X. H. Lu, K. X. Su, Appl. Catal. A 304 (2006) 178

[22] P. Tian, Z. Liu, Z. Wu, L. Xu, Y. He, Catal. Today 93-94 (2004) 735

[23] D. Dumitriu, R. Barjega, L. Frunza, D. Macovei, T. Hu, Y. Xie, V. I. Parvulescu, S. Kaliaguine, J. Catal. 219 (2003) 337

[24] E. Armengol, A. Corma, V. Fornes, H. Garcia, J. Primo, Appl. Catal. A 181 (1999) 305

[25] I. Sokmen, F. Sevin, J. Colloid Interface Sci. 264 (2003) 208

[26] T. Sooknoi, J. Limtrakul, Appl. Catal. A 233 (2002) 227

[27] R. Hariprasad, A. V. Ramaswamy, Appl. Catal. A 93 (1993) 123

[28] R. Neumann, M. Levin-Elad, Appl. Catal. A. 122 (1995) 85

[29] Y. W. Chen, Y. H. Lu, Ind. Eng. Chem. Res. 38 (1999) 1893

[30] N. K. Mal, A. V. Ramaswamy, J. Mol. Catal. 105 (1996) 149

[31] N. K. Mal, A. V. Ramaswamy, Appl. Catal. A 143 (1996) 75

[32] A. P. Singh, T. Selvam, J. Mol. Catal. 113 (1996) 489

[33] S. Gontier, A. Tuel, Appl. Catal. A 143(1996) 125

[34] Z. Zhang, J. Suo, X. Zhang, S. Li, Appl. Catal. A 179 (1999) 11

[35] G. A. J. Russell, J. Am. Chem. Soc. 79 (1957) 3871

SECTION D

[1] S. S. Bhoware, S. Shylesh, K. R. Kamble, A. P. Singh, J. Mol. Catal. A 255 (2006) 123

[2] S. K. Jana, P. Wu, T. Tatsumi, J. Catal. 240 (2006) 268

[3] N. K. Mal, A. V. Ramaswamy, Appl. Catal. A 143 (1996) 75

[4] S. Vetrivel, A. Pandurangan, J. Mol. Catal. A 217 (2004) 165

[5] T. H. Bennur, D. Srinivas, S. Sivasankar, V. G. Puranik, J. Mol. Catal. A 219 (2004) 209

[6] T. H. Bennur, D. Srinivas, S. Sivasankar, J. Mol. Catal. A 207 (2004) 163

[7] L.I. Matienko, L.A. Molosova, Russ. Chem. Bull. 46 (1997) 658.

[8] G.L. Tembe, P.A. Ganeshpure, S. Satish, J. Mol. Catal. A 121 (1997) 17

[9] C. Guo, Q. Peng, Q. Liu, G. Jiang, J. Mol. Catal. A 192 (2003) 295

[10] P. S. Singh, K. Kosuge, V. Ramaswamy, B. S. Rao, Appl. Catal. A. 177(1999) 149

[11] E. P. Reddy, R. S. Varma, J. Catal. 221 (2004) 93

[12] P. P. Toribio, J. M. C. Martin, J. L. G. Fierro, J. Mol. Catal. A 227 (2005) 101

[13] B. Notari, Stud. Surf. Sci. Catal. 60 (1991) 343

[14] N. K. Mal, V. Ramaswamy, S. Ganapathy, A.V. Ramaswamy, Appl. Catal. A 125 (1995) 233

[15] R. Neumann, M.L. Elad, Appl. Catal. A. 122 (1995) 85

[16] K.O. Xavier, J. Chako, K.K.M. Yusuff, Appl. Catal. A. 258 (2004) 251

[17] P. Kumar, R. Kumar, B. Pandey, Synlett (1995) 289

[18] S.L.H. Rebelo, M.M.Q. Simoes, M. Graca, P.M.S. Neves, J.A.S. Cavaleiro, J. Mol. Catal. A 201 (2003) 9

[19] S. Velusamy, T. Punniyamurthy, Tetrahedron Lett. 44 (2003) 8955

[20] P.P. Toribio, J.M.C. Martin, J.L.G. Fierro, Appl. Catal. A 294 2 (2005) 290

[21] L. Barrio, P.P. Toribio, J.M.C. Martin, J.L.G. Fierro, Tetrahedron 60 50 (2004) 11527

[22] S. Vetrivel, A. Pandurangan, Appl. Catal. A 264 (2004) 243

[23] S. Vetrivel, A. Pandurangan, Ind. Eng. Chem. Res. 44 (2005) 692

[24] R. Alcantara, L. Canoira, P.G. Joao, J.M. Santos, I. Vazquez, Appl. Catal. A 203 (2000) 259

[25] C. Guo, Q. Peng, Q. Liu, G. Jiang, J. Mol. Catal. A 192 (2003) 295

[26] R. Alcantara, L. Canoira, P. G. Goao, J. M. Santos, I. Vazquez, Appl. Catal. A 203 (2000) 259

****

CHAPTER 5

OXIDATIVE DEHYDROGENATION OF ETHYLBENZENE

Abstract

The utilization of relatively abundant and cheap alkanes in the chemical industry is always desirable. In the transformation of alkanes into valuable chemicals, selective oxidation is considered to be important. The production of light olefins from alkanes separated from natural gas, today largely available and cheap, is a desirable option to limit the dependence from oil. This can be obtained through endothermic reactions such as steam cracking and thermal catalytic dehydrogenation or through an exothermic reaction such as oxidative dehydrogenation. However, several problems still remain, such as the formation of coke on the catalyst, thermodynamic constraints, and a large amount of wasted energy in the form of excess steam. Energy saving and more economical dehydrogenation processes are therefore desirable. The oxidative dehydrogenation of ethylbenzene, based on an introduction of oxidant to the ethylbenzene feed, seems to be one of the promising methods.

5.1. Introduction

The catalytic dehydrogenation of ethylbenzene is now a days the main method of styrene production, which is one of the most important basic chemicals as a monomer of synthetic polymers. The process is performed at elevated temperatures (550-650°C) in the presence of potassium doped hematite catalysts[1]. Additional promoters (e.g. Cr_2O_3, Ce_2O_3, MgO and MoO_3) are used in order to enhance the activity and selectivity, as well as stability of the catalytic system. Ethylbenzene dehydrogenation is endothermic and limited by thermodynamic equilibrium. An excess of superheated steam is therefore used to supply the heat of reaction and shift the equilibrium to higher styrene yields by a decrease in the partial pressures of reactants[2,3]. Oxidative dehydrogenation of ethylbenzene was proposed as an alternative route in styrene production[4-6]. Due to the exothermic effect of oxydehydrogenation, a higher conversion of ethylbenzene at significantly lower temperatures can be obtained compared to that in a classical dehydrogenation process. The schematic representation of the ethylbenzene dehydrogenation is shown in scheme 5.1.

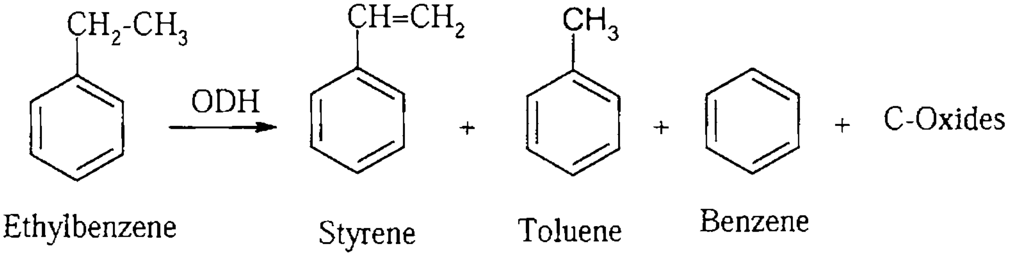

Scheme: 5.1: Reaction scheme of oxidative dehydrogenation of ethylbenzene

For this reaction, the economically preferred oxidant is air if high selectivity can be maintained. Various promoters like primary halides and sulphur compounds were tried[7,8]. Though these provided high conversions and selectivity, the severe problems arise in terms of corrosion, recovery, recycle of the catalyst and removal of the impurities from the reaction product. So these have not been extended into commercial processes. In oxydehydrogenation, the formation of carbon oxides is often a side reaction. The process economy rapidly deteriorates when ethylbenzene is extensively oxidized to carbon oxides. The formation of carbon oxides requires large quantities of oxygen, which limits the conversion to styrene. Moreover, formation of carbon oxides is extremely exothermic. Therefore the catalyst should be very selective in the minimum production of carbon oxides and reasonably active in order to limit the reactor size. Too much activity can cause problems with heat transfer and runway reaction. Thus most of the work on ethylbenzene has been devoted to the selection of suitable catalysts and appropriate reaction conditions for improved styrene yield and selectivity[9].

Figueiredo et al. investigated in detail the oxidative dehydrogenation of ethylbenzene over activated carbon catalysts and studied the catalytic deactivation[10-12]. They suggested a redox mechanism of the Mars-van-Krevelen type, where the quinone surface groups are reduced to hydroquinone by the adsorbed ethylbenzene, and reoxidised back to quinone by oxygen. The ODH of ethylbenzene was studied over $Mg_3(VO_4)_2$-MgO systems by Oganowski et al.[13] and their findings showed that magnesium orthovanadate forms with magnesium oxide an active biphasic system very efficient in the ODH of ethylbenzene to styrene.

Recently, CO_2 has been extensively utilized by several authors[14-23] for the last two decades in the oxidative dehydrogenation of ethylbenzene to styrene as oxidant as well as diluent for the replacement of superheated steam that is used in commercial plants for maintaining the high temperatures at 600-700°C over potassium promoted iron based catalysts[1]. Burri et al.[14]studied the influence of SBA-15 support on CeO_2-ZrO_2 catalyst for the oxidative dehydrogenation of ethylbenzene to styrene with CO_2. All their catalysts were effective in oxidative dehydrogenation and there was a sequential enhancement in the catalytic activity from individual oxides to mixed oxides followed by supported mixed oxide catalysts. The higher activity of the catalyst in the presence of CO_2 is due to the dissociation of CO_2 on the catalyst surface to produce active oxygen species. This active species oxidizes H_2 that is produced in the simple ethylbenzene dehydrogenation process into H_2O by reverse water-gas shift reaction and thereby releases the limitation of thermodynamic equilibrium. Cr-MCM-41 catalyst was found to be an effective catalyst with CO_2 for dehydrogenation of ethylbenzene[24]. It was suggested that the rate of CO formation during the dehydrogenation of ethylbenzene with CO_2 over Cr-MCM-41 was well accounted for by assuming parallel occurrence of two reactions, i.e., direct oxidative dehydrogenation of ethylbenzene with CO_2 and simple dehydrogenation of ethylbenzene thermodynamically assisted by reverse water-gas shift reaction. However, carbon dioxide introduced to the ethylbenzene stream acts both as an oxidizing agent and as a diluent similar to water vapour. The effectiveness of CO_2 as the oxidant is limited. On the other hand, it was found that the presence of CO_2 could favor the fast deactivation of a catalyst by the formation of catalytically inactive coke[25].

Nitrous oxide (N_2O) seems to be a more promising oxidizing agent than carbon dioxide. The utilization of N_2O is of additional interest as nitrous oxide has been recognized to be one of green house gases causing global warming. Coupling the N_2O decomposition with the ethylbenzene dehydrogenation over γ-Al_2O_3 supported transition metal (Fe, Cr and Cu) oxide catalysts led to high conversions of ethylbenzene and N_2O[26]. Furthermore, a replacement of the alumina support by mesoporous silicas (SBA-15, MCF, MCM-48 and MSU) characterized by high surface area gave the Fe-, Cr- and Cu- containing catalysts which were active in the oxidative dehydrogenation of ethylbenzene with N_2O[27]. Kustrowski[3] and co-workers studied the ODH of ethylbenzene with N_2O over vanadia supported on SBA-15. They observed an increase in the catalytic activity with raising the vanadium content. They proved that monomeric V^{5+} species were considerably more active and selective in styrene formation than oligomeric ones.

Spinel oxides were reported to be an active catalyst in the oxidative dehydrogenation of ethylbenzene. Krishnasamy et al.[28] studied the oxidative and nonoxidative dehydrogenation of ethylbenzene over Zn-Fe-Cr ternary spinel systems. They revealed that a redox cycle involving $Fe^{3+} \leftrightarrow Fe^{2+}$ is the active site for this reaction. Mathew et al.[29] prepared ferrites of copper and cobalt and studied the ODH of ethylbenzene. They have the same conclusion as proposed by Krishnasamy and explained the results with the mechanism of dehydrogenation of ethylbenzene proposed by Wang[30] and Krouse[31]. Strong basic sites facilitate the formation of toluene whereas strong acid centers result in high yield of benzene. The active site balanced with acidic and basic sites is important for an efficient ethylbenzene dehydrogenation.

This section presents the exhaustive investigation on vapour-phase oxidative dehydrogenation of ethylbenzene over different series of chromite spinels. It was observed that the catalytic performance of spinels for the oxidative dehydrogenation of ethylbenzene to styrene was fairly good. In all cases, some amount of benzene, toluene and carbon oxides was detected as by-products. A detailed discussion of process optimization by studying the effect of reaction temperature, flow rate and air flow rate are also included in this section.

5.2. Influence of Reaction Conditions

Various reaction parameters such as temperature, flow rate and airflow rate were optimized in order to maximize the product yield and selectivity. Effect of reaction conditions for oxidative dehydrogenation of ethylbenzene with air was initially assayed in non-optimized conditions with CCoCr-2 as the catalyst.

5.2.1. Effect of air flow rate

The dehydrogenation of ethylbenzene to styrene over oxide catalysts may take place in the presence or absence of oxygen. In the absence of oxygen, lattice oxygen directly participates in the reaction resulting in the bulk reduction of the catalyst[32,33]. The variation of ethylbenzene conversion and styrene selectivity with air flow is presented in figure 5.1.

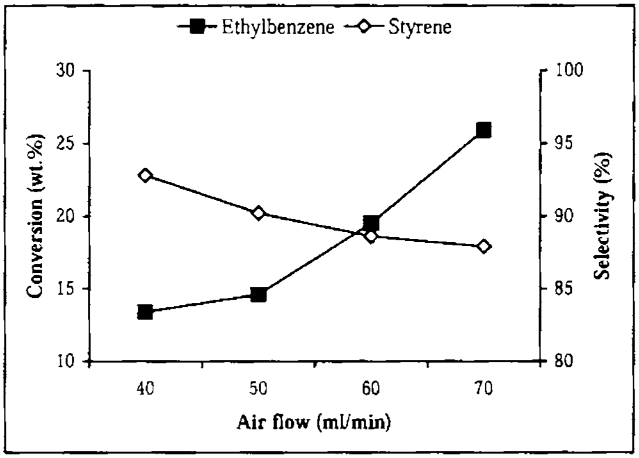

Reaction conditions: -Catalyst-CCoCr-2, Catalyst weight-0.5 g, Temperature-450°C, Flow rate- 4 ml/h, Time-2 h

Figure 5.1: Effect of air flow on ODH of ethylbenzene

It was observed that ethylbenzene conversion increased from 15.4% to 26% on increasing the air flow from 40 to 70 ml/min. Meanwhile, styrene selectivity decreased correspondingly. The percentage selectivity of the side products such as benzene and carbon oxides increased with more air. At higher air flow, styrene selectivity remained almost same. Therefore, 70 ml/min was selected as the optimized air flow for further studies.

5.2.2. Effect of Temperature

To study the effect of temperature on the oxidative dehydrogenation of ethylbenzene, reaction was carried out at various temperatures keeping other parameters constant. The results obtained are presented in figure 5.2.

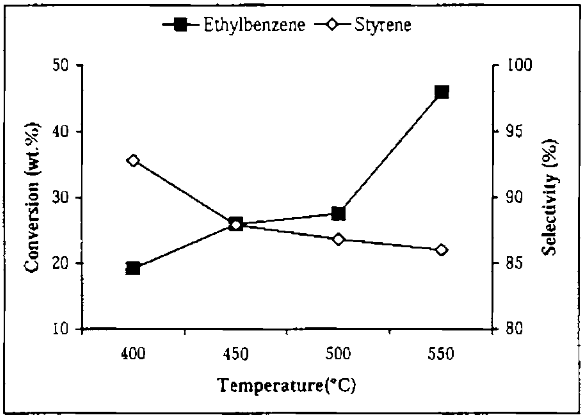

Reaction conditions: -Catalyst-CCoCr-2, Catalyst weight-0.5g, Air flow rate-70 ml/min, Flow rate-4 ml/h, Time-2 h.

Figure 5.2: Effect of temperature on ODH of ethylbenzene

Ethylbenzene conversion was 20% at 400°C, which increased remarkably to 46% at a temperature of 550°C. The results indicated that there was a direct relation between temperature and activity of the catalyst. Styrene selectivity decreased marginally when the temperature was increased from 400 to 550°C. The noticeable decrease in styrene selectivity at 550°C was due to cracking of ethylbenzene into benzene, toluene and carbon oxides[14]. An optimum temperature of 500°C was selected for further studies.

5.2.3. Effect of flow rate

The effect of flow rate on ethylbenzene conversion and styrene selectivity is presented in figure 5.3. The reaction was carried out at different flow rates of 3-6ml/h.

The conversion depends on the residing time of the reactant on the catalyst surface. Increase in flow rate decreased the residing time and hence lowered the conversion. Moderate conversion and styrene selectivity was obtained at a flow rate of 4ml/h and is selected for further studies.

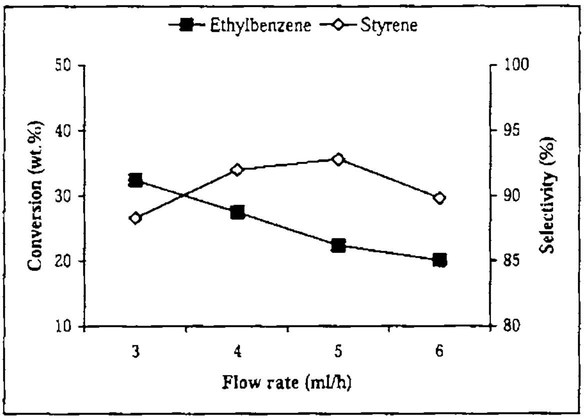

Reaction conditions: - Catalyst-CCoCr-2, Catalyst weight-0.5g, Temperature-500°C, Air flow rate-70 ml/min, Time-2 h

Figure 5.3: Effect of flow rate on ODH of ethylbenzene

The reaction was carried out over all the catalysts with the reaction conditions given in table 5.1.

Table 5.1: Optimized conditions for oxidative dehydrogenation of ethylbenzene

Reaction Parameters		Selected conditions
Temperature	:	500°C
Air flow rate		70 ml/min
Flow rate		4 ml/h
Time		2 h
Catalyst weight	:	0.5 g

5.2.4. Effect of time on stream

In order to check the catalytic stability, a set of reactions were carried out at 500°C for 8 h over five catalyst samples. The results obtained are presented in figure 5.4.

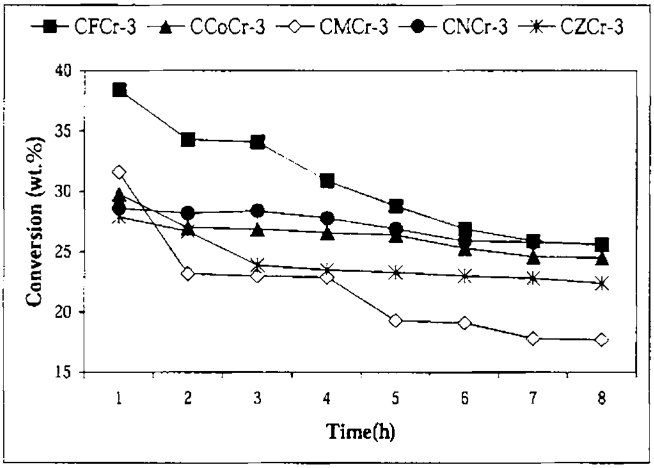

Reaction conditions: Temperature-500°C, Flow rate-4 ml/h, Air flow rate-70 ml/min, Catalyst weight-0.5g

Figure 5.4: Effect of time on stream on ODH of ethylbenzene

Deactivation was observed in all the catalysts with increase in time. Coke deposition may be the reason for the deactivation of catalysts under vapour phase reaction conditions. CZCr-3 showed a better stability upto 8 h.

5.3 Oxidative Dehydrogenation of Ethylbenzene over Prepared Catalysts

The reaction was carried out over all the catalysts prepared and the results obtained are presented in table 5.2.

Table 5.2: Oxidative dehydrogenation of ethylbenzene over the prepared catalysts

Catalyst	Ethylbenzene conversion (wt %)	Product selectivity (%)			
		Styrene	Benzene	Toluene	C-Oxides
CCr	29.0	88.7	3.2	2.7	5.3
CFCr-1	24.8	90.8	4.1	1.5	6.8
CFCr-2	30.9	87.9	5.1	2.3	4.5
CFCr-3	34.3	89.8	2.9	1.7	5.6
CF	25.9	90.4	1.0	1.0	7.6
CMCr-1	36.6	88.4	4.1	2.8	4.7
CMCr-2	28.7	87.3	4.2	2.1	6.4
CMCr-3	23.2	86.9	3.5	1.8	7.8
MCr	37.3	83.6	4.8	5.9	5.7
CCoCr-1	37.8	85.6	4.9	4.2	5.2
CCoCr-2	27.5	92.0	3.9	1.7	2.3
CCoCr-3	27.0	90.5	3.9	1.9	5.9
CoCr	33.9	87.3	4.7	2.6	5.4
CNCr-1	33.1	91.2	2.3	1.0	5.5
CNCr-2	21.6	88.9	1.7	1.0	8.4
CNCr-3	28.2	87.7	3.2	1.6	7.5
NCr	34.7	89.4	3.4	1.2	6.0
CZCr-1	23.9	87.9	3.0	1.3	7.7
CZCr-2	33.5	87.7	3.9	2.1	6.1
CZCr-3	26.7	86.0	5.1	2.7	6.3
ZCr	36.2	85.1	4.1	3.3	7.5

5.4. Discussions

The oxidative dehydrogenation of ethylbenzene to styrene in the presence of air was carried out at 500°C over all the spinel catalysts prepared. Moderate ethylbenzene conversion and more than 80% selectivity to styrene was achieved over all the catalytic systems studied. Toluene, benzene and carbon oxides were also formed as side products during this reaction.

According to Wang[30] and Krouse[31], the formation of toluene and benzene during the oxidative dehydrogenation reaction is caused by the interaction of acid-base centres on the catalyst surface. Strong basic sites can abstract the β- H of the adsorbed ethylbenzene, which facilitates the cleavage of side chain C-C bond resulting in the formation of toluene, whereas, strong acid centres can abstract α-hydrogen of ethylbenzene and facilitates the cleavage of phenyl-C bond resulting in the high yield of benzene. However, the formation of benzene and toluene require relatively high temperature. A balance of acid-base property is very important for an efficient ethylbenzene dehydrogenation.

In all the catalytic systems, the products benzene and toluene were formed in small quantities. From the ammonia TPD results, the amount of ammonia desorbed at higher temperatures (strong acid sites) is very low, which is in agreement with the benzene selectivity obtained during the oxidative dehydrogenation of ethylbenzene. Cyclohexanol decomposition reaction over the prepared catalysts produced the dehydrated product in major scale than the base catalyzed dehydrogenated product, cyclohexanone. In the ODH of ethylbenzene, toluene was produced in very small amount, which was in agreement with the results of cyclohexanol decomposition reaction.

5.5. Mechanism of the reaction

Several mechanisms have been proposed for the oxidative dehydrogenation of ethylbenzene. The most probable one is known as Mars-van Krevelen mechanism[34,35] which consists of abstraction of hydrogen from ethylbenzene by the lattice oxygen on the surface to form styrene through a π allyl intermediate and reoxidation of the catalyst[36,37]. A condition for the operation of this mechanism is that the catalyst must contain metal ion with variable valancies, notably transition metal ion able to cope with the varying degree of surface oxidation[38].

In non-oxidative dehydrogenation, the absence of gaseous oxygen may lower the activity. The following sequence was suggested by Tagawa et al.[39] on Si-Al systems. Hanuza and co- workers[37] also suggest the same sequence.

$$\text{EB} + [\text{O}] \longrightarrow \text{ST} + [\ ]$$
$$[\ ] + \tfrac{1}{2}\text{O}_2 \longrightarrow [\text{O}]$$

Where, EB is ethylbenzene, ST is styrene, [O] is the lattice oxygen and [ ] is anion vacancy.

According to Bautista[40], oxidation of ethylbenzene is a concerted process over the Lewis acid sites. According to this mechanism, direct transfer of two oxygen atoms to a triplet oxygen molecule is considered. Activation of the triplet state is achieved by the action of Lewis acid sites. The gas phase dehydrogenation mechanism is non-oxidative as well in oxidative conditions and can be explained within the framework of a concerted process. Alkhazov et al. assumed that in the ODH of ethylbenzene over modified alumina, ethylbenzene is adsorbed first on the acid centers of the catalyst surface[41]. They claimed that the reaction pathway depends on the strength of adsorption; stronger the adsorption, the greater is the ethylbenzene conversion. In this process, base centers on the catalyst surface also play an important role, as they activate the oxygen from the gas phase, which takes part in this reaction. Oxygen activated on strong base centers at higher temperature has been found to be responsible for the total oxidation of hydrocarbons. Therefore, such a catalyst, which has acid and base centers of moderate or weaker strength on its surface, is the most suitable for the ODH of ethylbenzene.

Bagnasco et al.[42] suggested that surface acid site of medium- high strength play significant role in the ODH of ethylbenzene. Hagemeyer et al.[43] claimed a redox process involving the dehydrogenation of ethylbenzene by contact with a catalyst containing a reducible metal oxide (Bi_2O_3, CeO_2 and Cr_2O_6) in the absence of oxygen and simultaneous reduction of the catalyst, followed by oxidation of reduced catalyst with an oxidizing agent. From the investigations over rare earth promoted sulphated tin oxide, Sugunan et al.[44] suggested that the strong acid sites generated by the sulphated treatment is accountable in the activation of ethylbenzene and enhance the catalytic activity. The strong basic site enhances the formation of the non-selective product, toluene.

A plausible mechanism for the oxidative dehydrogenation of ethylbenzene is described below. At first, ethylbenzene is coordinated to the acid site of the catalyst and the basic group adjacent to the acid site abstracts the α- hydrogen from the co-ordinated ethylbenzene to give a stable adsorbed species. The OH group thus formed over the catalyst surface then abstracts the β- hydrogen and the subsequent desorption of water activates the molecular oxygen. The reversibly adsorbed oxygen is converted to O^- species over the catalyst surface, which regenerates the active site.

5.6. Conclusions

The conclusions from the present results can be summarized as given below.

- ✓ Oxidative dehydrogenation of ethylbenzene over transition metal substituted copper chromite spinel catalysts showed good catalytic activity.
- ✓ Reaction variables such as air flow, temperature and flow rate had strong influence on ethylbenzene conversion and product selectivity.
- ✓ Reaction always gave styrene as the major product with trace amount of benzene, toluene and carbon oxides.
- ✓ A plausible reaction mechanism was proposed for the formation of styrene.

References

[1] E. H. Lee, Catal. Rev. 8 (1973) 285

[2] F. Cavani, F. Trifiro, Appl. Catal. A 133 (1995) 219

[3] P. Kustrowski, Y. Segura, L. Chmielarz, J. Surman, R. Dziembaj, P. Cool, E. F. Vasant, Catal. Today 114 (2006) 307

[4] G. Eming, H. Hofman, J. Catal. 84 (1983) 15

[5] F. Cavani, F. Trifiro, Appl. Catal. A 133 (1995) 219

[6] A. E. Lisovskii, C. Aharoni, Catal. Rev. - Sci. Eng. 36 (1994) 25

[7] S. W. Brown, Br. Pat. Appl. 913323, 1991

[8] L. Y. Litvintsv, Kinet. Catal. 34 (1993) 71

[9] D. R. C. Hytbrechts, Catal. Lett. 8 (1991) 273

[10] M. F. R. Pereira, J. J. M. Orfao, J. L. Figueiredo, Appl. Catal. A 196 (2000) 43

[11] M. F. R. Pereira, J. J. M. Orfao, J. L. Figueiredo, Appl. Catal. A 218 (2001) 307

[12] M. F. R. Pereira, J. J. M. Orfao, J. L. Figueiredo, Appl. Catal. A 184 (1999) 153

[13] W. Oganowski, J. Hanuza, L. Kepinski, Appl. Catal. A 171 (1998) 145

[14] D. R. Burri, K. M. Choi, J. H. Lee, D. S. Han, S. E. Park, Catal. Commun. 8

(2007) 43

[15] G. Towler, S. Lynn, Chem. Eng. Sci. 49 (1994) 2585

[16] M. Sugino, H. Shimada, T. Turuda, H. Miura, N. Ikenaga, T. Suzuki, Appl. Catal. A 121 (1995) 125

[17] N. Mimura, I. Takahara, M. Saito, T. Hattori, K. Ohkuma, M. Ando, Catal. Today 45 (1998) 61

[18] T. Badstube, H. Papp, P. Kustrowski, R. Dziembaj, Catal. Lett. 55 (1998) 169

[19] J. S. Chang, S. E. Park, M. S. Park, Chem. Lett. (1997) 1123

[20] M. S. Park, V. P. Vislovskiy, J. S. Changa, Y. G. Shul, J. S. Yoo, S. E. Park, Catal. Today 87 (2003) 205

[21] J. S. Chang, V. P. Vislovskiy, M. S. Park, D. Y. Hong, J. S. Yoo, S. E. Park, Green Chem. 5 (2003) 587

[22] S. E. Park, S. C. Han, J. Ind. Eng. Chem. 10 (2004) 1257

[23] J. N. Park, J. Noh, J. S. Chang, S. E. Park, Catal. Lett. 65 (2000) 75

[24] Y. Ohishi, T. Kawabata, T. Shishido, K. Takaki, Q. Zhang, Y. Wang, K. Takehira, J. Mol. Catal. A 230 (2005) 49

[25] R. Dziembaj, P. Kustowski, T. Badstube, H. Papp, Top. Catal. 11-12 (2000) 317

[26] P. Kustrowski, M. Zbroja, R. Dziembaj, H. Papp, Catal. Lett. 80 (2002) 1

[27] P. Kustrowski, L. Chmielarz, R. Dziembaj, P. Cool, E. F. Vansant, J. Phys. Chem. A 109 (2005) 330

[28] N. J. Jebarathinam, M. Eswaramoorthy, V. Krishnasamy, Appl. Catal. A 145 (1996) 57

[29] T. Mathew, S. Malwadkar, Shivanand Pai, C. P. Sebastian, C. V. Satyanarayana, V. V. Bokade, Catal. Lett. 91 (2003) 217

[30] I. Wang, W. H. Chang, R. J. Shiau, J. C. Wu, C. S. Chung, J. Catal 83 (1983) 438

[31] A. Krouse, Sci.Pharm.38 (1970) 266

[32] H. Norman, J. Coord. Chem. 19 (1988) 25

[33] R. Yu, F. Xiao, D. Wang, G. Pang, S. Feng, S. Qiu, R. Xu, Catal. Lett. 49 (1997) 49

[34] P. Mars, D. W. van der Krevelen, Chem. Eng. Sci. 8 (1954) 41

[35] A. Maltha, T. L. F. Favre, H. F. Kist, A. P. Zuur, V. Ponec, J. Catal. 149 (1994) 364

[36] Y. Murakami, K. Iwayama, H. Uchida, T. Hattori, T. Tagawa, J. Catal. 71 (1981) 257

[37] J. Hanuza, B. Jezowska, J. Mol. Catal. 4 (1978) 271

[38] S. Meijers, T. P. Pruys, V. Ponec, J. P. Jacobs, H. H. Brongersma, J. Catal. 161 (1996) 459

[39] T. Tagawa, T. Hattori, Y. Murakami, J. Catal. 75 (1982) 66

[40] F. M. Bautista, J. M. Campelo, A. Garcia, V. M. Marinas, J. Catal. 116 (1989) 338

[41] T. G. Alkhazov, A. E. Lisovski, M. Safarov, A. M. Dadasheva, Kinet. Catal. 13 (1972) 509

[42] G. Bagnasco, P. Ciambelli, M. Turco, A. La Ginestra, P. Partono, Appl. Catal. A 68 (1991) 69

[43] A. Hagemeyer, W. J. Poecel, W. Buechele, O. Hofstadt, A. Deimling, W. Hoffman, German Patent, DE 4422770 (1996)

[44] T. M. Jyothi, K. Sreekumar, M. B. Talwar, A. A. Belhekar, B. S. Rao, S. Sugunan, Bull. Chem. Soc. Jpn. 73 (2000) 1

****

CHAPTER 6

OXIDATION OF CARBON MONOXIDE

Abstract

Catalytic oxidation of carbon monoxide (CO) at ambient temperature has been of considerable interest recently due to its importance in human safety in mines, deep sea diving, space exploration as well as in many other applications such as indoor air cleaning, CO sensors and in minimizing the CO build-up in CO_2 lasers. In addition, CO oxidation is an elementary step in other important industrial processes such as water-gas shift reaction and production of methanol. The ability to oxidize CO at low temperatures is important in many applications. The use of a low temperature active catalyst can lower the emission during a cold-start of a car, and volatile organic compounds in exhaust gases from stationary sources might be treated without the need of preheating the gas. In this chapter, copper chromite and transition metal substituted copper chromites were chosen as a model catalyst for carbon monoxide oxidation. The catalytic activity at various temperatures was investigated and presented.

6.1. Introduction

The exhaust from internal combustion engines contains large amount of pollutants that must not be emitted to the atmosphere due to legislational and environmental aspects. For this reason today's petrol engine cars are equipped with a so called three way catalyst (TWC), which is able to simultaneously convert the pollutants CO, hydrocarbons (HC) and NO_x to the harmless substances CO_2, H_2O and N_2. The required reactions are thus oxidation of CO and HC to CO_2 and H_2O, and reduction of NO_x to N_2. Today's TWC perform well in these reactions if the catalyst temperature is above 200-250°C. Below this temperature the pollutants are not completely converted. When a cold- start is made with a car engine (i.e. when the car is started after the engine has been switched off for some time), both the engine and the catalytic converter is at ambient temperature. It thus takes a while before the catalyst has been heated by the exhausts to the temperature (200-250°C) where the catalytic reactions start. Before this the exhaust is emitted more or less untreated. To make things worse, the engine is run somewhat rich after the cold-start, leading to higher emissions of CO than during normal driving. About 80-90% of all emissions are released during the cold -start[1,2]. This problem is often referred to as the "cold-start problem" in car exhaust catalysis.

A problem somewhat similar to the cold-start problem is the emission of CO and volatile organic compounds (VOC) in ventilation air from chemical industries, restaurants and printeries. The desired reactions would be oxidation of CO and VOC over an oxidation catalyst placed in the exhaust gas flow. However, the temperature of the gas to be treated is too low to start the reaction. The difference from the cold-start problem is that this is a steady state process. The gas flow will always have approximately the same temperature, and this temperature is too low to start the reaction, while in the cold-start problem the exhaust gas will finally be heated up to a temperature at which the reactions on the catalyst can start.

Today's diesel engine vehicles are equipped with oxidation catalysts to oxidize CO and hydrocarbons in the exhaust gas from the engine. If the exhaust gas temperature is decreased too much, there will be a problem in heating the catalyst sufficiently to start the reaction[3]. This will lead to a problem similar to the VOC problem discussed above; where, at steady state conditions the exhaust gas temperature is too low to ignite the catalyst.

6.2. CO Oxidation over Metals

Oxygen adsorbs rapidly on most clean metal surfaces. The sticking probability is between 0.1 to 1 at room temperature, meaning that the activation energy for adsorption is low. At temperatures above around 0°C the oxygen molecule is dissociatively adsorbed, producing adsorbed O atoms on the metal surface. On clean metal surfaces the adsorption of CO is also rapid. The sticking probability is between 0.2 and 0.6; i.e. the activation energy for this process is also low. CO is adsorbed perpendicular to the metal surface with the carbon atom facing the surface[4]. Adsorption occurs via donation of electrons in the 5σ orbital on CO to the d_{xy} orbital of the metal and back-donation of metal d-electrons into the antibonding $2\pi^*$ orbital of CO[5]. Although this weakens the C-O bond, dissociative adsorption of CO is rare on Pt group metals. If the metal surface is exposed to oxygen and CO at the same time, reaction between adsorbed O atoms and adsorbed CO can occur and produce CO_2. However, if the metal surface is saturated with CO, no reaction can occur since there are no sites available for oxygen adsorption. This happens if the CO partial pressure is higher than the O_2 partial pressure or the temperature is too low to allow CO desorption. This state is called CO poisoning and occurs due to the strong adsorption of CO to the metal at low temperatures. When the temperature is raised CO desorbs from the metal surface, leaving sites available for oxygen adsorption. In the reverse case when the metal surface is completely covered with oxygen, no blocking occurs, since oxygen does not inhibit CO adsorption. Even an oxygen presorbed Pt surface leaves enough free sites for CO to adsorb[6]. This case will happen when the oxygen partial pressure is much higher than the CO partial pressure. The CO oxidation over metals is thought to follow a Langmuir-Hinshelwood mechanism.

$O_2 + 2^* \rightarrow 2\ O_{ads}$ LH-1

$CO + {}^* \rightarrow CO_{ads}$ LH-2

$CO_{ads} + O_{ads} \rightarrow CO_2 + 2^*$ LH-3

Where * depicts a free site on the metal surface. The CO_2 formed is only weakly adsorbed and will thus not affect the rate substantially, since it is quickly desorbed to gas phase. No surface carbonate species are formed as intermediates in this reaction. The rate of reaction will then be proportional to the surface coverage of O_{ads} and CO_{ads}. Sometimes an Eley-Ridel mechanism is supposed for the CO oxidation over metals. In this mechanism gas-phase CO reacts directly with adsorbed oxygen.

$O_2 + 2^* \rightarrow 2\ O_{ads}$ ER-1

$CO\ (g) + O_{ads} \rightarrow CO_2 + {}^*$ ER-2

6.3. CO Oxidation over Metal Oxides

The mechanism for CO oxidation over metal oxides differs from that over metals. The reaction is thought to follow a stepwise mechanism first suggested by Mars and van Krevelen[7] in 1954. The oxidation occurs in two steps. First the reactant (which may be a hydrocarbon as well as CO) is oxidized by surface lattice oxygen in the metal oxide. An oxygen vacancy is then created, reducing the neighboring metal ions to a lower oxidation state. In the second step the surface metal atoms are reoxidised by gas-phase oxygen.

$CO + O_{cat} \rightarrow CO_{2\,ads} + *$ MK-1

$CO_2, ads \rightarrow CO_2\,(g)$ MK-2

$\frac{1}{2} O_2 + * \rightarrow O_{cat}$ MK-3

Where * depicts an oxygen vacancy and O_{cat} is a surface lattice oxygen, probably O^{2-}. The oxidation over metal oxides thus takes place via a redox mechanism in which the metal ion changes oxidation state. The ability to change oxidation state is crucial for the activity of the metal oxide in the oxidation reaction. At higher temperatures (150-200°C) the reoxidation step (MK-3) is rather fast than the desorption of reaction products (MK-2). The withdrawal of oxygen from the catalyst in step one (MK-1) will then be rate determining. At lower temperatures (-80°C to +100°C) on the other hand desorption of reaction products will be rate determining[8]. At lower temperatures a conjugated mechanism may occur, where the desorption of reaction products and reoxidation of the metal oxide occurs simultaneously.

In CO oxidation over metal oxides, surface carbonates form as an intermediate product. Several types of carbonates may form on metal oxide surfaces. Holmgren[9] reported the formation of unidentate carbonate, bidentate carbonate, inorganic carboxylate and bridged carbonate after exposing CeO_2 to CO at room temperature. Surface carbonate species may be detected by infrared spectroscopy. Carbonate and carboxylate species[10] have characteristic absorption bands in the region 1000-1700 cm^{-1}. Boreskov[11] reviewed the CO oxidation activity for different metal oxides and found that the activity decreased in the following order:

$$Co_3O_4 > CuO > NiO > Mn_2O_3 > Cr_2O_3 > Fe_2O_3 > ZnO > V_2O_5 > TiO_2$$

Shelef et al.[12] found the following order for the CO oxidation activity:

$$Co_3O_4, CuCr_2O_4 > Cu_2O > Fe_2O_3 > MnO > NiO > Cr_2O_3 > V_2O_5$$

6.4. Literature Review

There is an increasing demand to reduce emissions from vehicles equipped with Otto engines. New and efficient engine control systems, together with new catalyst materials can convert most of the emissions during normal driving. However, during the first few minutes of driving before the catalyst has been heated, a large fraction of the total emissions is released[13,14]. This means that there is still a big challenge to find efficient catalysts that can convert the emissions immediately after a cold-start. During these first few minutes, the engine is running somewhat rich, which means that the exhaust contain relatively large amounts of carbon monoxide (1-7%), hydrogen (0.5-3%) and hydrocarbons[15] (0.1-0.7%). Although it is possible to convert hydrogen at low temperatures on an ordinary noble metal catalyst, CO and hydrocarbons need higher temperatures before the conversion starts. If at least one of either CO or some hydrocarbons could be converted at lower temperatures, not only would the harmful emissions be lowered, but also the catalyst would also be heated up faster due to the exothermicity of the chemical reactions. CO is probably the species most easily activated and is, therefore, put into focus in this study.

Several groups have studied the carbon monoxide oxidation over various catalysts since it has an importance in environmental applications. Gold has traditionally been known as a catalytically inactive material. However, it has been shown that small supported gold particles can be effective catalysts for CO oxidation[16-21]. The gold particle size and activity of gold catalyst depend critically on the support material, the synthesis method and activation procedure[22-29]. To date, explanations for the catalytic activity of small gold particles have mainly focused on the size of the particle and nature of the support material and include electronic quantum size effects, strain, oxygen diffusion via the support and the oxidation state of the gold particles[30-32.] Janssens et al. studied the relation between nano scale gold particle structure and activity for CO oxidation on supported gold catalyst[33]. A number of oxide supported gold catalysts were prepared by Moreau and co-workers who studied the carbon monoxide oxidation over those catalysts[34]. Gold nano particles confined in mesoporous aluminosilicates Al-SBA-15 were found to be effective in CO oxidation[35]. The high-temperature hydrogen reduction of the aluminosilicate materials produced defect sites for oxygen adsorption to give the super oxide species, which facilitates the CO oxidation. Catalysts containing gold supported on CeO_2, ZrO_2 and La_2O_3[36] were reported to be active in CO oxidation.

Recently, there has been interest in examining the oxidation of carbon monoxide on perovskite type oxides[37-42]. Taguchi et al. synthesized perovskite type of $(La_{1-x}Ca_x)\ FeO_3$ at low temperature and studied CO oxidation over those catalysts[43]. They found that catalytic activity for CO oxidation increased with increasing value of x. According to Voorhoeve et al.[44], CO oxidation occurs at the metal ions of the perovskite-type oxide surface. Catalytic activity for CO oxidation depends strongly on both the metal ion content of the surface and surface crystallinity. CO_2 is produced by the reaction of CO with oxygen adsorbed on the metal ions of the outermost surface. After CO_2 has been desorbed from the surface, oxygen is again adsorbed on the metal surface.

Cerium oxide has attracted much attention in environmental catalysis, either as effective promoter or supporting material based on its high oxygen storage capacity and facile Ce^{4+}/Ce^{3+} redox cycle[45]. CuO/CeO_2 catalysts have been shown to be very active for CO oxidation, exhibiting specific activities for superior to the conventional copper-based catalysts and even comparable with or superior to platinum catalyst[46-48]. Another similar CuO/samaria-doped ceria catalyst was also reported to be highly active in total CO oxidation[49]. In principle, an excellent CuO/CeO_2 catalyst should have the ability to facilitate the copper species in changing their valence and to supply suitable oxygen species. The so-called metal-support interaction between copper and ceria is often regarded as the key factor in determining the redox features and consequently the catalytic behavior[50-56]. Arias et al. studied the catalytic behavior of CuO/CeO_2 and $CuO/ZrCeO_4$ catalysts for CO oxidation[57]. A greater CO oxidation activity was exhibited by the CuO/CeO_2 catalyst. A comparison of both catalysts and analysis of the redox properties of the different copper entities present in the catalysts indicated that the active copper sites for CO oxidation are located on the copper oxide clusters.

CuO/TiO_2 catalysts synthesized by deposition-precipitation method were applied as catalysts for low temperature CO oxidation[58]. Recently copper-manganese oxides were reported to be an active catalyst for low temperature CO oxidation[59]. Hutchings and co-workers studied the effect of preparation conditions on the catalytic performance of copper manganese oxide catalyst for CO oxidation[60]. They concluded that catalysts containing copper/manganese mixed phases are found to be the most active. Copper-zinc oxide and ceria promoted copper-zinc oxide are highly active for low temperature oxidation of carbon monoxide[61]. The reducibility and susceptibility to variation in the oxidation states of copper oxides are critical to the activity of the catalyst. It was found that addition of CeO_2 brings out a significant improvement in the catalytic stability over an extended reaction period as well as at elevated reaction temperature.

The surface catalytic reaction of CO oxidation on Pt surfaces is central to controlling CO emissions, and continues to demand greater understanding. A new microscopic model, based on DFT/LDA modeling is suggested for the Langmuir-Hinshelwood reaction of catalytic CO oxidation in co-adsorbed O-CO layer on Pt (111)[62]. It was found that only the oxygen atoms occupying threefold hollow sites of hcp type were chemically active. Addition of alkali metal ions such as Li, Na, K, Rb and Cs to Pt/Al_2O_3 enhanced CO conversion and selectivity of CO oxidation[63]. The selective low temperature oxidation of CO was studied in hydrogen-rich streams over $Pt\text{-}Co\text{-}Ce/Al_2O_3$ catalysts[64]. The results obtained proved that this catalyst had great potential for removing CO in the hydrogen stream from a fuel processor for fuel cell applications, considering the fact that it may operate at significantly lower temperature and O_2/CO ratios compared to other alternatives reported in the literature. Bernado and co-workers studied the carbon monoxide oxidation reaction over Pt-Y zeolite membrane[65]. They had shown that the catalytically active particles are entrapped in a thin zeolite layer, avoiding the by-pass problems, generally shown in catalyst pellets. Nakao et al. reported a comparative study of CO_2 formation in CO oxidation by O_2, NO and N_2O on Pd (110) surface using infrared chemiluminescence[66]. Their results showed that the activated complex of CO_2 in the CO+NO reaction had more bent structure than those in the CO+O_2 and CO+N_2 reactions. Carbon monoxide oxidation reaction was studied over $PdO/Ce_{0.8}Y_{0.2}O_{1.9}$ catalysts by Luo and co-workers[67]. Their catalytic activity indicated that both the highly dispersed and crystalline PdO were the active site for CO oxidation.

Spinels are another group of catalysts over which the carbon monoxide oxidation reaction had widely studied. Recently, Ruszel et al.[68] used chromium spinels as a support for gold nano particles in the oxidation of carbon monoxide. They found that the activity depends on the nature of the bivalent cation of the spinel and reducibility of the catalyst. Carbon monoxide oxidation over copper chromite were studied by various groups[69,70] and their results showed that Cu species in tetrahedral co-ordination leads to higher activity and both Cu^0 and Cu^+ are involved in the mechanism of CO oxidation. Laberty et al. studied CO oxidation over nonstoichiometric nickel manganite spinels and a detailed mechanism was proposed for the reaction[71]. Copper manganese oxide mixture based on $CuMn_2O_4$ is a long established catalyst for the removal of toxic gases and vapors since its discovery in 1920[72]. Spinel based pigment system containing Mn, Cu and Fe oxides[73], nickel ferrites[74], $NiMn_2O_4$[75] and cobalt aluminate[76] were also applied as catalyst for CO oxidation.

6.5. Carbon Monoxide Oxidation over the Prepared Catalysts

Carbon monoxide oxidation was performed in a glass micro reactor fixed in a furnace. About 0.5 g of the catalyst was loaded to the reactor previously loaded with glass balls. Nitrogen, oxygen and carbon monoxide of composition 1% carbon monoxide, 5% oxygen and the rest nitrogen (using outlet flow is set to ~15000 ml/h so as to get the space velocity factor of 30 h^{-1}). The furnace temperature was raised slowly through the required temperature profile and analyzed the outlet gas sample for CO and CO_2 using GC with FID detector and Pouropack column. After separation at the column, CO and CO_2 were detected with FID by converting them to methane by passing through a Ni based catalyst kept at 400°C. From the amount of CO and CO_2, percentage conversion was calculated. Simultaneously, flow at different temperatures can also be measured through the valves provided.

The results obtained on performing the carbon monoxide oxidation over the five series of spinels showed that all the catalysts are highly active in this reaction. Substitution of transition metals on copper chromite spinel had an enhanced activity towards CO oxidation. At room temperature and below 200°C, the activity was less and showed increased activity around 200-350°C. Above 350°C, 100% CO conversion was achieved over all the catalysts.

The results obtained for CO oxidation over iron substituted copper chromites are presented in figure 6.1. Copper chromite showed CO conversion of only 20% at a temperature of 300°C and after that the conversion increased. Around 92% conversion was achieved at 450°C. Iron substitution had a remarkable influence on activity. On CFCr-1 catalyst a sharp increase in conversion from 31%-99% was observed in the temperature range 250°-350°C. In CFCr-2 such a sharp increase was observed in temperature between 200°C-300°C. The same trend was observed on other iron-substituted catalysts.

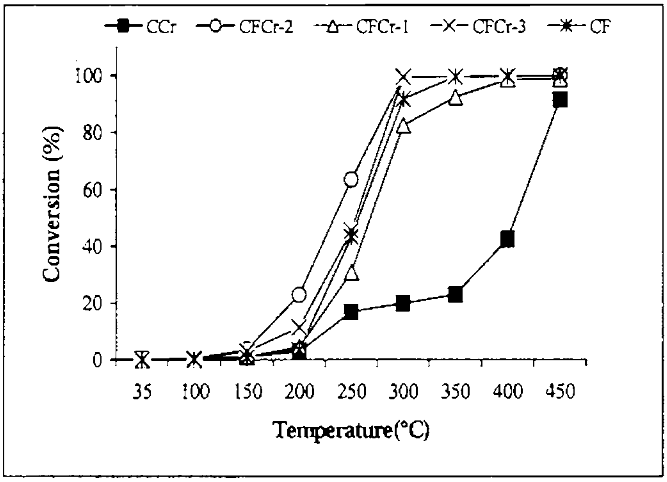

Figure 6.1: CO Oxidation over $CuCr_{2-x}Fe_xO_4$ series spinels

Manganese substitution had a remarkable influence on the catalytic activity of copper chromite for CO oxidation. The results obtained over the manganese series spinels are presented in figure 6.2. At a temperature range of 150°C to 250°C, catalysts CMCr-1 and CMCr-2 showed a sharp increase in the CO conversion rate. Other catalysts CMCr-3 and MCr showed this sharp increase around 250°C to 350°C range. Above 350°C, all the catalysts showed 100% CO conversion.

The results obtained for carbon monoxide oxidation over cobalt substituted copper chromite spinels are presented in figure 6.3. The catalyst CCoCr-1 showed a higher activity even at low temperatures. A sharp increase in conversion from 9% to 100% was obtained in the temperature range of 100-200°C. Other catalysts such as CCoCr-2 and CCoCr-3 showed higher activity in the range of 150-250°C. In the case of cobalt chromite, 47%-98% conversion was achieved in the temperature range of

250-300°C. All the catalysts showed 100% conversion above 350°C, which showed that all the catalysts were very active in carbon monoxide oxidation.

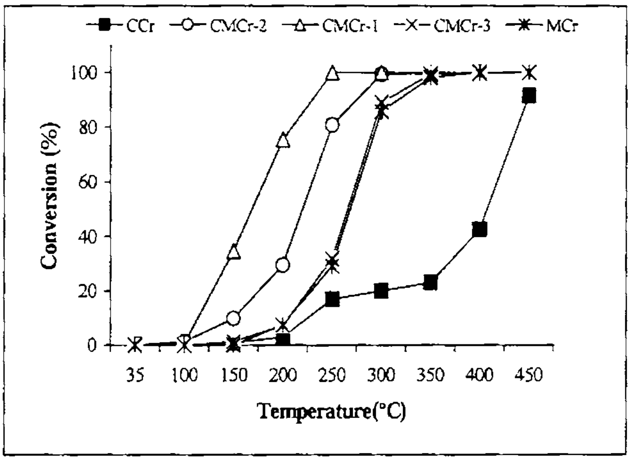

Figure 6.2: CO Oxidation over $Cu_{1-x}Mn_xCr_2O_4$ series spinels

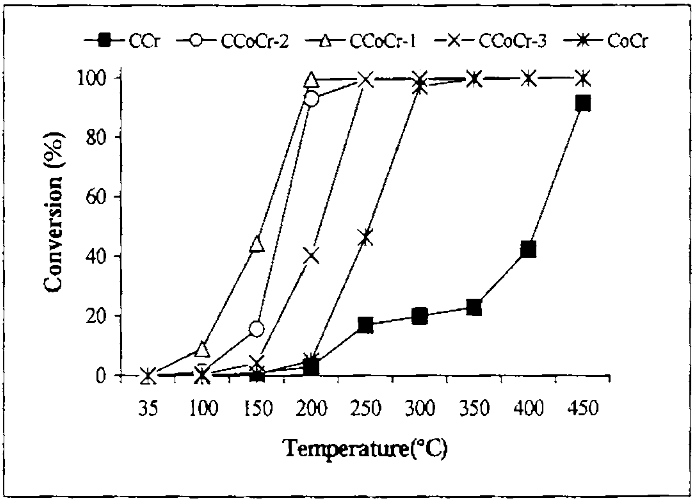

Figure 6.3: CO Oxidation over $Cu_{1-x}Co_xCr_2O_4$ series spinels

Nickel substituted catalysts showed catalytic activity towards carbon monoxide oxidation only above 200°C. The results obtained over these catalytic systems are presented in figure 6.4. Considerable increase in catalytic activity was observed in the temperature range of 250-400°C in all the catalysts and above 400°C all the catalysts showed 100% conversion.

Figure 6.5 depicts the results obtained for carbon monoxide oxidation over zinc substituted copper chromite spinels. At a temperature range of 200-250°C, a sharp increase in conversion was shown by CZCr-1, CZCr-2 and CZCr-3 catalysts and these systems gave 100% conversion above 250°C. Zinc chromite showed considerable activity only above 300°C and showed 100% conversion above 400°C.

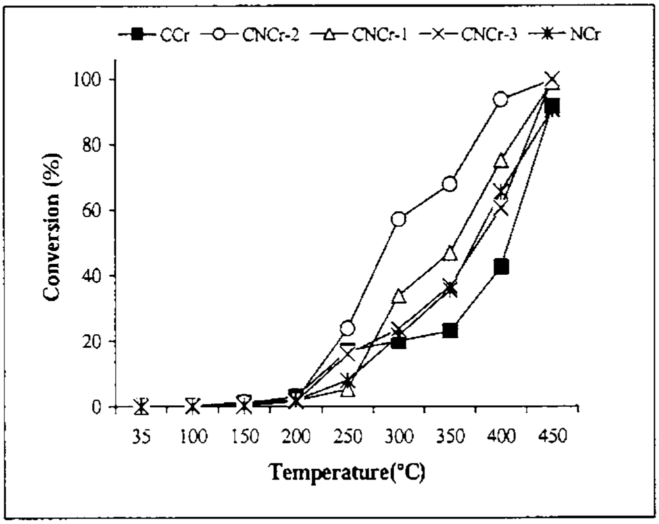

Figure 6.4: CO Oxidation over $Cu_{1-x}Ni_xCr_2O_4$ series spinels

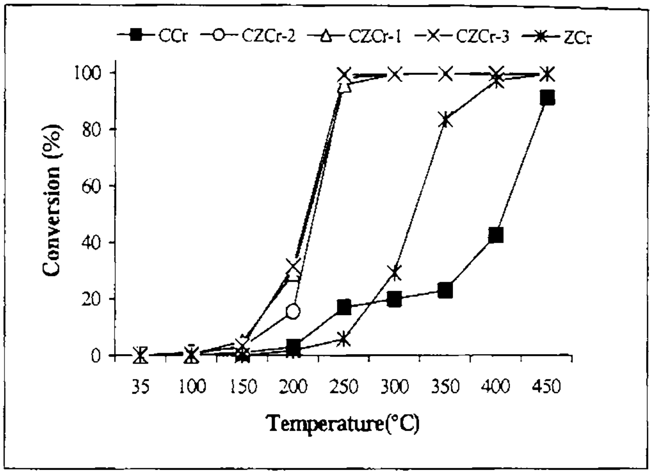

Figure 6.5: CO Oxidation over $Cu_{1-x}Zn_xCr_2O_4$ series spinels

6.6. Mechanism of the Reaction

Different mechanisms have been suggested for the oxidation of carbon monoxide over metals and metal oxides. They are Langmuir-Hinshelwood mechanism, Eley-Ridel mechanism and Mars van Krevelen mechanism[4-7].

The CO oxidation over metals is thought to follow a Langmuir-Hinshelwood mechanism.

$$O_2 + 2^* \rightarrow 2\ O_{ads}$$

$$CO + {}^* \rightarrow CO_{ads}$$

$$CO_{ads} + O_{ads} \rightarrow CO_2 + 2^*$$

Where * depicts a free site on the metal surface. The CO_2 formed is only weakly adsorbed and will thus not affect the rate substantially, since it is quickly desorbed to the gas phase. No surface carbonate species are formed as intermediates in this reaction. The rate of reaction will then be proportional to the surface coverage of O_{ads} and CO_{ads}.

Sometimes an Eley-Ridel mechanism is supposed for the CO oxidation over metals. In this mechanism gas-phase CO reacts directly with adsorbed oxygen.

$$O_2 + 2^{*} \rightarrow 2\ O_{ads}$$

$$CO\ (g) + O_{ads} \rightarrow CO_2 + {}^{*}$$

The CO oxidation over metal oxides is thought to follow the Mars van Krevelen mechanism. The oxidation occurs in two steps. First the reactant is oxidized by surface lattice oxygen in the metal oxide. An oxygen vacancy is then created, reducing the neighboring metal ions to a lower oxidation state. In the second step the surface metal atoms are reoxidised by gas-phase oxygen.

$CO + O_{cat} \rightarrow CO_{2,\ ads} + *$ Step 1

CO_2, ads $\rightarrow CO_2\ (g)$ Step 2

$\frac{1}{2} O_2 + * \rightarrow O_{cat}$ Step 3

Where * depicts an oxygen vacancy and O_{cat} is a surface lattice oxygen, probably O^{2-}. The oxidation over metal oxides thus takes place via a redox mechanism in which the metal ion changes oxidation state. The ability to change oxidation state is crucial for the activity of the metal oxide in the oxidation reaction. At higher temperatures (150-200°C) the reoxidation step (Step-3) is rather fast than the desorption of reaction products (Step-2). The withdrawal of oxygen from the catalyst in step one (Step-1) will then be rate determining. At lower temperatures (-80-100°C) on the other hand desorption of reaction products will be rate determining. At lower temperatures a conjugated mechanism may occur, where the desorption of reaction products and reoxidation of the metal oxide occurs simultaneously.

A plausible mechanism for CO oxidation over spinel metal oxides is described below. It is supposed to take place by a stepwise process [The Mars van Krevelen mechanism]. Carbon monoxide first is oxidized by surface lattice oxygen causing an oxygen vacancy, followed by a re-oxidation of the metal oxide by gas phase oxygen. In order to facilitate this process, the metal atoms change oxidation state during the repeated reduction and oxidation of the lattice surface.

6.7. Conclusions

The important conclusions of the carbon monoxide oxidation reaction are presented below.

- Copper chromite and transition metal substituted copper chromites were very effective in carbon monoxide oxidation.
- Catalytic activity of copper chromite was enhanced by transition metal substitution.
- In almost all catalysts studied, 100% conversion of carbon monoxide was achieved above 400°C.
- A plausible mechanism for carbon monoxide oxidation over spinel catalysts was also proposed.

References

[1] G. Lenaers, Sci. Total Environment 189/190 (1996) 139

[2] R. C. Rijkeboer, Catal. Today 11 (1991) 141

[3] S. Erkfeldt, E. Jobson, M. Larsson, Proc. CAPoC5, Brussels, April 2000, Vol. 1, p. 143 (2000)

[4] R. Masel, Principles of adsorption and reaction on solid surfaces, John Wiley and Sons, New York (1996)

[5] G. K. Boreskov, “Catalysis: Science and Technology" (J. R. Anderson and M. Boudart, Eds.) Vol. 3 p. 39. Springer-Verlag, Berlin (1982)

[6] Y. Mergler, J. Hoebink, B. E. Nieuwenhuys, J. Catal. 167 (1997) 305

[7] P. Mars, D. W. Van Krevelen, Chem. Eng. Sci. 3 (suppl) (1954) 41

[8] K. Klier, J. Catal. 8 (1967) 14

[9] A. Holmgren, Doctoral Thesis, Chalmers University of Technology, Gothenburg, Sweden (1998)

[10] A. A. Davydov, Infrared Spectroscopy of Adsorbed Species on the Surface of Transition Metal Oxides, ed. C. H. Rochester, John Wiley and Sons, New York (1990)

[11] G. K. Boreskovin, "Catalysis: Science and Technology" (J. R. Anderson and M. Boudart, Eds.) Vol. 3 p. 39. Springer-Verlag, Berlin (1982)

[12] M. Shelef, K. Otto, H.Gandhi, J. Catal. 12 (1968) 361

[13] G. Lenaers, Sci. Total Environ. 190 (1996) 139

[14] T. Krichner, A. Donnerstag, A. Konig, G. Eigenberger, Stud. Surf. Sci. Catal. 116 (1998) 125

[15] G. Ertl, H. Knozinger, J. Weitkamp, Handbook of Heterogeneous Catalysis, Vol. 4, Wiley-VCH, Weinheim, Germany, 1997

[16] G. C. Bond, D.T. Thomson, Catal. Rev. Sci. Eng. 41 (1999) 319

[17] M. Haruta, N. Yamada, T. Kobayashi, S. Ijima, J. Catal. 115 (1989) 301

[18] M. Haruta, Catal. Today 36 (1997) 153

[19] V. Schwartz, D. R. Mullins, W. Yan, B. Chen, S. Dai, S. H. Overbury, J. Phys. Chem. B. 108 (2004) 15782

[20] M. Valden, X. Lai, D. W. Goodman, Science 281 (1998) 1647

[21] X. Lai, T.P. St Clair, M. Valden, D.W. Goodman, Prog. Surf. Sci.59 (1998) 25

[22] J. D. Grunwaldt, C. Kiener, C. Wogerbauer, A. J. Baiker, J. Catal. 181 (1999) 223

[23] W. C. Li, M. Comotti, F. Schuth, J. Catal. 237 (2006) 190

[24] A. I. Kozlov, A. P. Kozlova, H. Liu, Y. Iwasawa, Appl. Catal. A 182 (1999) 9

[25] Y. Yuan, K. Asakura, H. Wan, K. Tsai, Y. Iwasawa, Catal. Lett. 42 (1996) 15

[26] G. K. Bethke, H. H. Kung, Appl. Catal. A 194-195 (2000) 43

[27] D. Boyd, S. Golunski, G.R.Hearne, T. Magadzu, K. Mallick, M.C. Raphulu, A. Venugopal, M. S. Scurrell, Appl. Catal. A 292 (2005) 76

[28] J. H. Yang, J.D. Henao, M. C. Raphulu, Y. Wang, T. Caputo, A. J. Groszek, M. C. Kung, M.S. Scurrell, J. T. Miller, H. H. Kung, J. Phys. Chem. B. 109 (2005) 10319

[29] M. S. Chen, D.W. Goodman, Catal. Today 111 (2006) 22

[30] M. Valden, X. Lai, D. W. Goodman, Science 281 (1998) 1647

[31] X. Lai, T. P. St. Clair, M. Valden, D. W. Goodman, Prog. Surf. Sci. 59 (1998) 25

[32] X. Lai, D. W. Goodman, J. Mol. Catal. A 162 (2000) 33

[33] T.V.W. Janssens, A. Carlsson, A. P. Molina, B.S. Clausen, J. Catal. 240 (2006) 108

[34] F. Moreau, G. C. Bond, Catal. Today 114 (2006) 362

[35] C. W. Chiang, A. Wang, C.Y. Mou, Catal. Today 117 (2006) 220

[36] N. Russo, D. Fino, G. Saracco, V. Specchia, Catal. Today 117 (2006) 214

[37] K. Rida, A. Benabbas, F. Bouremmad, M. A. Pena, A. M. Arias, Catal. Commun. 7 (2006) 963

[38] Y. Z. Steenwinkel, L. M. Zande, H. L. Castricum, A. Bliek, Appl. Catal. B 54 (2004) 93

[39] P. Ciambelli, S. Cimino, S. D. Rossi, G. Minelli, P. Porta, G. Russo, Appl. Catal. B. 29 (2001) 239

[40] P. Ciambelli, S. Cimino, G. Lasorella, L. Lisi, S.D. Rossi, M. Faticanti, G. Minelli, P. Porta, Appl. Catal. B 37 (2002) 231

[41] Y. Teraoka, H. Nii, S. Kagawa, K. Jansson, M. Nygren, Appl. Catal. A 194-195 (2000) 35

[42] P. Ciambelli, L. Lisi, S. D. Rossi, M. Faticanti, P. Porta, Appl. Catal. B 43 (2003) 397

[43] H. Taguchi, Y. Masunaga, K. Hirota, O. Yamaguchi, Mater. Res. Bull. 40 (2005) 773

[44] R. J. H. Voorhoeve, D. W. Johnson, J. P. Remeika, P. K. Gallegher, Science 195 (1977) 827

[45] X. Tang, B. Zhang, Y. Li, Y.Xu, Q. Xin, W. Shen, Appl. Catal. A 288 (2005) 116

[46] W. Lu, M. F. Stephanopoulos, J. Catal. 153 (1995) 304

[47] W. Lu, M. F. Stephanopoulos, J. Catal. 153 (1995) 317

[48] W. Lu, M. F. Stephanopoulos, Chem. Eng. J. 64 (1996) 283

[49] J. B. Wang, W. H. Shih, T. J. Huang, Appl. Catal. A 203 (2000) 191

[50] L. Kundakovic, M. F. Stephanopoulos, J. Catal. 179 (1998) 203

[51] S. Hocevar, J. Batista, J. Levec, J. Catal. 184 (1999) 39

[52] C. Kleinlogel, L. J. Gauckler, Adv. Mater. 13 (2001) 1081

[53] Y. Li, Q. Fu, M. F. Stephanopoulos, Appl. Catal. B 27 (2000) 179

[54] J. Cunningham, G. H. Al- Sayyed, J. A. Cronin, J. Fierro, C. Healy, W. Hirschwald, M. Ilyas, J. Tobin, J. Catal. 102 (1986) 160

[55] M. Iwamoto, H. Yahiro, N. Mizuno, W. X. Zhang, Y. Mine, S. Furkaga, J. Phys. Chem. B 96 (1992) 9360

[56] W. Shen, Y. Ichihashi, Y. Matsumura, Catal. Lett. 83 (2002) 33

[57] A. M. Arias, M. Fernandez, O. Galvez, J.M. Coronado, J.A. Anderson, J.C. Conesa, J. Soria, G. Munuera, J. Catal. 195 (2000) 207

[58] J. Huang, S. Wang, Y. Zhao, X. Wang, S. Wang, S. Wu, S. Zhang, W. Huang, Catal. Commun. 7 (2006) 1029

[59] M. Kramer, T. Schmidt, K. Stowe, W.F. Maier, Appl. Catal. A 302 (2006) 257

[60] G. J. Hutchings, A. A. Mirzaei, R.W. Joyner, M.R.H. Siddiqui, S. H. Taylor, Appl. Catal. A 166 (1998) 143

[61] U. R. Pillai, S. Devi, Appl. Catal. B 65 (2006) 110

[62] I. N. Yakovkin, N. V. Petrova, Surf. Sci. 600 (2006) 2600

[63] Y. Minemura, M. Kuriyama, S. Ito, K. Tomishige, K. Kunimori, Catal. Commun. 7 (2006) 623

[64] T. Ince, G. Uysal, A. N. Akin, R. Yildirim, Appl. Catal. A. 292 (2005) 171

[65] P. Bernardo, C. Algieri, G. Barbieri, E. Drioli, Desalination, 200 (2006) 702

[66] K. Nakao, S. Ito, K. Tomishige, K. Kunimori, Surf. Sci. 600 (2006) 4221

[67] M. F. Luo, Z. Y. Pu, M. He, J. Jin, L.Y. Jin, J. Mol. Catal. A 260 (2006) 152

[68] M. Ruszel, B. Grzybowska, K. Samson, I. Gressel, A. Klisinska, Catal. Today 112 (2006) 126

[69] F. Severino, J.L. Brito, J. Laine, J. L. G. Fierro, A. L. Agudo, J. Catal. 177 (1998) 82

[70] J. Ghose, K. S. R. C. Murthy, J. Catal. 162 (1996) 359

[71] C. Laberty, C. M. Alvarez, C. Drouet, P. Alphonse, C. Mirodatos, J. Catal. 198 (2001) 266

[72] A. B. Lamb, W. C. Bray, J. C. Frazer, J. Ind. Eng. Chem. 12 (1920)

[73] S. Pal Dey, S. Gedevanishvili, W. Zhang, F. Rasouli, Appl. Catal. B 56 (2005) 241

[74] M. M. Rashad, O. A. Fouad, Mater. Chem. Phys. 94 (2005) 365

[75] D. Mehandjiev, A. Naydenov, G. Ivanov, Appl. Catal. A 206 (2001) 13

[76] P. Thromahlen, E. Fridell, N. Cruise, M. Skoglundh, A. Palmqvist, Appl. Catal. B 31 (2001) 1

****

CHAPTER 7

SUMMARY AND CONCLUSIONS

Abstract

More and more new ideas, emerging from basic research in catalysis promise a break though that may change the profile of industries in future. Current and future chemists are being trained to design products and processes with an increased awareness for environmental input. The goal of a catalyst manufacturer is to produce and reproduce a commercial product, which can be used as a stable, active and selective catalyst. With chemists under increasing pressure to perform atom economic processes with minimal or no environmentally unfriendly by-products, development of novel catalyst system that facilitates some industrially important reactions should be of great importance. The importance of environmentally friendly catalysts in the modern age forms the basis of the present research work. The major objectives of the present work consist of preparation of some chromite spinels, physico-chemical characterization and their activity towards some oxidation reactions. This chapter deals with the summary and conclusions of the results of the present work and the scope for further research in this field.

7.1. Introduction

The prime intension of the present work was a synthetic investigation of the preparation, surface properties and catalytic activity of some transition metal substituted copper chromite catalysts. Homogeneous co-precipitation method is employed for the preparation of catalysts. Since the knowledge about the structure and composition of the surface is critical in explaining the reactivity and selectivity of a solid catalyst, a systematic investigation of the physico-chemical properties of the prepared systems was carried out. The catalytic activity of these systems has also been measured in several oxidation reactions of industrial as well as environmental relevance. The thesis is dedicated to several aspects of chromite spinels giving emphasis to its preparation, characterization and catalytic performance towards oxidation reactions.

7.2. Summary

The chapter wise organization of the thesis is as follows.

Chapter 1 covers an introduction to heterogeneous catalysis and literature survey on catalysis by spinel chromites. A detailed description on various methods of preparation of chromites, spinel structure, acid-base properties and catalytic effectiveness for various oxidation reactions is also given in this chapter.

Chapter 2 deals with the various materials and experimental methods adopted for the synthesis and characterization of the catalyst systems. It also gives a brief account of the relevant theory of each method of characterization employed. Surface acidity determination by different techniques, including the test reactions like cumene conversion and cyclohexanol decomposition are the additional features of this chapter. The experimental procedures used to evaluate the catalytic activity are also incorporated in this chapter.

Chapter 3 describes the results of physico-chemical characterization of the prepared catalytic systems. The catalytic systems were characterized by X-ray diffraction analysis, surface area and pore volume measurements and FT-IR spectroscopy. Thermal stability of the samples was revealed by thermo gravimetric analysis and elemental composition of the prepared systems was obtained from energy dispersive X-ray analysis. Scanning electron microscopy was used to know the topology of the catalysts. Surface acidic properties of the catalysts were examined by temperature programmed desorption of ammonia and by test reactions like cumene conversion and cyclohexanol decomposition.

Chapter 4 focuses on the application of the catalytic systems for liquid-phase oxidation reactions. Oxidation of benzyl alcohol is achieved by H_2O_2 and that of styrene, cyclohexane and ethylbenzene by TBHP. The influence of various reaction conditions on the catalytic activity and selectivity is subjected to investigation. Plausible mechanisms have been drawn out in each case based on the experimental observations.

Chapter 5 illustrates the catalytic activity of the systems towards oxidative dehydrogenation of ethylbenzene. The catalytic activity and selectivity of all the systems were measured under optimized reaction conditions such as temperature of the reaction, air flow, time on stream and flow rate of ethylbenzene.

Chapter 6 narrates the performance of the catalytic systems for the gas phase oxidation of carbon monoxide to carbon dioxide. A plausible reaction mechanism is proposed and described in this chapter.

Chapter 7 presents the summary, important conclusions and future prospects of the present work.

7.3. Conclusions

The major conclusions that can be drawn from the present research work are the following.

- Homogeneous co-precipitation method was found to be an efficient method for the preparation of spinel chromites. The modification of copper chromite spinel by transition metals showed improvement in the physico- chemical characteristics.
- XRD patterns of the prepared systems revealed the characteristic peaks of spinels. The spinel phase formation was again confirmed by the appearance of two bands at 620 and 510cm^{-1} in the FT-IR spectra.
- Chemical composition of the catalysts obtained from EDX analysis was in agreement with the theoretical values indicated the correct stoichiometry.
- Enhancement in surface area, pore volume and total acidity was observed in all the transition metal substituted copper chromite spinels.
- Scanning electron microscopy of the catalysts gave an idea about surface morphology of the catalysts.
- The general observation that acid sites favor dehydration and both acidic and basic sites favor dehydrogenation was confirmed by the cyclohexanol decomposition reaction carried out over different spinel systems.

- Cumene conversion reaction gave α-methyl styrene as the major product indicated the presence of more Lewis acid sites in the catalyst.
- Activity of the catalysts towards liquid-phase oxidation of hydrocarbons such as benzyl alcohol, styrene, cyclohexane and ethylbenzene was measured and they effectively catalyzed the oxidations.
- Vapour- phase oxidative dehydrogenation of ethylbenzene over the catalytic systems yielded styrene as the major product along with small amounts of benzene, toluene and carbon oxides. Increase in temperature and decrease in flow rate enhanced the conversion of ethylbenzene.
- Carbon monoxide oxidation was carried out over the prepared catalysts and found to be effective in the oxidation

Future outlook

Catalysis is a mature field with extensive practical applications in today's society. Indeed, the catalysis of petroleum refining, fine chemical synthesis and emission control demands the production of catalysts in bulk quantities. The observations we have obtained during the research work on "Studies on surface properties and catalytic activity of some chromites and related spinels" point to the importance of some chromium containing spinel oxides for some important oxidation reactions. Since these catalysts are efficient in oxidation reactions, further research work can be made in the field of oxidation reactions. Further, more studies on the removal of exhaust gases is desirable.

****